JOURNAL OF GEOPHYSICAL RESEARCH

The continuation of

TERRESTRIAL MAGNETISM AND ATMOSPHERIC ELECTRICITY

(1896-1948)

An International Quarterly

VOLUME 58 September, 1953 NUMBER 3

CONTENTS

(Contents concluded on outside back cover)

Address all correspondence to

JOURNAL OF GEOPHYSICAL RESEARCH

5241 BROAD BRANCH ROAD, NORTHWEST

WASHINGTON 15, D.C., U.S.A.

THREE DOLLARS AND FIFTY CENTS A YEAR SINGLE NUMBERS, ONE DOLLAR

PRINTED BY

THE WILLIAM BYRD PRESS, INC.

P. O. Box 2-W—Sherwood Ave. and Durham St., Richmond 5, Virginia

JOURNAL OF GEOPHYSICAL RESEARCH

The continuation of

Terrestrial Magnetism and Atmospheric Electricity

(1896-1948)

An International Quarterly

Founded 1896 by L. A. BAUER *Continued 1928–1948 by* J. A. FLEMING

Fields of Interest

Terrestrial Magnetism
Atmospheric Electricity
The Ionosphere
Solar and Terrestrial Relationships
Aurora, Night Sky, and Zodiacal Light
The Ozone Layer
Meteorology of Highest Atmospheric Levels
The Constitution and Physical States of the Upper Atmosphere
Special Investigations of the Earth's Crust and Interior, including experimental seismic waves, physics of the deep ocean and ocean bottom, physics in geology
And similar topics

This Journal serves the interests of investigators concerned with terrestrial magnetism and electricity, the upper atmosphere, the earth's crust and interior by presenting papers of new analysis and interpretation or new experimental or observational approach, and contributions to international collaboration. It is not in a position to print, primarily for archive purposes, extensive tables of data from observatories or surveys, the significance of which has not been analyzed.

Forward *manuscripts* to one of the Associate Editors, or to the editorial office of the Journal at 5241 Broad Branch Road, Northwest, Washington 15, D. C., U. S. A. It is preferred that manuscripts be submitted in English, but communications in French, German, Italian, or Spanish are also acceptable. A brief abstract, preferably in English, must accompany each manuscript. A *publication charge* of $4 per page will be billed by the Editor to the institution which sponsors the work of any author; private individuals are not assessed page charges. Manuscripts from outside the United States are invited, and should not be withheld or delayed because of currency restrictions or other special difficulties relating to page charges. Costs of publication are roughly twice the total income from page charges and subscriptions, and are met by subsidies from the Carnegie Institution of Washington and international and private sources.

Back issues and *reprints* are handled by the Editorial Office, 5241 Broad Branch Road, N.W., Washington 15, D.C., U.S.A.

Subscriptions are handled by the Editorial Office, 5241 Broad Branch Road, N.W., Washington 15, D.C., U.S.A.

Entered as second-class matter at the Post Office at Richmond, Virginia, under the act of March 3, 1879.

Journal of
GEOPHYSICAL RESEARCH

The continuation of

Terrestrial Magnetism and Atmospheric Electricity

VOLUME 58 SEPTEMBER, 1953 No. 3

DISSOCIATIVE RECOMBINATION IN THE *E*-LAYER*

BY E. GERJUOY

University of Pittsburgh,
Pittsburgh, Pennsylvania

AND

M. A. BIONDI

Westinghouse Research Laboratories,
East Pittsburgh, Pennsylvania

(Received December 10, 1952)

ABSTRACT

The present paper discusses the consequences of the assumption that dissociative recombination determines electron removal in the *E*-layer. The observation that the apparent recombination coefficient, α, does not depend markedly on the altitude of the *E*-layer, electron density, or time of day imposes restrictions on the rates of the various atomic collision processes. It is shown that α must be very nearly equal to the actual dissociative recombination coefficient of O_2^+ ions and electrons. The conversion of O^+ to O_2^+ by charge transfer is consistent with ionospheric observations provided that the transfer cross-section is $\gtrsim 10^{-17}$ cm^2. In addition, the negative ion concentration is required to remain smaller than the electron concentration at all times. It is concluded that dissociative recombination is far more satisfactory than ion-ion recombination in explaining the *E*-layer observations, and that most of the atomic processes proposed for this mechanism are subject to accurate laboratory measurement.

*Scientific paper 1708, October 31, 1952.

I—MAGNITUDE OF THE RECOMBINATION COEFFICIENT

The difficulties involved in explaining the observed values of the effective electron recombination coefficient in the E- and $F1$-layers were first discussed in detail by Bates and Massey [see 1 of "References" at end of paper]. These authors suggested dissociative recombination of electrons as a means of accounting for the large effective recombination coefficient. We proceed to examine, rather more quantitatively than heretofore, the consequences of assuming that electrons in the ionized layer disappear mainly by dissociative recombination. We confine our detailed analysis to the E-layer where the constituents are better known.

If electrons are destroyed mainly by dissociative recombination,

$$\frac{dN_e}{dt} = Q - \alpha_d N(O_2^+) N_e \quad \ldots\ldots (1)$$

where N_e , $N(O_2^+)$ are, respectively, the electron and positive molecular ion concentrations, Q is the total rate of production of electrons by the primary photoionization processes giving rise to the layer, and α_d is the dissociative recombination coefficient of the reaction:

$$O_2^+ + e \rightarrow O' + O'' \quad \ldots\ldots (2)$$

Defining

$$\lambda' = \frac{N(O_2^+)}{N_e} \quad \ldots\ldots (3)$$

the effective recombination coefficient α, defined by $dN_e/dt = Q - \alpha N_e^2$, is

$$\alpha = \lambda' \alpha_d \quad \ldots\ldots (4)$$

Thus dissociative recombination focuses attention on the positive molecular ion to electron ratio λ', in contrast to the theory based on ion-ion recombination in which attention is focused on the negative ion ratio λ,

$$\lambda = \frac{N^-}{N_e} \quad \ldots\ldots (5)$$

with N^- the negative ion concentration.

It is the consensus of opinion [1,14] that in the E-layer, $\alpha = 1 \times 10^{-8}$ cc/sec, very nearly independent of pressure, time of day, or electron density. Since α_d should not depend on pressure or electron density, equation (4) implies a similar independence for λ'. Laboratory studies [2] of recombination between He_2^+ and electrons have yielded the only measurements in which the recombining ion has been identified as diatomic. Here a coefficient $\alpha_d = 1.7 \times 10^{-8}$ cc/sec is observed at $T = 300°$ K. Measurements of recombination in oxygen [3] yield values of the order of 10^{-7} cc/sec at low pressures, but the identity of the recombining ion (that is, O_2^+ , O_3^+ , etc.) has not been established. Thus the laboratory results are not inconsistent with a value $\alpha_d \simeq 10^{-8}$ cc/sec in the ionosphere, which would imply that $\lambda' \simeq 1$. As explained below, there are strong reasons for believing the value of λ' actually is close to unity. Consequently, when dissociative recombination is included, the observed recombination coefficient in the E-layer is, if anything,

too small judging from the laboratory results, rather than too large as is the difficulty [1] when the theory of the layer is developed without dissociative recombination.

II—THE POSITIVE MOLECULAR ION RATIO

The investigation of the daytime and nocturnal behavior of λ' can be simplified by assuming the number of negative ions is negligibly small during the day and night. With this assumption, which is discussed in Section III, O^+ is created solely by photo-ionization

$$O + h\nu \rightarrow O^+ + e \quad \ldots\ldots\ldots\ldots\ldots\ldots\ldots\ldots (6)$$

and, in the absence of negative ions, is destroyed solely by the charge transfer reaction

$$O^+ + O_2 \rightarrow O_2^+ + O \quad \ldots\ldots\ldots\ldots\ldots\ldots\ldots\ldots (7)$$

Radiative recombination and dielectronic recombination of electrons with O^+ occur far too slowly [1] to account for the observed recombination coefficient α. Consequently,

$$\frac{dN(O^+)}{dt} = Q_1 - \gamma N(O^+)N(O_2) \quad \ldots\ldots\ldots\ldots\ldots\ldots (8)$$

where Q_1 , $\gamma N(O^+)\ N(O_2)$ are the rates of equations (6) and (7), respectively. At all times the layer is essentially neutral, that is,

$$N(O_2^+) + N(O^+) = N_e + N^- \quad \ldots\ldots\ldots\ldots\ldots\ldots (9)$$

It can now be argued, as do Massey and Burhop [7], that the daytime value of λ' is very nearly unity. From equations (8) and (9), with N^- assumed to be zero, the equilibrium daytime value of λ' is

$$\lambda' = 1 - \frac{Q_1}{\gamma N_e N(O_2)} \quad \ldots\ldots\ldots\ldots\ldots\ldots\ldots\ldots (10)$$

The marked [5, 6] altitude dependence of the molecular oxygen concentration $N(O_2)$ implies by equation (4) that α will be markedly pressure dependent, contrary to observation, unless the second term in equation (10) is small compared to unity. Since α does not vary appreciably in a 24-hour period, it can be concluded also that the nocturnal value of λ' is close to unity.

It is observed that the nocturnal values of N_e obey the equation

$$(N_e)_t = \frac{1}{\frac{1}{(N_e)_o} + \alpha t} \quad \ldots\ldots\ldots\ldots\ldots\ldots\ldots\ldots (11)$$

which is the integral of

$$\frac{dN_e}{dt} = -\alpha N_e^2 \quad \ldots\ldots\ldots\ldots\ldots\ldots\ldots\ldots (12)$$

with α constant. Time t is measured from nightfall, and the subscripts t, o indicate, respectively, values at time t and just before sunset. Assuming, as justified below, that $N(O_2)$ is approximately constant during the night, then equation (9) again with $N^- = 0$, equation (8) with $Q_1 = 0$, and equation (11) yield

$$(\lambda')_t = 1 - \frac{N(O^+)_t}{(N_e)_t} = 1 - [1 - (\lambda')_o][1 + \alpha(N_e)_o t]e^{-\gamma N(O_2)t} \quad \ldots\ldots (13)$$

Equation (8) is essential to the dissociative recombination theory. Since equation (11) is experimentally verified, and equation (9) is certainly true, equation (13) can be false only if equation (8) [which is used to deduce equation (13)] is false. We consider the observations of equation (11) good enough to rule out a variation in α exceeding a factor of two. It follows, recalling equation (4), that the variation in λ' predicted by equation (13) can at most equal a factor of two, if the dissociative recombination theory is to be valid.

The maximum electron density in the E-layer is not very altitude dependent; a representative value [1] is $(N_e)_o = 1.5 \times 10^5$ e/cc. Consequently, if $\gamma N(O_2)t > 10$, the exponential term in equation (13) will be negligible by the end of a 12-hour night (4.3×10^4 sec), thereby implying $(\lambda')_t \simeq 1$, independent of the value of $(\lambda')_o$. The rate of charge transfer $\gamma = \sigma_c \bar{v}$, where σ_c is the cross-section for charge transfer, equation (7), and $\bar{v}$ is the mean relative velocity for O^+ and O_2, $\simeq 10^5$ cm/sec at 500° K. At 110 km, $N(O_2)$ cannot be much less [5, 6] than 10^{11} per cc. Thus, at this altitude, $\gamma N(O_2)t > 10$ implies $\sigma_c > 2.3 \times 10^{-20}$ cm^2. Massey and Burhop [7] consider 10^{-17} cm^2 a reasonable estimate of σ_c, an estimate the order of magnitude of which appears justified by the measurements of Hasted [9]. At 120 km, where $N(O_2)$ is close to 10^9 cc^{-1}, $\sigma_c > 2.3 \times 10^{-18}$ cm^2 guarantees $(\lambda')_t = 1$ at the end of the night. Equation (13) predicts, therefore, that by morning $(\lambda')_t \simeq 1$, independent of the sunset value $(\lambda')_o$, at E-layer altitudes up to and even above 120 km, unless σ_c is appreciably less than 10^{-17} cm^2.

At an altitude of 110 km, the increase in λ' predicted by equation (13), from $(\lambda')_o$ at sunset to$(\lambda')_t \simeq 1$, takes place in an interval too short to be observable. At 120 km and above, however, with $\gamma = 10^{-12}$, the time constant $[\gamma N(O_2)]^{-1}$ of equation (13) exceeds 1,000 seconds and furthermore, because of the factor $[1 + \alpha(N_e)_o t]$, $(\lambda')_t$ just about equals $(\lambda')_o$ at $t = 1{,}000$ seconds. Thus it must be true that $1/2 < (\lambda')_o \leq 1$; otherwise equation (13) predicts a change in λ' of more than a factor of two during an observable interval, at altitudes $\geq$ 120 km. Unless $(\lambda')_o$ is very close to 1, a value of γ much less than 10^{-12} in equation (13) makes the nocturnal variation of λ' even more marked. Moreover, in further contradiction to observation, it predicts λ' is altitude dependent at the end of the night.

In summary, consistency of the nocturnal observations of N_e with the dissociative recombination theory requires that γ be not much less than 10^{-12} cc/sec, and that $(\lambda')_o \simeq 1$. It is noteworthy that this conclusion concerning $(\lambda')_o$ is obtained solely from considerations of the nocturnal dependence of N_e, and in no way appeals to the daytime observations. Of course, once it is granted that α is approximately constant over a 24-hour period, the argument following equation (10) can be inverted. Namely, having justified $\lambda' \simeq 1$ at the end of the night, it follows immediately that $\lambda' \simeq 1$ during the day. The above analysis demonstrates, however,

that the correctness of the dissociative recombination theory *necessitates* approximate equality of the daytime and nocturnal values of α.

During the night, $N(O_2)$ increases at a rate of approximately $9 \times 10^{-21}[N(O)]^2$ per second, as a result of recombination of neutral oxygen atoms [6]. At 120 km, assuming [5, 6] $N(O) = 2 \times 10^{12}$, this recombination produces an additional 1.5×10^9 molecules of O_2 per cc over the course of an entire 12-hour night. This nocturnal increase in the density of $N(O_2)$ somewhat decreases the time required for λ' to become very close to unity, at altitudes of 120 km and above, but does not otherwise affect the argument based on equation (13).

III—THEORY INCLUDING NEGATIVE IONS

In the preceding Section, the number of negative ions was assumed negligible throughout the day and night. This assumption is open to question so that the arguments of the preceding Section require closer examination. At all times we may write

$$\frac{dN(O^+)}{dt} = Q_1 - \gamma N(O^+)N(O_2) - \alpha_e N(O^+)N_e - \alpha_i N(O^+)N^- \quad \ldots\ldots(14)$$

$$\frac{dN(O_2^+)}{dt} = Q_2 + \gamma N(O^+)N(O_2) - \alpha_e N(O_2^+)N_e - \alpha_i N(O_2^+)N^- - \alpha_d N(O_2^+)N_e \quad \ldots\ldots(15)$$

$$\frac{dN^-}{dt} = \eta N^\circ N_e - \rho N^- - KN^-N^\circ - \alpha_i N^+ N^- \quad \ldots\ldots(16)$$

$$\frac{dN_e}{dt} = Q_1 + Q_2 - \eta N^\circ N_e + \rho N^- + KN^-N^\circ - \alpha_e N^+ N_e - \alpha_d N(O_2^+)N_e \quad \ldots\ldots(17)$$

where $N^+ = N(O^+) + N(O_2^+)$, α_i is the mean coefficient of ion-ion recombination [1], α_e is the sum of the mean radiative and dielectronic recombination coefficients, N° is the neutral particle density, η is the mean attachment coefficient, K is the mean collision detachment coefficient, and ρ is the photo-detachment rate per negative ion per second [1]. For simplicity, the ions O^+ and O_2^+ are assumed to have the same values of α_i and α_e . Equations (14) to (17) are consistent with equation (9). From equations (16) and (17) there results the recombination law

$$\frac{dN_e}{dt} = \frac{Q}{1+\lambda} - \alpha N_e^2$$

with $Q = Q_1 + Q_2$ and

$$\alpha = \alpha_e + \frac{\lambda'}{1+\lambda}\alpha_d + \lambda\alpha_i + \frac{1}{(1+\lambda)N_e}\frac{d\lambda}{dt} \quad \ldots\ldots(18)$$

During the day, equating to zero the derivative in equation (16), and using equation (9),

$$\eta N^\circ - \lambda\rho - KN^\circ\lambda - \alpha_i\lambda(1+\lambda)N_e = 0 \quad \ldots\ldots(19)$$

Thus the equilibrium daytime value of λ satisfies

$$\lambda = \frac{\eta N^\circ}{\rho + KN^\circ + \alpha_i(1+\lambda)N_e} < \frac{\eta N^\circ}{\rho} \quad \ldots\ldots(20)$$

In other words, as is apparent from the fact that α_d does not appear in equation (16), the existence of dissociative recombination does not affect the usual analysis [1] whereby the inequality in equation (20) places an upper limit on the daytime value of λ.

Past estimates of this upper limit have assumed attachment and photo-detachment involve atomic oxygen only, *via* the inverse reactions

$$O + e \rightleftarrows O^- + h\nu \quad \ldots\ldots\ldots\ldots\ldots\ldots\ldots\ldots (21)$$

With this simplification the ratio $\eta N^\circ/\rho$ depends mainly on statistical factors, and can be confidently stated to lie between [7] about 6×10^{-3} and 7×10^{-2}, with the larger value less probable. In a recent article, Bates [8] quotes simply $\lambda < 6 \times 10^{-3}$.

It can be shown that this limit for λ is not altered by the presence of molecular oxygen in the E-layer. The attachment cross-section to atomic oxygen *via* reaction (21) is probably about equal to 10^{-22} cm^2, though a cross-section some 30 times larger cannot be ruled out [7]. Laboratory measurements [4] have indicated that the total cross-section for attachment of thermal (300° K) electrons to O_2 is also of the order of 10^{-22} cm^2. Since the concentration of O_2 is considerably smaller than that of O in the E-layer, attachment occurs mainly to atomic oxygen. Therefore, the aforementioned estimate $\lambda < 6 \times 10^{-3}$ could be seriously wrong only if the mean photo-detachment rate is much smaller than the estimated rate of equation (21), which can be seen to imply the unlikely eventuality that the total rate of detachment from O_2^- is very much smaller than the total rate of detachment from O^-, by a factor as large as 10^3 or 10^4.

From the foregoing discussion, it appears reasonable to assume that the number of negative ions is negligibly small throughout the day. However, when the sun sets, photo-detachment ceases to limit λ, so that the negative ion ratio may be expected to increase during the night.

As in the preceding Section, information concerning the nocturnal variation of λ as well as λ' is obtained from the requirement that equations (14) to (17), which are quite general, be consistent with the observation that the recombination coefficient is constant or nearly so throughout the night. During the night, equation (19) is replaced by

$$\frac{d\lambda}{dt} = \eta N^\circ - KN^\circ\lambda + (\alpha - \alpha_i)N_e\lambda - \alpha_i N_e\lambda^2 \quad \ldots\ldots\ldots\ldots (22)$$

so that the last two terms in equation (18) are given by

$$\lambda\alpha_i + \frac{1}{(1+\lambda)N_e}\frac{d\lambda}{dt} = \frac{\lambda\alpha}{1+\lambda} + \frac{\eta N^\circ - KN^\circ\lambda}{(1+\lambda)N_e} \quad \ldots\ldots\ldots\ldots (23)$$

$(1 + \lambda)N_e = N_e + N^- = N^+$ decreases during the night from its initial value of 1.5×10^5 . ηN° exceeds [7] 2×10^{-3}. Consequently, $KN^\circ\lambda$ must be close to ηN° during the entire interval $1{,}000 < t < 4.3 \times 10^4$; otherwise variations in α by more than a factor of two should be noticeable during the night. Moreover, since as will be argued below $N(O^+) \ll N(O_2^+)$, implying $\lambda' = 1 + \lambda$ in equation (18), it follows from equation (23) that λ must be <1, to keep the nocturnal

value of α near its daytime value α_d. It is necessary, therefore, that $KN^\circ > 2 \times 10^{-3}$ in order that $KN^\circ\lambda \simeq \eta N^\circ$. Here N° means $N(O)$; in the E-layer, collisions with neutral molecular oxygen or nitrogen do not result in detachment [1]. At 120 km, where $N(O) \simeq 2 \times 10^{12}$, the above inequality implies $K > 10^{-15}$ which, while a large value of K, is not unreasonable [1]. The present condition, $KN^\circ > \eta N^\circ$, may be compared with the condition $KN^\circ \gg \rho$ which is required to insure pressure independence of the daytime value of α in the theory based on ion-ion recombination. Since ρ is much larger than ηN°, as demonstrated by the small limit of λ resulting from equation (20), the present condition is seen to be much less restrictive.

We next proceed to demonstrate that $\lambda'/(1 + \lambda)$ in equation (18) is always close to unity during the night. Defining $\mu = N(O^+)/N(O_2^+)$, equations (14) and (15) imply

$$\frac{d}{dt} \log \mu = -\gamma N(O_2)(1 + \mu) + \alpha_d N_e \quad \ldots\ldots\ldots\ldots\ldots\ldots (24)$$

In equation (24) the terms involving α_i and α_e have disappeared. Moreover,

$$N(O^+) + N(O_2^+) = (1 + \mu)N(O_2^+) = N_e + N^- = (1 + \lambda)N_e$$

so that

$$\frac{\lambda'}{1 + \lambda} = \frac{1}{1 + \mu} = 1 - \frac{1}{1 + \lambda} \frac{N(O^+)}{N_e} \quad \ldots\ldots\ldots\ldots\ldots\ldots (25)$$

The first equality of equation (25) shows that the second term in equation (18) is independent of α_i and α_e, and can be evaluated with these coefficients equal to zero in equations (14) to (17). With $\alpha_i = \alpha_e = 0$, equation (14) reduces to equation (8). Since $\lambda < 1$, comparison of equations (13) and (25) shows that the conclusions based on equation (13) are modified only slightly by including negative ions. If anything, the increase in λ during the night causes the nocturnal value of α to be larger and closer to α_d than in Section II, while simultaneously $1 - (\lambda')_o$ may be somewhat larger, by a factor <2, than previously permitted. These conclusions have been based on the assumption that α_i is the same for both O^+ and O_2^+, and α_e is unimportant. However, at 120 km, with $\gamma N(O_2) = 10^{-3}$, and α_i as large as 10^{-7}, $\alpha_i N^- < \gamma N(O_2)$ in equations (14) and (15) if $N^- \lesssim 10^4$. Since $\lambda < 1$, N^- obeys this condition for most of the night (at $t = 4.3 \times 10^4$, $N_e = 2.3 \times 10^3$), and therefore these conclusions will not be modified significantly by a more accurate analysis which takes into account the differences in the ion-ion recombination rates for O^+ and O_2^+.

It may be noted that equation (22) is a Riccati equation for λ which, because of the form of equation (11), can be solved by standard methods in terms of confluent hypergeometric functions [10]. Thus the time dependence of λ is determinable for arbitrary values of K and α_i. However, in view of the present uncertainties in the values of these coefficients, more detailed calculations than those given in this Section are not warranted at this time.

IV—SUMMARY AND CONCLUSIONS

The presumed validity of the observations, (1) that the daytime value of the apparent recombination coefficient, α, is practically independent of pressure,

time of day, or electron density, and (2) that the nocturnal variation of the electron density N_e obeys equation (11), with α nearly equal to its daytime value, implies restrictions on the possibility that dissociative recombination [equation (2)] can explain the observed magnitude of α. These restrictions may be summarized as follows:

(*a*) The ionospheric α must turn out to be close to the laboratory value (at the same temperature) of the coefficient α_d of the reaction (2). A difference of more than a factor of two between α and α_d should probably be considered a serious discrepancy. This situation contrasts with the theory based on ion-ion recombination, in which event α can differ by large factors from the ionic recombination coefficient [1], depending on the value of the negative ion to electron ratio λ.

(*b*) The ratio μ of O^+ to O_2^+ concentrations must be small, day and night, which in turn implies the ratio $\lambda'/(1 + \lambda)$ must be close to unity, day and night, with λ' the concentration ratio of O_2^+ to electrons.

(*c*) The rate γ of the charge transfer reaction (7) cannot be much less than 10^{-12} cc/sec. These restrictions have been deduced previously [7] from observation (1) above. It appears to be a new result that they are also implied by the nocturnal observations (2).

(*d*) In addition, the observed nocturnal variation of N_e implies that $\lambda < 1$ during the night. The daytime value of λ is limited to small values by photo-detachment, irrespective of other processes, as previously known [7]. At sunset, photo-detachment ceases and λ increases, at least for a time, its maximum value depending on the relative values of the ion-ion recombination coefficient α_i, the collision detachment coefficient K, and the attachment rate β.

(*e*) In any event, λ must be close to $\eta N^\circ/KN^\circ$ during the observable portion of the night, with N° the density of oxygen atoms. Since $\lambda < 1$, this implies $KN^\circ > \eta N^\circ$. This is considerably less restrictive than the inequality $KN^\circ \gg \rho$, where ρ is the photo-detachment rate per negative ion per second, which is needed to keep α independent of pressure when ionic recombination is assumed to dominate.

(*f*) Evidently, measurements of the various reaction rates involved in the theory are urgently needed, particularly an improved measurement of the dissociative recombination coefficient α_d. From laboratory studies we do not expect that α_d is smaller than 10^{-8}, consequently the ionospheric value $\alpha = 10^{-8}$ is as small as possible for consistency with dissociative recombination.* Examination of

*It may be noted that our conclusions have not required the assumption that O_2^+ is formed principally by charge transfer. The argument of Section II rests solely on the validity of equation (8), which describes the destruction of O^+, and is not concerned with other mechanisms for forming O_2^+. In the more accurate treatment of Section III, Q_2 denotes the total rate of formation of O_2^+ by processes other than charge transfer. Presumably, Q_2 results predominantly from photo-ionization, including pre-ionization. However, in Section III the only assumption concerning Q_2 was the reasonable one that $Q_2 = 0$ during the night. In other words, our discussion has been concerned primarily not with the sources of electrons in the *E*-layer, but with considerations involving the rates of electron destruction. In conclusion (c) above, we have assumed additionally that there is a non-negligible rate of formation of O^+. Should $Q_1 = 0$ in equation (10), implying negligible O^+ formation, electrons arise primarily from ionization of O_2. These electrons must eventually recombine with O_2^+. In this event, no conclusions concerning the rate of charge transfer can result, and, in fact, in Section II, if $Q_1 = 0$, $\lambda' = 1$ day or night, independent of the value of γ.

the preceding Sections shows that if anything the daytime value of α will be less than its nocturnal value, with the daytime value definitely less than α_d , whereas the nocturnal value may exceed α_d . For this reason, a somewhat larger value of α would be desirable. Piddington [11] has argued, from analysis of the time dependence of N_e during eclipses, that the value of α should be as high as 10^{-7}. We do not place any special credence in Piddington's conclusion, but point to it as evidence that the nocturnal value of α (to which eclipse observations correspond) may still be an open question. Baral and Mitra [12] report that the value of α over Calcutta is definitely greater at night, which is in agreement with our conclusions. However, they find $10^{-9} < \alpha < 2 \times 10^{-9}$ cc/sec, which disagrees with measurements of other observers.

Finally, if dissociative recombination is responsible for the observed value of α, calculations assuming a temperature dependence of the form $\alpha = (T/T_0)^{-r}$, with $r \sim 1$, as have been made by Mitra [13] and others, appear somewhat unrealistic, since the temperature dependence of dissociative recombination need not be of this form. Mitra justifies the relation $\alpha = (T/T_0)^{-1}$ through $\alpha = \lambda\alpha_i$, based on the theory of ionic recombination, with $\lambda = \beta/KN^e$, and assuming β inversely proportional to temperature. This argument does not apply if electrons are destroyed mainly by dissociative recombination.

References

[1] D. R. Bates and H. S. W. Massey, The basic reactions in the upper atmosphere I and II, Proc. R. Soc., A, **187**, 261-296 (1946), and A, **192**, 1-16 (1947).

[2] M. A. Biondi and S. C. Brown, Measurements of ambipolar diffusion in helium, Phys. Rev., **75**, 1700 (1949). Identification of the ion responsible for the recombination in the helium afterglow was made by A. V. Phelps and S. C. Brown, Positive ions in the afterglow of a low pressure helium discharge, Phys. Rev., **86**, 102 (1952).

[3] M. A. Biondi and S. C. Brown, Measurement of electron-ion recombination, Phys. Rev., **76**, 1697 (1949). M. A. Biondi and T. Holstein, Concerning the mechanism of electron-ion recombination I and II, Phys. Rev., **82**, 962 (1951), and **83**, 1078 (1951).

[4] M. A. Biondi, Attachment of thermal electrons in oxygen, Phys. Rev., **84**, 1072A (1951).

[5] R. Penndorf, The vertical distribution of atomic oxygen in the upper atmosphere, J. Geophys. Res., **54**, 7-38 (1949).

[6] H. E. Moses and Ta-You Wu, Self-consistent calculation of the dissociation of oxygen in the upper atmosphere, Phys. Rev., **83**, 109-121 (1951), and **87**, 628-632 (1952).

[7] H. S. W. Massey and E. H. S. Burhop, Electronic and ionic impact phenomena, London, Oxford University Press, 641 ff. (1952).

[8] D. R. Bates, Ionization and recombination in the upper atmosphere, Proceedings of the Conference on Ionospheric Physics (July 1950), Part A, Geophysics Research Division, Air Force Cambridge Research Center, Cambridge, Mass., 225-234 (April 1952).

[9] J. B. Hasted, The exchange of charge between ions and atoms, Proc. R. Soc., A, **205**, 421-438 (1951).

[10] E. Kamke, Differentialgleichungen, New York, Chelsea Publishing Co., Vol. 1, 22 and 427 (1948).

[11] J. H. Piddington, The modes of formation of the ionized layers, J. Geophys. Res., **56**, 409-429 (1951).

[12] S. S. Baral and A. P. Mitra, Ionosphere over Calcutta, J. Atmos. Terr. Phys., **1**, 95-105 (1950).

[13] A. P. Mitra, Effects of the variations of recombination coefficient, Indian J. Phys., **26**, 79-102 (1952).

[14] S. K. Mitra, The upper atmosphere, Calcutta, Asiatic Society of Bengal, 2nd ed., Chap. 6 (1952).

THE PHYSICAL BASIS OF FIELD PHENOMENA

BY GUSTAVE R. HOLM

4849 West Belden Avenue, Chicago 39, Illinois

(Received January 16, 1953)

ABSTRACT

This article seeks to extend further the views which served as a basis for my article "Gravitation and gyromagnetism," in the December 1952 issue (Vol. 57, No. 4) of this JOURNAL. Instead of attempting to explain phenomena in space in terms of many independent hypotheses, it seems simpler and more logically satisfying to assign the known physical characteristics to a single basic structure, explaining all field phenomena, including radiation, in terms of this one structure. Most of the mathematical relations are well established and are not considered in detail here. The purpose is rather to show the application of the basic concepts, deriving a physical structure to complement and interpret the known mathematical relations.

Among the many views on field phenomena which have been proposed, the theories which have sought to describe the physical background of field phenomena have in general proved inadequate to account for the mathematical relations involved, while the mathematical theories have not attempted to set up a descriptive physical background. There is a wide gap between the two viewpoints, and it is a fundamental problem of physics to bring the two closer together. The approach here outlined is designed to do just this.

Very successful theories have been developed which deal primarily with the two basic concepts of space and time, and with the coordinate systems usefully applicable to them. Still a universe fashioned of space and time alone must remain a mathematical abstraction, empty and uneventful, devoid of physical content. A third basic concept, that of energy, is needed to give physical content to our universe and to the events which compose it.

We live in a changing world. Science is concerned with our attempts to observe, measure, compare, and interpret the changes taking place about us. The measurement and comparison of unchanging things offer little difficulty. Our problem lies rather in the determination of what to regard as unchangeable. It is here that the principle of Conservation of Energy may serve as our starting point, as we require an unchanging aspect of changing things before we can form a basis for physical equations.

The energy concept provides us with a consistent quantitative measure of the changes taking place within our framework of time and space. It is a meeting

point of constancy and change, a basic measure of change which is itself unchanging, a criterion of description in terms of which we may equate cause and effect. The principle of Conservation of Energy makes ENERGY our fundamental invariant, but it imposes no limitation on the forms which energy may take; it specifies only that the measure of one form be consistent with that of another.

The absence of a simple, consistent physical theory has left the application of this principle to the field problem somewhat obscure. Such a principle provides only a passive, unchanging factor, and does not of itself serve to originate or explain field phenomena. We need a second principle to complement it, to serve as an active motivating basis. Energy does manifest another characteristic which appears equally general and fundamental. Energy always seeks a level, seeks uniformity, symmetry. Differences of level, potential, temperature, etc., tend to equalize. The principle involved here can be regarded as a generalization of the second law of thermodynamics. It includes that law and the usual equipartition laws. It implies a trend toward equality, uniformity, applicable to field energy, and might be referred to as a Principle of Symmetry; the word symmetry seems suitable for denoting such equal measure. As the principle of conservation of energy symbolizes the reversible aspect of nature, so does the principle of symmetry symbolize the irreversible aspect.

The principle implies that the bulk of energy in the field is symmetrical and produces no observable effect at the ordinary scale of magnitude. Field energy attains most complete symmetry in regions remote from matter. In such regions the energy forms a uniform, isotropic structure. If we specify three coordinate axes, the energy will be equally divided between them. If we further subdivide the energy into energy of linear motion and energy of rotational motion, these components will also be equal.

To account for observable field phenomena we presume that modifications of this basic structure are possible. Observed forces originate in small modifications of the basic symmetrical pattern. Energy differences associated with individual field components give us the group of phenomena designated as "electromagnetic." This group manifests polarity, that is, changes can either add to or subtract from the normal field background. The three components associated with the energy of linear motion constitute the electric field, the components associated with the energy of rotational motion constitute the magnetic field. Thus an electric charge modifies the energy of linear motion along radial lines in the region about the charge. If the charge is in motion we also have differences in rotational energy, the curl of a vector potential, a magnetic field.

The bulk of the mass or energy of matter which does not manifest electromagnetic attributes maintains a high degree of isolation and produces only a small, indirect modification of our field. This effect, gravitation, is associated with differences in total density of field energy, affecting all six components equally. In a gravitational field the local, small-scale symmetry of our field structure is maintained to a high approximation; the flux of gravitation is distributed equally among the six field components.

For stationary states the forces of the field satisfy the simplest law of symmetry, the inverse square law. More generally we must take propagation into account. Our description then may take the form of retarded potential functions. These

satisfy a characteristic "equation of propagation" which leads directly to the Maxwell field equations. To describe the electromagnetic field we need only assign potential functions satisfying equations of propagation and continuity in free space; the small-scale discontinuity of the field is disregarded in these equations.

The Lorentz transformation has the same structural form as the equation of propagation and depends on the same physical fact, namely, the existence of a basic velocity c associated with the energy of our field background, and also with the intrinsic energy of a localized entity. The Lorentz transformation relates these two patterns of energy; it is the energy concept which gives direct physical significance to this transformation law.

Since we are regarding the field as a physical reality, the term "absolute motion" has a meaning, albeit a more subtle and elusive one than in the concept of a stationary ether. In describing motion we may conveniently make use of the concept of "lines of symmetry." In regions of space remote from matter, any line at rest with respect to our basic symmetrical pattern is a line of symmetry. These lines form a single reference system in such regions, at least approximately uniform over vast distances. In a region containing a concentration of matter at rest with respect to our basic pattern, the lines of symmetry are simply radial lines. Matter in motion includes directional energy in conjunction with the symmetrical energy which the matter would possess at rest. In a symmetrical field this directional energy is maintained unchanged, and we may interpret Newton's first law as a direct consequence of the principle of conservation of energy. Mass or total energy content is not in general a simple scalar quantity, although the approximation is adequate for low velocities, with momentum and kinetic energy evaluated specifically; such a separation is not valid at high velocities.

In the vicinity of matter in motion we have a shifting of the lines of symmetry of the field, since the energy of the moving pattern tends to remain symmetrical within itself. We cannot extend lines of symmetry unbroken from remote regions of space to concentrations of matter in motion, but must consider a transition region, where we can still picture these lines locally. The exact solution of this problem requires a detailed interpretation of small-scale structure, but it seems obvious at once that the extent of a transition region is related to the amount of matter in motion. For small portions of matter such a region is effectively confined within molecular dimensions. The field here shows no analogy to the traditional ether, no hint of frictional forces or the long-sought "ether drag."

In a region of space at the earth's surface, we have vertical lines of symmetry moving with substantially the same speed as the earth's surface. Our field structure is symmetrical with respect to these lines except for rotation; the principle of symmetry does not operate to cancel out this component. We have direct internal evidence of the earth's rotation, such as the Foucault pendulum and the earth's magnetic field. In contrast, effects associated with translation are difficult to detect, but not necessarily beyond the border line of the observable.

When we deal with phenomena on a very small scale, evidences of finite discontinuity in our field structure begin to appear. The general laws of the field are of the nature of statistical laws, representing the summation of a myriad complexity of motions and actions. These laws do not determine the detailed pattern

of our field energy but are in fact quite independent thereof. The customary potential functions express statistical net results and are a valid mathematical device for this purpose. These quantities have the form of continuous functions and suggest that we are regarding the field as a continuous structure, but we have no reason to assume *a priori* that the field structure is actually continuous. A continuous field structure would imply a region in which no changes whatever are taking place, that is, a region of zero energy. Field quantities serve rather to express resultant energy differences directly; they are in fact defined in terms of such energy differences.

Time and space in the philosophical sense cannot be regarded as discontinuous, but time and space in the physical sense, in the sense of serving as a physical field background, can and must be regarded as possessing a discontinuous aspect. This does not require us to assign any profound and mystical discontinuity to these concepts; rather, the quantum may be regarded as an intrinsic part of a small-scale physical process present at all times and places. General physical laws are extended to phenomena on an atomic scale only with the aid of Planck's constant as the connecting link. This constant is a measure of the basic discontinuity in our field. It not only plays a part in the structure of the atom, and in all phenomena on a similar scale of magnitude, but it is basic to the very existence of the electron. The field here serves as a matrix in time and space through which small-scale phenomena are sifted.

It is not necessary to regard either wave length or frequency as an intrinsic attribute of an individual photon; the concept of wave length belongs to the statistical distribution of a group of photons. A photon is not an entity in itself but rather a transient modification of the normal field pattern in space, a quantity of momentum (energy) transmitted as a unit through the field. The photon partakes of the velocity of the field in the direction of propagation, while transversely its structure involves a displacement from the normal symmetry of the field, an aspect symbolized by a vector perpendicular to the propagation. The velocity of light in any region of space is characteristic of the field in that region, and can have no dependence on any observer. This velocity will be symmetrical under symmetrical conditions, that is, with reference to the "lines of symmetry" of the field in any region. The result of the Michelson-Morley experiment is in accord with this; any motion of our lines of symmetry with respect to the earth would be very small, even at a short distance from the earth's surface.

The phenomenon of aberration is significant here. Aberration involves a modification in the propagation of a photon as it enters the field of our moving earth. The photon acquires a component of momentum with respect to our moving field pattern which it did not possess with respect to the remote field. The photon in a remote region may be described as having a direction "A" in the field in that region. The photon as it enters the observer's telescope may be described as having a direction "B" in the moving field pattern in that region, the difference in the directions "A" and "B" constituting our angle of aberration. The two descriptions are *not* equivalent, in spite of the fact that the direction of propagation remains unchanged with respect to the remote field. The remote field pattern no longer plays a part in the process of propagation, and cannot be correctly used in its

description. In other words, we are to regard the propagation of a photon as a local phenomenon at any instant, and its motion is to be described only with reference to the local field at that instant. Velocity at intermediate points, while not directly observable, is not essential to the problem. When the photon reaches the observer's telescope, it has a definite direction with respect to the field in this region. If we change the velocity of the photon at this point, by filling our telescope with water or in any other manner (the Airy experiment), no further alteration in direction occurs.

To summarize: We have here assumed the existence of a single basic field structure in space, modified to produce observable field phenomena. Electric, magnetic, and gravitational fields are no longer regarded as independent physical concepts; they become simply classifying names for specific types of energy differences in space. The quantum constant forms an intrinsic part of the same structure, directly accounting for both the wave and particle attributes of radiation. Our description is expressed in terms of three physical concepts—space, time, and energy; these three are necessary and sufficient for our purpose.

JOURNAL OF GEOPHYSICAL RESEARCH VOLUME 58, NO. 3 SEPTEMBER, 1953

OPTIC AXES AND CRITICAL COUPLING IN THE IONOSPHERE*

BY NORMAN DAVIDS

Ionosphere Research Laboratory, The Pennsylvania State College, State College, Pennsylvania

(Received February 2, 1953)

ABSTRACT

Critical coupling arises when, for a certain critical $N = N_c$ and $\nu = \nu_c$ the coupling factor, which measures the degree of interaction between the ordinary and extraordinary modes, becomes infinite. Instead of attempting to solve the standard coupled wave equations at or near this singularity, a different reference system is introduced based on the principal directions of the three-dimensional dielectric ellipsoid. These directions depend only on the direction of the earth's field, and are thus essentially constant over the ionosphere.

Analogy with crystals, as pointed out by Lange-Hesse, suggests the possibility of optic axes in the ionosphere. It is shown here that such axes can exist in the presence of collisions and that this is precisely the condition for critical coupling. The ionosphere acts isotropically at such a level, with no principal modes being singled out. Some application to data at 150 kc/sec is made.

INTRODUCTION

The doubly-refracting propagation characteristics of the ionosphere suggest an analogy with similar behavior in crystals. The extent of this analogy has been discussed by various writers [see 1, 2, and 9 of "References" at end of paper]. Of special interest is the question of "optic axes." These are preferred directions in a crystal along which the principal indices of refraction become equal—that is, the medium acts isotropically for these directions and there is no longer a distinction between ordinary and extraordinary modes.

In this work we shall show that optic axes can exist in the ionosphere—a condition for such axes, surprisingly enough, is the presence of damping collisions between electrons and heavy particles. We shall also show how these axes shed new light on the "coupling problem," which is to determine the degree of interaction between the ordinary and extraordinary modes—mathematically to solve the coupled wave equations. For the ionosphere models of interest, the difficulty encountered at low frequencies is that, especially under night-time conditions, the coupling (as measured by a parameter appearing in the differential equations) attains a sharp, narrow peak when plotted as a function of height and, indeed, becomes infinite for a certain critical value of electron density N and collision

*The research reported in this paper has been supported by the Geophysics Research Division of the Air Force Cambridge Research Center under Contract AF 19 (122)-44.

frequency ν. This effect appears to be of practical interest since these critical values are believed to be approached, if not actually attained, under certain conditions of ionospheric propagation. It seems difficult to interpret this coupling singularity as being analogous to a resonance effect since, as will be shown, it requires damping for its occurrence.

We shall show that the coupling singularity conditions for N and ν are precisely those which make the direction of wave propagation (here assumed vertical) an optic axis.

Unlike the usual approach in [3], which seeks an apparent simplification by eliminating the z-component of the electric field, thereby two-dimensionalizing the problem, our approach is to retain this wave component and seek the principal axes of the three-dimensional dielectric tensors. This leads to several advantages, notably their directions are independent of the ionospheric model and do not undergo the rapid fluctuations with height as do the conventional polarizations near the coupling singularity.

I. THE MAGNETO-IONIC FORMULAS

The basic equations of the magneto-ionic theory have been treated in detail by many authors; see for instance [3], [4], [5]. We shall, however, briefly note some of the required fundamentals.

The displacement $\mathbf{r}$ of an electron in an ionized medium under the influence of an electric field $\mathbf{E}$ and magnetic field $\mathbf{H}_0$ is given by the equation of motion

$$m\ddot{\mathbf{r}} = -e\mathbf{E} - m\nu\dot{\mathbf{r}} - (e/c)(\dot{\mathbf{r}} \times \mathbf{H}_0) \quad \ldots\ldots\ldots\ldots\ldots\ldots (1.1)$$

(For explanation of symbols, see Table of Notations, Section VII.) We choose a right-handed system of coordinate axes with positive x in the direction of magnetic east, y magnetic north, and z vertically upward. If we then suppose all varying quantities to contain the time in the form $\exp(i\,\omega\,t)$ and introduce the polarization vector through the relation $\mathbf{P} = Ne\mathbf{r}$, we obtain from (1.1) the linear vector relationship

$$\begin{bmatrix} E_x \\ E_y \\ E_z \end{bmatrix} = -4\pi \begin{bmatrix} \frac{\omega^2}{\omega_0^2}\left(1 - i\frac{\nu}{\omega}\right) & -i\gamma_L & i\gamma_T \\ i\gamma_L & \frac{\omega^2}{\omega_0^2}\left(1 - i\frac{\nu}{\omega}\right) & 0 \\ -i\gamma_T & 0 & \frac{\omega^2}{\omega_0^2}\left(1 - i\frac{\nu}{\omega}\right) \end{bmatrix} \begin{bmatrix} P_x \\ P_y \\ P_z \end{bmatrix} \quad \ldots\ldots (1.2)$$

or, abbreviated,

$$\mathbf{E} = \lambda\mathbf{P} \quad \ldots\ldots\ldots\ldots\ldots\ldots\ldots\ldots (1.3)$$

where we call λ the "polarization tensor." By introducing the dielectric displacement vector $\mathbf{D} = \mathbf{E} + 4\pi\mathbf{P}$, we can obtain the equivalent relation, familiar in electrostatics,

$$\mathbf{D} = \varepsilon\mathbf{E} \quad \ldots\ldots\ldots\ldots\ldots\ldots\ldots\ldots (1.4)$$

where ε is the dielectric tensor.

Maxwell's equations for the wave field are given by

$$\left.\begin{aligned} \operatorname{curl} \mathbf{H} &= \frac{1}{c}\dot{\mathbf{D}} \qquad \operatorname{div} \mathbf{D} = 0 \\ \operatorname{curl} \mathbf{E} &= -\frac{1}{c}\dot{\mathbf{H}} \qquad \operatorname{div} \mathbf{H} = 0 \end{aligned}\right\} \quad \ldots\ldots\ldots\ldots\ldots\ldots (1.5)$$

If we assume the ionosphere, as well as the incident wave-front, to be horizontally stratified (that is, all quantities vary with z only), and neglect any constant electric fields, these equations reduce to

$$\left.\begin{aligned} E_x'' + \frac{\omega^2}{c^2}(E_x + 4\pi P_x) &= 0 \\ E_y'' + \frac{\omega^2}{c^2}(E_y + 4\pi P_y) &= 0 \end{aligned}\right\} \quad \ldots\ldots\ldots\ldots\ldots\ldots (1.6)$$

$$D_z = E_z + 4\pi P_z = 0 \quad \ldots\ldots\ldots\ldots\ldots\ldots\ldots\ldots (1.7)$$

where primes denote differentiations with respect to z. Note the contrast between the relationship for the z-components and the other two. From this and div $\mathbf{H} = 0$ we conclude $\mathbf{D}$ and $\mathbf{H}$ are transverse to the direction of propagation (that is, horizontal). However, $\mathbf{E}$ is not.

The relations (1.2), (1.6), and (1.7) form a system of six equations for the six unknown field components E_x , E_y , E_z , P_x , P_y , P_z .

II. THE COUPLED WAVE EQUATIONS AND CRITICAL COUPLING

The conventional approach at this point is to use the transversality condition (1.7) to eliminate the vertical components, thereby reducing the field problem to a system of four equations for the four quantities E_x , E_y , P_x , P_y . Two are differential equations and two are linear equations of the form

$$\begin{pmatrix} E_x \\ E_y \end{pmatrix} = -4\pi \begin{pmatrix} \lambda_{xx} & \lambda_{xy} \\ \lambda_{yx} & \lambda_{yy} \end{pmatrix} \begin{pmatrix} P_x \\ P_y \end{pmatrix} \quad \ldots\ldots\ldots\ldots\ldots\ldots (2.1)$$

analogous to (1.2). In order to reduce the problem still further, these linear equations are "uncoupled" by transforming to the standard ordinary and extraordinary modes $\mathbf{E}^{(1)}$, $\mathbf{E}^{(2)}$, for which we are left with only a pair of differential equations. If we introduce the polarizations $u = E_y/E_x$, and form new components by rotating* through a certain complex angle θ,

$$\pi_1 = E_x^{(1)} \cos\theta + iE_y^{(1)} \sin\theta$$

$$\pi_2 = -E_x^{(2)} \sin\theta + iE_y^{(2)} \cos\theta$$

*The representation of the principal modes by rotations in a complex space was first discussed by Saha, Banerjea, and Guha in [4]. It is also discussed by Davids in [6].

then these principal components satisfy the coupled differential equations

$$\left.\begin{aligned} \pi_1'' + \left(\frac{\omega^2}{c^2}\epsilon_1 + M^2\right)\pi_1 &= -\pi_2 M' - 2\pi_2' M \\ \pi_2'' + \left(\frac{\omega^2}{c^2}\epsilon_2 + M^2\right)\pi_2 &= -\pi_1 M' - 2\pi_1' M \end{aligned}\right\} \quad \ldots\ldots\ldots\ldots (2.2)$$

where ϵ_1 , ϵ_2 are the respective indices of refraction of the principal modes and

$$M = -i\theta' = \frac{u'}{1 - u^2} \quad \ldots\ldots\ldots\ldots\ldots\ldots\ldots\ldots (2.3)$$

We can consider M as the "coupling factor" since the equations (2.2) become uncoupled when $M = 0$. Fortunately, this is the case over all but local regions of the ionosphere so that we have essentially independent propagation of the principal modes, except in the coupling region. Here M and M' fluctuate rapidly in a small height interval, thereby making standard approximation techniques difficult for handling the equations (2.2).

The singular limiting case occurs when the polarization $u = \pm 1$. Since u satisfies the quadratic relation

$$u^2 + 2iu\delta_u + 1 = 0 \quad \ldots\ldots\ldots\ldots\ldots\ldots\ldots\ldots (2.4)$$

where

$$\delta_u = \frac{\gamma_T^2}{2\gamma_L} \frac{1}{1 - \dfrac{\omega^2}{\omega_0^2}\left(1 - i\dfrac{\nu}{\omega}\right)} \quad \ldots\ldots\ldots\ldots\ldots\ldots (2.5)$$

we have, when $u = \pm 1$, $\delta_u = \pm i$, which gives, upon equating real and imaginary parts, the "critical coupling" conditions

$$\omega^2 = \omega_0^2 \qquad \nu/\omega = \mp\gamma_T^2/2\gamma_L = \mp \frac{\omega_H}{\omega} \frac{\sin^2 \theta_P}{2 \cos \theta_P} \quad \ldots\ldots\ldots\ldots (2.6)$$

We note that in the northern magnetic hemisphere the downward direction of $\mathbf{H}_0$ makes $\cos \theta_P$ negative, so that only the upper sign has physical significance; conversely in the lower hemisphere. In either case, the "critical collision frequency" is given by

$$\nu_c = \tfrac{1}{2}\omega_H \sin^2 \theta_P / \cos \theta_P \quad \ldots\ldots\ldots\ldots\ldots\ldots (2.7)$$

At State College we have $\nu_c = 5.348 \times 10^5$ sec, independent of the operating frequency. The critical electron density, for 150 kc sec, is $N_c = m\omega^2/4\pi e^2 = 278$ cc.

If there is a level at which $N = N_c$ and $\nu = \nu_c$ simultaneously, then the coupling factor M is infinite, unless N' and ν' are both zero at that point. For, since $u = 1$, we have to show that u' in (2.3) is not zero. Differentiating equation (2.4),

$$u' = -iu\delta_u'/u + i\delta_u$$

which shows that u' is infinite when $u = 1$, $\delta_u = i$ unless $\delta_u' = 0$. But this would give, from (2.5),

$$\delta_u' = \left(\frac{\gamma_T^2}{2\gamma_L}\right) \frac{2\frac{\omega}{\omega_0}\left(\frac{\omega}{\omega_0}\right)'\left(1 - i\frac{\nu}{\omega}\right) - \frac{\omega^2}{\omega_0^2}\left(-i\frac{\nu'}{\omega}\right)}{\left[1 - \frac{\omega^2}{\omega_0^2}\left(1 - i\frac{\nu}{\omega}\right)\right]^2} = 0$$

Since the denominator is not zero when $\omega_0 = \omega$, $\nu = \nu_c$, this would require, for the real and imaginary parts of the numerator to go to zero, that $N' = \nu' = 0$.

The exceptional case $N' = \nu' = 0$ leaves M indeterminate. If the medium is constant in some interval about the point, then $u' = 0$, hence $M = 0$. This situation is not of physical interest here.

We have, thus, seen that the attempt to reduce the number of independent equations is paid for by the complicated character of the differential equations near the critical coupling point. In the next section we shall discuss a geometric interpretation of this behavior.

III. THE PRINCIPAL DIELECTRIC AXES

Instead of calculating the principal axes of the two-dimensional tensor given in equation (2.1), we go back to the three-dimensional polarization tensor λ, equation (1.2). To find its principal axes, we equate to zero its secular determinant,

$$|\lambda_{ij} - \lambda\,\delta_{ij}| = (\eta - \lambda)^3 - \gamma_T^2(\eta - \lambda) - \gamma_L^2(\eta - \lambda) = 0$$

where λ is a variable and $\eta = (\omega^2/\omega_0^2)[1 - i(\nu/\omega)]$. The roots are

$$\left.\begin{aligned} \lambda_1 &= \frac{\omega^2}{\omega_0^2}\left(1 - i\frac{\nu}{\omega}\right) \\ \lambda_2 &= \frac{\omega^2}{\omega_0^2}\left[\left(1 - i\frac{\nu}{\omega}\right) + \frac{\omega_H}{\omega}\right] \\ \lambda_3 &= \frac{\omega^2}{\omega_0^2}\left[\left(1 - i\frac{\nu}{\omega}\right) - \frac{\omega_H}{\omega}\right] \end{aligned}\right\} \quad \text{.....(3.1)}$$

To find the corresponding principal directions, we substitute $\lambda = \lambda_i$ $(i = 1, 2, 3)$ in the equations

$$\lambda\mathbf{P} - \lambda_i\mathbf{P} = 0$$

Written out componentwise:

$$\begin{aligned} (\eta - \lambda_i)P_x - i\gamma_L P_y + i\gamma_T P_z &= 0 \\ i\gamma_L P_x + (\eta - \lambda_i)P_y &= 0 \\ -i\gamma_T P_x + (\eta - \lambda_i)P_z &= 0 \end{aligned}$$

If we denote by $P^{(i)}$ $(i = 1, 2, 3)$ a solution to this set of equations corresponding to the root λ_i, we have

$$\begin{aligned} P_x^{(1)} : P_y^{(1)} : P_z^{(1)} &= 0, & \sin\theta_P, & & \cos\theta_P \\ P_x^{(2)} : P_y^{(2)} : P_z^{(2)} &= i, & \cos\theta_P, & & -\sin\theta_P \\ P_x^{(3)} : P_y^{(3)} : P_z^{(3)} &= i, & -\cos\theta_P, & & \sin\theta_P \end{aligned}$$

The quantities on the right are direction numbers for the principal axes of λ. We note at once: *The first principal axis is along the direction of the earth's field.* The others are orthogonal to this direction—provided one defines orthogonality of two complex vectors **A** and **B** by the condition

$$\mathbf{A} \cdot \mathbf{B}^* = 0$$

where $\mathbf{B}^*$ is the complex conjugate of **B**. The corresponding unit vectors, expressed in terms of their x, y, and z components, are

$$\mathbf{i}_1 = (0, \sin \theta_P , \cos \theta_P)$$

$$\mathbf{i}_2 = \left(\frac{i}{\sqrt{2}} , \frac{\cos \theta_P}{\sqrt{2}} , - \frac{\sin \theta_P}{\sqrt{2}}\right)$$

$$\mathbf{i}_3 = \left(\frac{i}{\sqrt{2}} , - \frac{\cos \theta_P}{\sqrt{2}} , \frac{\sin \theta_P}{\sqrt{2}}\right)$$

all satisfying the condition $| \mathbf{i}_k |^2 = \mathbf{i}_k \mathbf{i}_k^* = 1$.

We note at once that *the directions of the principal dielectric axes depend only on that of the earth's magnetic field.* They are, thus, constant through the ionosphere where the latter can be assumed constant. However, the lengths of the axes do change, of course. We also note that the principal directions for the dielectric tensor $\boldsymbol{\epsilon}$ [see equation (1.4)] are identical with those above for λ. However, their magnitudes are determined from the relations

$$\epsilon_i = 1 - 1/\lambda_i \qquad i = 1, 2, 3 \ldots\ldots\ldots\ldots\ldots\ldots (3.2)$$

which follows from $\mathbf{D} = \mathbf{E} + 4\pi\mathbf{P}$. We then have

$$D_i = \epsilon_i E_i \qquad i = 1, 2, 3 \ldots\ldots\ldots\ldots\ldots\ldots (3.3)$$

where the subscripts denote components in the principal directions.

IV. FRESNEL'S EQUATIONS FOR THE INDICES OF REFRACTION

We shall now develop the equations for vertical propagation in terms of the principal dielectric axes just found. We first transform the differential equations (1.6) and the transversality relation (1.7) to the reference system based on the above-found principal axes. The transformation equations are

$$E_x = E_1 \cos (x, \mathbf{i}_1) + E_2 \cos (\mathbf{x}, \mathbf{i}_2) + E_3 \cos (\mathbf{x}, \mathbf{i}_3)$$

$$= - \frac{i}{\sqrt{2}} (E_2 + E_3)$$

where $\cos (\mathbf{x}, \mathbf{i}_k) = \mathbf{i}_x \cdot \mathbf{i}_k^*$, etc. Similarly

$$E_y = E_1 \sin \theta_P + (E_2 - E_3) \frac{\cos \theta_P}{\sqrt{2}}$$

$$E_z = E_1 \cos \theta_P - (E_2 - E_3) \frac{\sin \theta_P}{\sqrt{2}}$$

Equations (1.6) and (1.7) become, using also (3.3),

$$\text{(I)} \qquad (E_2'' + E_3'') + \frac{\omega^2}{c^2}(\epsilon_2 E_2 + \epsilon_3 E_3) = 0$$

$$\text{(II)} \qquad \left(E_1'' + \frac{\omega^2}{c^2}\epsilon_1 E_1\right)\sin\theta + \left[E_2'' - E_3'' + \frac{\omega^2}{c^2}(\epsilon_2 E_2 - \epsilon_3 E_3)\right]\frac{\cos\theta}{\sqrt{2}} = 0$$

$$\text{(III)} \qquad \epsilon_1 E_1 \cos\theta - (\epsilon_2 E_2 - \epsilon_3 E_3)\frac{\sin\theta}{\sqrt{2}} = 0$$

These three equations for the determination of the three field components $E_1\ E_2\ E_3$ replace the original system of equations.

In an isotropic medium with dielectric coefficient ϵ, the index of refraction is given by $n = \sqrt{\epsilon}$. We seek the extension to this relation. If an upgoing wave is propagated through a medium with index of refraction n, its variation with z is expressed by the factor $e^{-i\omega nz/c}$. Consequently, equations (I) to (III) become, after replacing d^2/dz^2 by $-(\omega^2/c^2)n^2$,

$$(\epsilon_2 - n^2)E_2 + (\epsilon_3 - n^2)E_3 = 0$$

$$(\epsilon_1 - n^2)\sin\theta\, E_1 + (\epsilon_2 - n^2)\frac{\cos\theta}{\sqrt{2}}E_2 - (\epsilon_3 - n^2)E_3\frac{\cos\theta}{\sqrt{2}} = 0$$

$$\epsilon_1\cos\theta\, E_1 - \epsilon_2\frac{\sin\theta}{\sqrt{2}}E_2 + \epsilon_3\frac{\sin\theta}{\sqrt{2}}E_3 = 0$$

For this system of linear homogeneous equations to have a solution requires that the determinant of its coefficients vanish:

$$\begin{vmatrix} 0 & \epsilon_2 - n^2 & \epsilon_3 - n^2 \\ (\epsilon_1 - n^2)\sin\theta & (\epsilon_2 - n^2)\dfrac{\cos\theta}{\sqrt{2}} & -(\epsilon_3 - n^2)\dfrac{\cos\theta}{\sqrt{2}} \\ \epsilon_1\cos\theta & -\epsilon_2\dfrac{\sin\theta}{\sqrt{2}} & \epsilon_3\dfrac{\sin\theta}{\sqrt{2}} \end{vmatrix} = 0$$

Upon expansion and dividing through by $2\epsilon_1\epsilon_2\epsilon_3$, we obtain the quadratic in n^2:

$$An^4 + Bn^2 + C = 0$$

where

$$\left.\begin{aligned} A &= \frac{1}{\epsilon_2\epsilon_3}\cos^2\theta + \left(\frac{1}{\epsilon_1\epsilon_3} + \frac{1}{\epsilon_1\epsilon_2}\right)\frac{\sin^2\theta}{2} \\ B &= -\left(\frac{1}{\epsilon_2} + \frac{1}{\epsilon_3}\right)\cos^2\theta - \left(\frac{2}{\epsilon_1} + \frac{1}{\epsilon_2} + \frac{1}{\epsilon_3}\right)\frac{\sin^2\theta}{2} \\ C &= 1 \end{aligned}\right\} \quad \ldots\ldots\ldots(4.1)$$

which, apart from sign, gives us two, in general, numerically distinct values for n.

The above equation is a special case of Fresnel's equations for anisotropic media (see Born [7], p. 224).

V. THE OPTIC AXES AND CRITICAL COUPLING

The optic axes correspond to a double root of the determinantal equation (4.1). When this occurs there are then no principal modes, and the direction of propagation is said to be an optic axis. We shall now show: *The direction of propagation (z-axis) becomes an optic axis when critical coupling occurs, that is,* $\omega = \omega_0$, $\nu = \nu_e$ [see (2.6) and (2.7)].

For, we obtain the double root for n^2 by setting the discriminant of (4.1) equal to zero. We obtain, after calculation, the equation

$$B^2 - 4AC = \left(\frac{1}{\epsilon_3} - \frac{1}{\epsilon_2}\right)^2 + \left(\frac{2}{\epsilon_1} - \frac{1}{\epsilon_3} - \frac{1}{\epsilon_2}\right)^2 \left(\frac{1}{2}\frac{\sin^2\theta}{\cos\theta}\right)^2 = 0$$

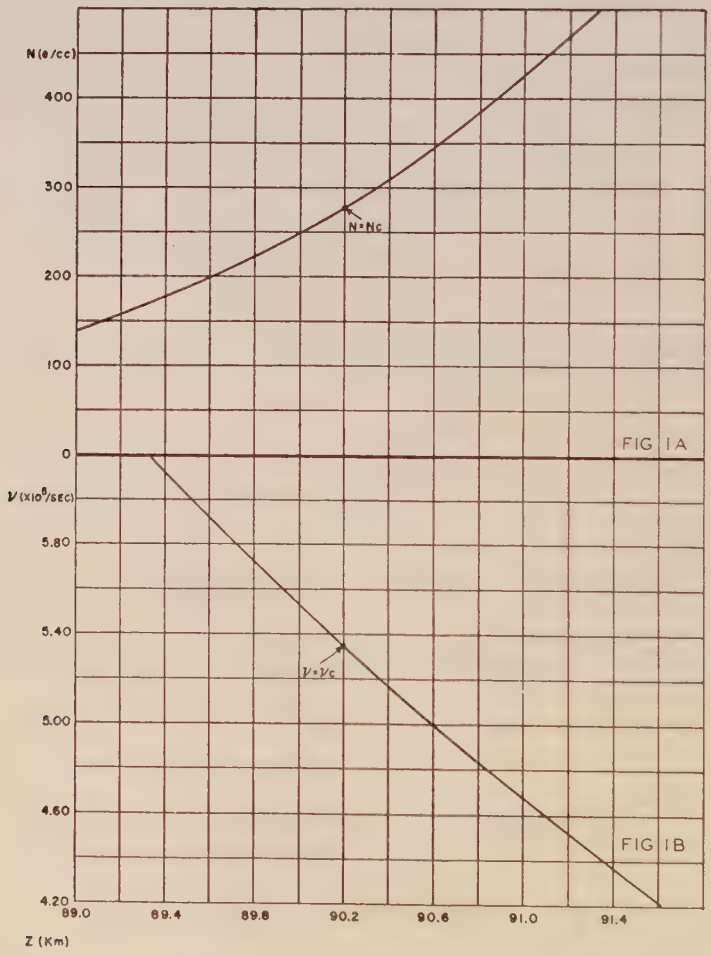

FIG. 1A—ASSUMED CHAPMANLIKE DISTRIBUTION OF ELECTRON DENSITY N FOR CRITICAL COUPLING

FIG. 1B—ASSUMED DISTRIBUTION OF COLLISION FREQUENCY ν FOR CRITICAL COUPLING

Expressed in terms of λ_i , from (3.2), and using (2.7), this equation reads

$$\frac{(\lambda_2 - \lambda_3)^2}{(\lambda_3 - 1)^2(\lambda_2 - 1)^2} + \left(\frac{2\lambda_1}{\lambda_1 - 1} - \frac{\lambda_3}{\lambda_3 - 1} - \frac{\lambda_2}{\lambda_2 - 1}\right)^2 \left(\frac{\nu_c}{\omega_H}\right)^2 = 0$$

Using the values for λ_i given by (3.1), and also putting $\omega^2 = \omega_0^2$, we have

$$\left(-\frac{2\omega\omega_H}{\nu^2 + \omega_H^2}\right)^2 + \left(\frac{2i\omega\omega_H^2}{\nu(\nu^2 + \omega_H^2)}\right)^2 \left(\frac{\nu_c}{\omega_H}\right)^2 = 0$$

When solved for ν this gives at once $\nu = \nu_c$.

VI. A NUMERICAL APPLICATION

We illustrate the above analysis by reference to a possible ionospheric distribution for conditions at our Laboratory. Figure 1*A* shows the distribution of ν as a function of height in the neighborhood of $\nu = \nu_c$. The curve for ν is based on the work of Nicolet [8]. According to this model, the critical coupling point occurs at a height of $z = 90.2$ km. In Figure 1*B* is shown a variation of electron density N which was calculated so that the critical $N = N_c = 278$/cc occurred at the same height.* Both curves are practically linear over the "coupling region."

Figure 2 shows the variation of the principal dielectric quantities ϵ_1, ϵ_2 , ϵ_3 , as given by (3.2) in this height interval. The points on each curve indicate the height in kilometers. It shows that the greatest change occurs in the direction of the axis oriented along the earth's field. The rate of change along this axis, with height, is increasing through the coupling region. Its absolute value appears to go through a minimum here, although whether this has any physical significance is not presently known.

The quantities ϵ_2 and ϵ_3 are approximately real, are reciprocal to each other, vary very slowly, and do not differ from unity very appreciably in the region of interest.

In order to obtain some idea of the dispersive characteristics of the model, the dielectric quantities for two side-band frequencies of 140 kc/sec and 160 kc/sec are also shown in Figure 2. Dispersion is only apparent along the dielectric axis directed along the earth's field. Its amount, qualitatively indicated by the spread among the curves, increases rather steadily with rising height as the main reflection region is approached.

Figure 3 shows how the indices of refraction behave in the neighborhood of the critical coupling point. The arrows show the directions along the curves to be traversed for an upgoing wave. Instead of a pair of distinct curves, which would occur if $N = N_c$ were above $\nu = \nu_c$ or *vice versa*, the two modes merge at the critical point in a branch point, as is, of course, expected classically and from the point of view of optic axes. Which part of the curve is to be considered as ordinary and which as extraordinary is immaterial physically, and is, as a matter of fact, arbitrary.

*This calculation was based on an assumed Chapman distribution, neglecting variation with zenith angle χ and assuming constant scale height of 10. This was on grounds of physical reasonableness.

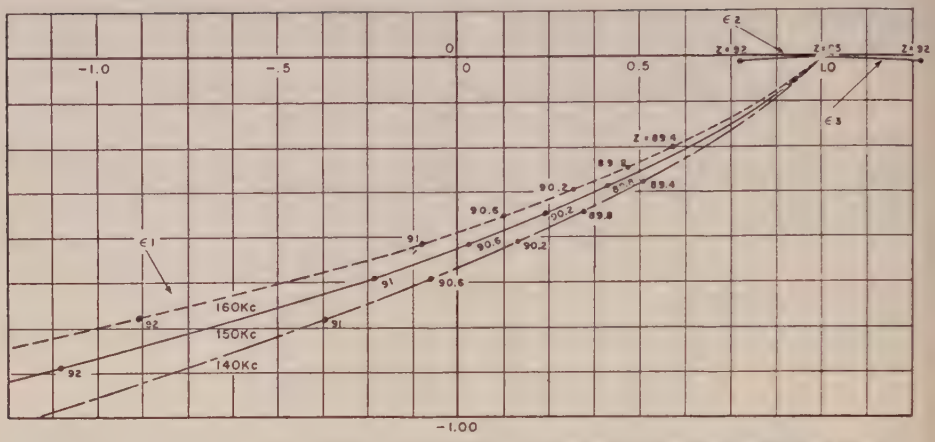

FIG. 2—VARIATION OF DIELECTRIC FACTORS IN COMPLEX PLANE WITH HEIGHT

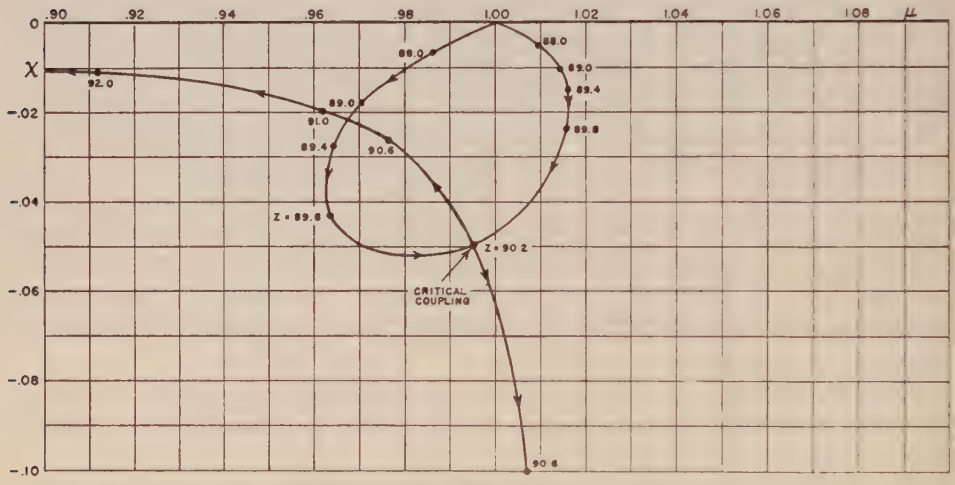

FIG. 3—VARIATION OF INDICES OF REFRACTION IN THE COMPLEX PLANE WITH HEIGHT IN THE NEIGHBORHOOD OF CRITICAL COUPLING FOR 150 KC

A detailed mathematical analysis of "forward" and "back-scattering" from the coupling region requires a wave-theory treatment of the differential equations (I) and (II). This work will be reported elsewhere and also covers the "high coupling" problem where $N = N_c$ is near (both above and below) $\nu = \nu_c$.

Thus, we have shown that the conditions for "optic axes" may occur in the actual ionosphere, for certain times of day and year. The level coincides with what would be the classical reflection level in the absence of collisions.

Acknowledgment is due especially to R. Parkinson, who arranged the computations and diagrams for this report, and to others of the Ionosphere Research Laboratory for helpful discussions.

VII—TABLE OF NOTATIONS

$\mathbf{r}$ = displacement vector
$\mathbf{E}$ = incident electric field vector

$\mathbf{H}_0$ = earth's magnetic field vector
$\mathbf{H}$ = magnetic vector of an electromagnetic field
m = mass of electron
e = numerical value of electronic charge
ν = collision frequency between electrons and heavy particles
c = velocity of electromagnetic waves in free space
N = number of electrons per cm^3
$\mathbf{P} = Ne\mathbf{r}$ = dielectric polarization vector
$\mathfrak{\lambda}$ = polarization tensor, defined by $\mathbf{E} = \mathfrak{\lambda}\,\mathbf{P}$
ω = circular operating frequency ($= 2\pi f$)
$\omega_0 = (4\pi Ne^2/m)^{\frac{1}{2}}$ = "critical" frequency
$\omega_H = eH_0/mc$ = gyromagnetic frequency
θ_P = angle between $\mathbf{H}_0$ and the positive z-axis
$\gamma_L = \omega\omega_H/\omega_0^2 \cos\theta_P$ = "reduced longitudinal component" of H
$\gamma_T = \omega\omega_H/\omega_0^2 \sin\theta_P$ = "reduced transverse component" of H
$\mathbf{D} = \mathbf{E} + 4\pi\mathbf{P}$ = dielectric displacement vector
$\mathfrak{e}$ = dielectric tensor, defined by $\mathbf{D} = \mathfrak{e}\,\mathbf{E}$
u = polarization (E_y/E_x)
n = index of refraction
M = coupling factor
π_i = wave function for i-th mode

References

[1] G. Lange-Hesse, Vergleich der Doppelbrechung im Kristall und in der Ionosphäre, Arch. Elektr. Ubertragung, **6**, 149-158 (1952).
[2] H. Poeverlein, Über Wellen in Anisotropen Ausbreitungsverhaltnissen, Zs. Naturf., **5a**, 492-498 (1950).
[3] O. E. H. Rydbeck, On the propagation of radio waves, Trans. Chalmers Inst. Tech., Gothenburg, No. 34 (1950).
[4] M. N. Saha, B. K. Banerjea, and U. C. Guha, Vertical propagation of electromagnetic waves in the ionosphere, Proc. Nat. Inst. Sci. India, **17**, 205-226 (1951).
[5] W. Becker, Ein Beitrag zur Frage der Dreifachaufspaltung in der Ionosphäre, Zs. Angew. Phys., **3**, 83-88 (1951).
[6] N. Davids, Theoretical group heights of reflection of 150 kc/s radio waves vertically incident on the ionosphere, J. Atmos. Terr. Phys., **2**, 324-336 (1952).
[7] M. Born, Optik, Julius Springer, Berlin (1933).
[8] M. Nicolet, The collision frequency of electrons in the ionosphere, to be published in J. Atmos. Terr. Phys.
[9] K. C. Westfold, The wave equations for electromagnetic radiation in an ionized medium in a magnetic field, Aust. J. Sci. Res., A, **2**, 168-183 (1949).

Journal of Geophysical Research Volume 58, No. 3 September, 1953

PROPAGATION MEASUREMENTS IN THE IONOSPHERE WITH THE AID OF ROCKETS

By J. Carl Seddon

United States Naval Research Laboratory, Washington 25, D. C.

(Received February 19, 1953)

ABSTRACT

Daytime measurements of electron density, ion density, electron collision frequency, and earth's magnetic field in the ionosphere were made during V-2 rocket flights at the White Sands Proving Ground, New Mexico. Two CW harmonically related frequencies were radiated from the rocket to two ground stations to obtain measurements of the ordinary and extraordinary indices of refraction in the region around the rocket. The results for one flight show an ion layer with a maximum of 5×10^8 ions/cc and a small electron layer with a maximum of 7,500 el/cc just below the $E1$-layer. On a September day the $E1$-layer remained dense up to the $E2$-layer, while on a January day the density apparently decreased above the $E1$-layer maximum to much lower values. It is shown that the Lorentz polarization term should not be used in the E-layer at 4 Mc.

INTRODUCTION

The Naval Research Laboratory began using rockets in 1946 to make measurements in the upper atmosphere. Data have now been obtained that are unavailable by any ground measurement. This paper discusses a propagation method of measuring electron density, ion density, electron collision frequency, and earth's magnetic field in the ionosphere and the results of three V-2 rocket flights at the White Sands Proving Ground, New Mexico. The first attempt was made in June, 1946, but various instrumentation problems [see 1 of "References" at end of paper] prevented success until March, 1947. Continuous measurements of electron density have since been made up to an altitude of 150 km. In addition, ion density measurements were made from 81 to 96 km, and values were obtained for the earth's magnetic field and electron collision frequency at 105 km. Due to multipath propagation, it was frequently possible to obtain checks on the values obtained.

The method makes possible the measurement of the indices of refraction of the medium immediately around the rocket. While this only provides two unknown quantities, and the propagation equation requires information concerning six unknowns to determine the indices of refraction, it is nevertheless possible to obtain most of the information desired. This is done by measuring the earth's magnetic field and the electron collision frequency at one altitude, and showing that the Lorentz polarization term can be neglected. The variation of the earth's

field with altitude follows a known law, so that this provides no further difficulty. The angle of magnetic dip varies so slowly with altitude that a ground measurement suffices for this. The variation in the electron collision frequency with altitude is not well known, but an average scale height of 8 km provides an approximate value. It is then usually possible to show that the effect of this factor on one or both of the indices of refraction is small enough to be neglected. The result is usually two equations with two unknowns, namely, the electron and ion density.

A somewhat similar method for measuring electron densities was recently reported by Berning [2], but as the frequencies used were quite high, the accuracy for low densities is questionable. Berning's results obtained for the *D*-layer, for example, cannot be correct within an order of magnitude, because at the densities reported, the electron collision frequency would cause complete absorption of any frequency that could reflect from the *E*-layer, whereas the $P' - f$ virtual height records at that time show the *E*-layer reflections. However, the high electron density of the *F*2-layer caused a large enough effect to yield apparently good data.

THE BASIC EXPERIMENT

Two harmonically related CW frequencies were radiated from the rocket to two stations on the ground, located six miles apart and approximately in the plane of the rocket trajectory. With the high-altitude short-range trajectory used, nearly vertical propagation was obtained. The frequencies used were 4.274 and its sixth harmonic 25.644 Mc. The higher frequency is practically unaffected by the *E*-layer, and serves as a reference frequency. These frequencies were received at the ground stations, where the ordinary and extraordinary components of the low frequency were separated by means of crossed dipoles and a cable-type Magic-T. After frequency multiplication by a factor of 6, each component was heterodyned separately with the reference frequency. The resulting beat frequency contains the information from which the index of refraction of the medium can be calculated. This is shown in the following discussion, where the assumption is made that the index of refraction of the medium in the vicinity of the rocket does not vary rapidly with height and that time variations of the ionosphere below the rocket are very slow. If c' and λ are the phase velocity and wavelength of the lower frequency f_l, then the received frequency on the ground is

$$\frac{c'}{\lambda + \Delta\lambda} = \frac{c'}{\frac{1}{f_l}(c' + v)} = \frac{f_l}{1 + v/c'}$$

where v is the radial velocity of the rocket from the ground station. As v is very small compared to c', and $c' = c/n$, where c is the velocity of light in vacuo and n is the index of refraction, the received frequency is $f_l\,(1 - nv/c)$. The higher frequency received has a frequency of $f_h\,(1 - v/c)$ if it is not affected by the charged particles present. Heterodyning this frequency with the sixth harmonic of the lower frequency yields a beat frequency of $f_b = (6 f_l v/c)\,(1 - n)$. Thus a measurement of the beat frequency and the radial velocity of the rocket made possible the determination of the index of refraction of the medium around the rocket.

Actually, the situation is somewhat more complicated than this. There are two downcoming rays, one ordinary and one extraordinary due to magneto-ionic splitting, and also two similar rays that are reflected from a higher level in the ionosphere. Figure 1 shows the frequency relationships, where O refers to the

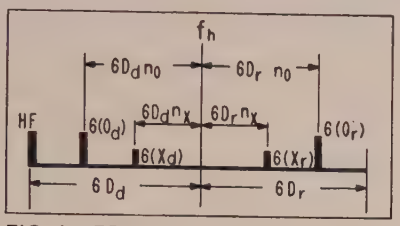

FIG. 1—FREQUENCY DISTRIBUTION ASCENDING ROCKET

ordinary ray, X to the extraordinary ray, and the subscripts r and d refer to the reflected and direct rays. D is used for the free-space Doppler shift $f_t\ v/c$ for the lower frequency. In order to calculate D_r it is necessary to know the height of reflection, and the height used was the virtual height of reflection obtained from $P' - f$ data taken during the flight by the Bureau of Standards ionosphere recording station at White Sands. The high frequency was high enough that no reflection was possible at the nearly vertical incidence involved. The line marked f_h is the transmitter frequency of 25.644 Mc. At the ground stations, this frequency is indicated by HF, a lower frequency because of the Doppler shift. The beat frequency for the direct ordinary ray is readily seen with the aid of Figure 1 to be

$$f_{bd} = 6(O_d) - HF = 6D_d(n_h - n_o) \quad \ldots\ldots\ldots\ldots\ldots\ldots (1)$$

where n_h is the index of refraction at the higher frequency and is equal to unity in general. A similar equation can be written for the extraordinary ray.

The ordinary and extraordinary beat frequencies were recorded on a Hathaway oscillograph simultaneously with the receiver AVC voltages. Due to the frequent presence of the reflected ray, the beat frequency was often quite complex, particularly when the ratio of the amplitudes of the direct and reflected rays was near unity. The situation became still more complicated when other components were present, as was sometimes the case. Methods have been worked out to determine the beat frequencies present provided that not more than three major components of one polarization are present, but these will not be discussed. The ordinary reflected-ray beat frequency f_{br} can be used to calculate the ordinary index of refraction by the equation

$$f_{br} = 6D_d n_h + 6D_r n_o \quad \ldots\ldots\ldots\ldots\ldots\ldots\ldots\ldots (2)$$

which is easily obtained by reference to Figure 1. As n_o is obtained from a difference of two large quantities, this equation will not give as accurate results as Equation (1).

At times the beat frequency record was unreadable due to the fact that the direct and reflected rays were nearly equal in amplitude, or due to the presence of noise. However, an approximate value of the ordinary index for the E-layer was

FIG. 2—OBSERVED AND CALCULATED FREQUENCIES FOR DIRECT RAYS, 10:00 HOURS, SEPT. 29, 1949, WSPG, N.M.

obtained from the ordinary receiver AVC record by noting that the resultant signal amplitude varies with a frequency of $(O_r) - (O_d)$. Thus,

$$f_{AVC} = n_o(D_d + D_r) \quad \ldots\ldots\ldots\ldots\ldots\ldots\ldots\ldots\ldots\ldots (3)$$

In order to plot the various results in a way that would permit a comparison to be made, the indices calculated from Equations (2) or (3) were substituted in Equation (1) to obtain a calculated value of f_{bd} . The value of D_r was not known with the certainty that D_d was known because it was determined from a virtual reflection height from records made at ground level, not from the appropriate levels in the ionosphere. The propagation was at times sufficiently far from vertical to introduce some error if the proper reflection height was not used. It was therefore desirable to calculate the direct beat frequency by the relation

$$f_{bd} = f_{br} - 6f_{AVC} \quad \ldots\ldots\ldots\ldots\ldots\ldots\ldots\ldots\ldots\ldots (4)$$

which is derived by eliminating D_r from Equations (2) and (3) with the aid of Equation (1). Thus, while the method of Equation (1) is by far the most desirable, there are actually three independent methods for obtaining the indices of refraction from the basic data. Also, as the data were recorded simultaneously at two stations, there are thus several ways of checking the results.

DATA OBTAINED ON SEPTEMBER 29, 1949

Figures 2*A*, 2*B*, and 2*C* show the frequencies obtained for the upward leg of the flight of September 29, 1949, take-off at 10:00 a.m. Only a small amount of data is available for the downward leg. The dashed lines in Figure 2*A* are portions that are considered unreliable, because of various factors such as semi-automatic antenna matching, antenna pattern, or severe noise. Note that the ordinary and extraordinary frequencies may be equal to each other and yet not be zero. This indicates the index is due mostly to ions, which are too heavy to cause magnetoionic splitting. Also, note that an additional frequency appears on the ordinary AVC record. The appearance of this additional frequency is also the cause of the irregularities at 127, 136, and 143 seconds after take-off. At the points where this additional frequency difference is plotted, there was at least one other ray present that was of greater amplitude than the ordinary direct ray. The reason for the existence of this ray is not known, but it is suspected that it may be due to mode coupling in the region just below the rocket.

Above 135 km, the data became somewhat irregular with sudden variations, so that the frequency determination became more difficult. It may be that the points plotted as ordinary direct values are the unknown component definitely identified in the lower altitudes. However, it is not believed that the unknown component was the one actually measured because the index of refraction was then nearly zero, while in previous measurements the unknown component consistently had an apparent index close to unity.

LORENTZ POLARIZATION TERM

There has been considerable disagreement for some time as to whether the Lorentz polarization term should be used in propagation calculations in the

ionosphere. The effects, if any, of this term on any quantity measurable on the ground, are so small as to be almost impossible to measure with sufficient accuracy to determine definitely whether or not the term (or part of it) should be used. This problem was resolved in this experiment by plotting the simultaneously observed indices of refraction on the theoretical Appleton-Hartree [3,4] curves in which the Lorentz polarization term was first included and then omitted.

The Appleton-Hartree formula for zero electron collision frequency was plotted for the condition of vertical propagation at White Sands, and ignoring the Lorentz term, as shown by the curves drawn in Figure 3. The value of the earth's field used was that for 100-km altitude, obtained by extrapolating the ground value by means of the inverse cube law. The abscissa x is proportional to electron density; namely, $x = Ne^2/\pi\, mf_i^2$, where e is the charge of an electron, m is its mass, N is the electron density, and f_i is the frequency of the radiation. The experimental points were plotted in the following manner: An experimentally determined value of the ordinary index of refraction was located on the upper curve, and the simultaneous experimental value of the extraordinary index of refraction was plotted for the same value of x. The disagreement in the first part (small values of x) was attributed to the presence of ions. The slight disagreement in the central portion was partially explainable by the combination of high electron density and electron collision frequency with neutral molecules. About 25 per cent can be ascribed to this cause. The remainder may be due to the presence of ions. At higher densities the collision frequency becomes low enough due to the higher altitude to permit agreement, except for the last point where the theoretical curve becomes very sensitive to collision frequency. Figure 4 was obtained in the same manner as Figure 3, except that the Lorentz polarization term of 1 3 was used in computing the Appleton-Hartree curves. The good agreement of Figure 3 and the disagree-

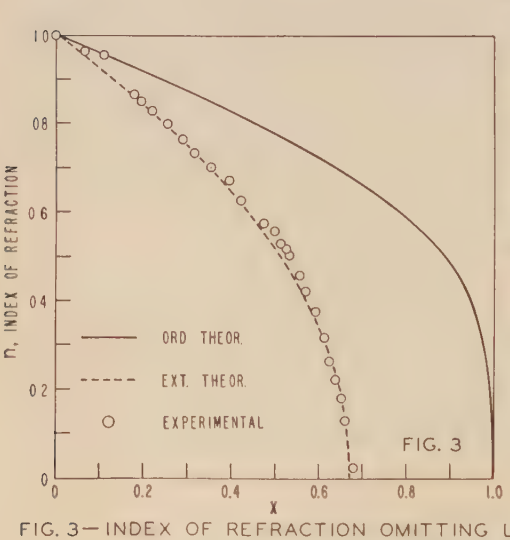

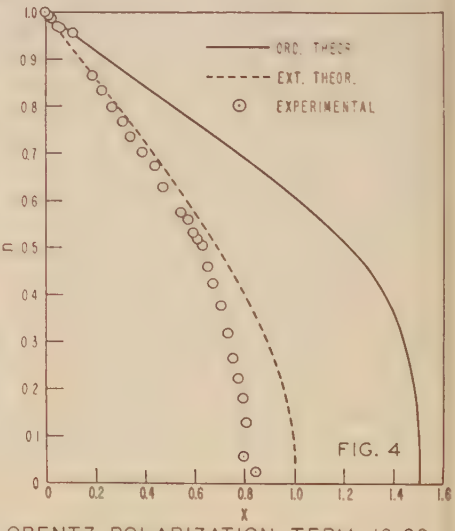

FIG. 3—INDEX OF REFRACTION OMITTING LORENTZ POLARIZATION TERM, 10:00 HOURS, SEPT. 29, 1949, WSPG, N.M.

FIG. 4—INDEX OF REFRACTION USING LORENTZ POLARIZATION TERM, 10:00 HOURS, SEPT. 29, 1949, WSPG, N.M.

ment of Figure 4 show that the Lorentz polarization term should be omitted at 4.274 Mc (and therefore also at higher frequencies).

EARTH'S MAGNETIC FIELD

Since the electron density where the extraordinary index of refraction becomes zero in the absence of collisions is dependent on the magnitude of the earth's magnetic field, it is possible to make a determination of the earth's magnetic field if the collision frequency ν is not too high. It is shown later that ν is low enough to be ignored in this computation. This zero point was determined by noting the altitude at which the reflected extraordinary ray dropped out on the AVC record. This was determined by plotting the logarithm of the AVC voltage as a function of altitude, and noting the altitude at which the slope first becomes constant. In two flights it was found that at this point there was a definite irregularity in the beat frequency. The electron density at this altitude was determined from the ordinary index of refraction by assuming that there were less than 10^7 ions per cc present at that altitude. The magnetic field was then determined from the gyrofrequency $f_g = He/mc$ by the relation

$$1 - x_H = \frac{f_g}{f_i} \qquad \ldots\ldots\ldots\ldots\ldots\ldots\ldots\ldots\ldots\ldots (5)$$

where x_H is the value of x determined from the electron density above. This formula is derivable from the Appleton-Hartree formula by solving for x with n_x set equal to zero. The magnetic field was computed to have a value of 0.497 oersted at 105 km, which agrees with the extrapolated ground value to a higher accuracy than exists in the available ground measurement from Coast and Geodetic Survey data.

ELECTRON COLLISION FREQUENCY

Where the electron density and the electron collision frequency with neutral molecules are both at high levels, the absorption of the radio wave is large enough that the rate of change of the received signal intensity provides a means of determining the collision frequency if the electron density is known. This was the case at 105 km in the flight of September 29, 1949. As there was no evidence of ions just below 105 km, the electron density could be determined from the ordinary index of refraction alone, the collision frequency not being high enough to affect this index at that electron density. The absorption index for the extraordinary wave was found from the slope of the AVC curve (discussed in the previous paragraph) to be 0.0105 per meter over a 190-meter path at 105 km. Using families of theoretical absorption curves plotted with various collision frequencies as a parameter, it was found that, at the observed electron density of 1.54×10^5 electrons per cc, the collision frequency must be 1.0×10^5 per second.

[*Note added in proof, August 24, 1953*: The original manuscript value for electron density was 1-1/2 per cent lower; the revised figure given here was obtained by graphical integration. It raised the final value of collision frequency by a factor of two. The corrected value is stated above.]

MEAN MOLECULAR CROSS-SECTION

With the electron collision frequency measured, an attempt was made to determine the mean molecular cross-section of the molecules present with respect to the free electrons. Data on pressure and density being known from rocket data [5], the calculation of the cross-section was made by substitution into the well-known kinetic theory formula

$$A = \frac{\nu}{s\sqrt{\frac{8kT}{\pi m}}} \qquad (6)$$

where ν is the electron collision frequency with neutral molecules, k is Boltzmann's constant, T is the absolute temperature, s is the number of molecules (or atoms) present per cc, and m is the mass of an electron. By use of the relations

$$s = \frac{\text{Avogadro's number} \times \text{density}}{\text{molecular weight}} = \frac{6.02 \times 10^{23} d}{M}$$

and

$$T = 4.65 \times 10^{-4} p/d$$

where p is pressure in mm of Hg and d is density in grams per cc, Equation (6) becomes

$$A = \frac{M\nu}{8.07 \times 10^{27}\sqrt{pd}} \quad \text{sq cm}$$

or

$$A = \frac{M\nu}{2.24 \times 10^{11}\sqrt{pd}} \quad \text{atomic units} \qquad (7)$$

Substitution of values for p and d gave a value for A of 44 atomic units at 105 km on the assumption that the mean molecular weight was 29. As N_2 and O_2 are both about 20 atomic units, the discrepancy was accounted for by the presence of atomic oxygen at this level, which had been previously reported by Friedman [6]. Atomic oxygen has an extremely high cross-section which has not been accurately measured or computed to date, but is probably more than 1,000 atomic units.

ELECTRON AND ION DENSITIES

With the Lorentz polarization term, earth's magnetic field, and electron collision frequency determined, the next step was to compute the electron and ion densities at all altitudes possible. The assumption was made that the values of the magnetic field at 100 km and the ground angle of dip could be used from 50 to 150 km without making larger errors than are involved in the determination of the beat frequencies. This simplified the calculations considerably, and seemed to be justified in that at altitudes where an appreciable change might result, such changes were smaller than the variations in the plotted points at those altitudes. The collision frequency at 105 km was used, with an assumption of a scale height of 8 km. This was done to

justify the method used in computing the various quantities. Goubau [7] has shown the theoretical effect of ions on the index of refraction of an ion-electron mixture. The Appleton-Hartree equation can be written for a given frequency at a particular location in the form $n^2 = F(x, \nu)$, where $x = Ne^2/\pi mf^2$ and ν is the electron collision frequency. The actual form of F is

$$F = 1 - \frac{x}{1 - j\frac{\nu}{k_1} - \frac{k_2}{1 - x - j\frac{\nu}{k_1}} \pm \sqrt{\frac{k_2^2}{\left(1 - x - j\frac{\nu}{k_1}\right)^2} + k_3}}$$

where the k's are constants and $j = \sqrt{-1}$. The index of refraction n_i due to an ion-electron mixture is obtained from the following equation:

$$n_i^2 = n_i^2 F(x/n_i^2, \nu) \quad \ldots\ldots(8)$$

where n_i is the index of refraction of the ions alone, which can be written in general

$$n_i^2 = 1 - \frac{x_i}{1 - j\frac{\nu_i}{\omega}} \quad \ldots\ldots(9)$$

where $\omega = 2\pi f_i$. Thus, the complete equation for both ions and electrons is

$$n_i^2 = 1 - \frac{x}{1 - j\frac{\nu}{\omega} - \frac{y_T^2}{2\left(1 - \frac{x}{n_i^2} - j\frac{\nu}{\omega}\right)} \pm \sqrt{\frac{y_T^4}{4\left(1 - \frac{x}{n_i^2} - j\frac{\nu}{\omega}\right)^2} + y_l^2}} - \frac{x_i}{1 - j\frac{\nu_i}{\omega}} \quad \ldots\ldots(10)$$

where

$$y_T = \frac{H_T e}{\omega mc} \qquad x_i = \frac{N_i e_i^2}{\pi m_i f_i^2}$$

$$H_T = H \cos\theta$$

$$y_l = \frac{H_l e}{\omega mc} \qquad \nu_i = \text{ion collision frequency with neutral molecules}$$

$$H_l = H \sin\theta$$

$$\theta = \text{angle of magnetic dip}$$

The experimental data show that in the lower altitudes, the values of x and x_i do not exceed 0.04. Under these conditions, the n_i^2 term in Equation (10) has no appreciable effect and can be ignored. Equation (10) then can be written:

$$n_i^2 = 1 - A - B \quad \ldots\ldots(11)$$

where A has two values but B only one. Note that $A = F_1(x, \nu)$ and $B = F_2(x_i, \nu_i)$ for a given location and operating frequency. Calculations of the collision fre-

quencies through the range where data were obtained show that through the 80- to 100-km range the ion collision frequency with neutral molecules contributed nothing significant to B. The collision frequency was calculated on the kinetic theory basis that the ion collision frequency would be approximately one-fortieth of that of the electrons. Thus B can be taken equal to x_i . Considering the A term, it was noted that from 80 to 98 km the extraordinary index was not affected appreciably by the calculated collision frequencies. Below 80 km the collision frequency was high enough to alter the results. However, as the actual collision frequency was not known, the electron densities were calculated on the assumption of zero collision frequency. Consequently, the values given below 80 km are minimal values, that is, the actual electron density must exceed these values. Using a scale height of 8 km, the collision frequency at 60 km would be 2.9×10^7 per second, but this high a value will cause the ordinary frequency to be higher than the extraordinary, as the electron density must exceed 2,000 el./cc. This was not observed, so the average scale height must be slightly greater than 8 km. An upper limit of 2.5×10^7 per second can be set for the collision frequency at the 60-km level, as the beat frequencies would be equal at this value of collision frequency.

Above 100 km it was not possible to make ion density calculations from the data available unless a collision frequency was assumed for each height. Even then, there might be appreciable error, as the Appleton-Hartree equation does not take into account electron collisions with positive ions. The term A was considered to be only a function of x under the restrictions as given above. Equation (11) can then be written as two equations with only two unknowns, x and x_i . The results obtained for x_i are shown plotted as a function of height in Figure 5. If the ionic mass were known, the number of ions could be calculated. On the assumption that the ions present consisted of N_2^+ and O_2^- of equal mass, a curve of ion density was plotted, as in Figure 6. Above 100 km it was assumed that the ion

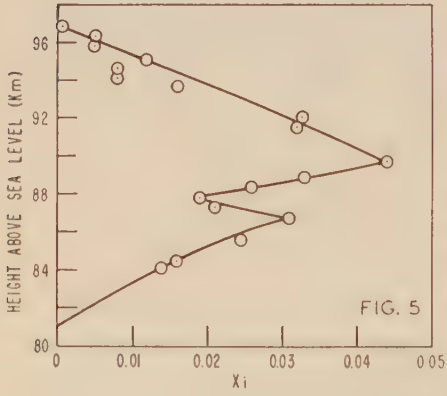

FIG. 5—X_i MEASURED AT 4.274 MC, 10:00 HOURS, SEPT. 29, 1949, WSPG, N. M.

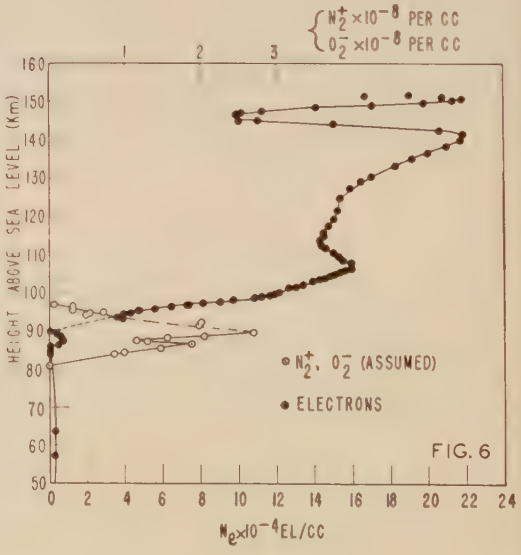

FIG. 6—ELECTRON AND ION DISTRIBUTION, 10:00 HOURS, SEPT. 29, 1949, WSPG, N.M.

density was less than 10^7 per cc and therefore could be ignored. This left one equation and one unknown. The results are also shown in Figure 6.

DISCUSSION OF RESULTS

The fact that the electron density did not drop much above the $E1$-layer maximum causes the virtual heights of reflection to be far greater than the actual reflection heights. As a result, the usual $P' - f$ curves can be quite misleading. For example, a numerical summation of the delays for passage of a 4-Mc wave gives a result of approximately 207 km for the virtual height, with the actual reflection height being 137 km. Examination of the $P' - f$ records (Fig. 7) taken during the flight by the Bureau of Standards shows a virtual height at 4 Mc of about 210 km. The $F1$-layer reflections ran smoothly into the $E2$-layer reflections. This fact, in conjunction with the observed discrepancy between E-layer virtual

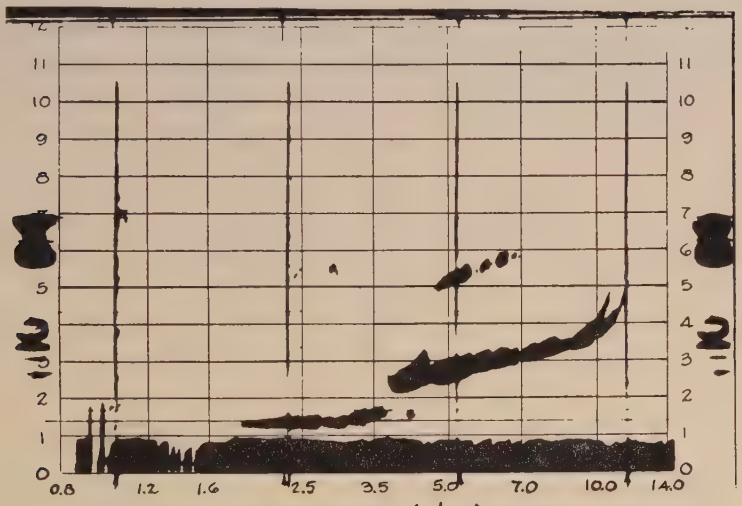

FIG. 7—BUREAU OF STANDARDS (P'-f) RECORD FOR 10:06 HOURS, SEPT. 29, 1949, WSPG, N.M.

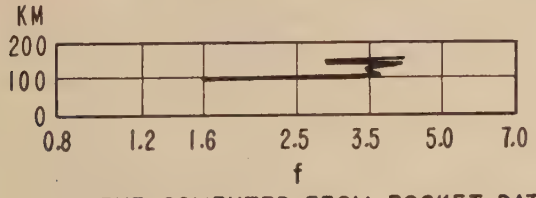

FIG. 8— P-f CURVE COMPUTED FROM ROCKET DATA, 10:00 HOURS, SEPT. 29, 1949, WSPG, N.M.

heights and actual heights (Fig. 8) leads to the conclusion that the E-layers and the $F1$-layer are all at lower altitudes than the $P' - f$ record would suggest. Part of the difference is undoubtedly due to using the previously accepted method of measuring the virtual heights by means of the leading edge of the ground and echo pulses. The remainder is due to the ions and electrons below the level of reflection.

It is probable that the rocket almost reached the $F1$-layer. The rocket data yield a value of 4.19 Mc for the critical frequency of the $E2$-layer at the actual altitude of 142 km. The $P' - f$ data give the virtual height of 215 km at 4.19 Mc, and the $F1$ critical frequency as 4.4 Mc. As 4.19 Mc is 95 per cent of 4.4 Mc, it is evident that the $F1$-layer is not much higher in altitude than the $E2$-layer. It is possible that the rising density at 150 km (Fig. 6) is the lower portion of the $F1$-layer.

RESULTS OF OTHER FLIGHTS

Some data were obtained with previous rockets, but the magneto-ionic components were not received separately at that time, and the records were very complex. No results could be given with assurance until after the 1949 flight which cleared up many confusing points. Even so, the results may be in error by a factor of 2 because of some necessary assumptions. Figure 9 shows the effective electron density for the flight of March 7, 1947, take-off time 11:23 a.m. A sudden ionospheric disturbance (S.I.D.) occurred just before take-off, and the resultant sporadic-E stopped the signals at 111 km, and no further data were obtained.

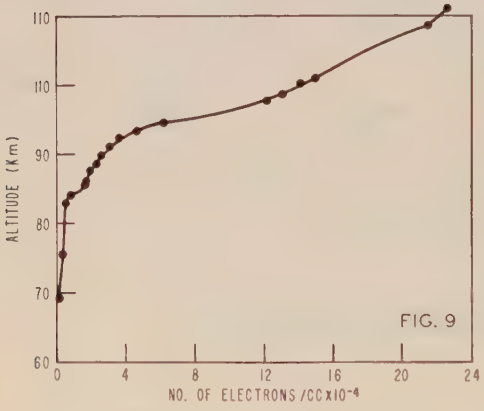

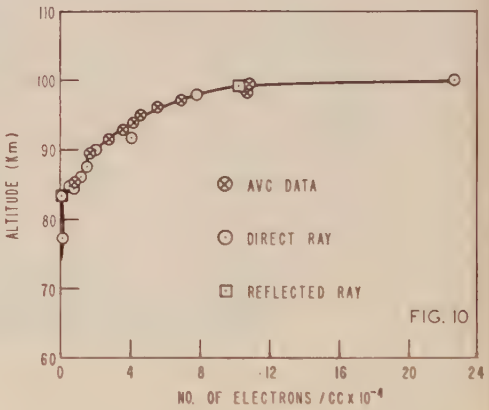

FIG. 9—EFFECTIVE ELECTRON DENSITY DISTRIBUTION, 11:25 HOURS, MAR. 7, 1947, WSPG, N.M.

FIG. 10—EFFECTIVE ELECTRON DENSITY DISTRIBUTION, 13:14 HOURS, JAN. 22, 1948, WSPG, N.M.

Figure 10 shows the effective electron density obtained for the flight of January 22, 1948, take-off at 1:12 p.m. It is interesting to note that in both this and the previous flight the curve has a peculiar shape in the vicinity of 85 km, which is also the altitude where temperature inversion occurs. There was some sporadic-E which caused the signal to drop out at 100 km. However, it decreased slightly later, so that a few points were obtained at higher altitudes:

km	Density (el/cc) $\times 10^{-4}$
122.6	2.0
130.7	4.0
158.0	6.0
158.2	22.4
158.3	22.6

If the low densities calculated above are actually due to the direct ordinary ray, these results indicate that in winter there is a much lower minimum above the $E1$-layer maximum than in early autumn.

CONCLUSIONS

The harmonic-frequency CW method described seems to provide an accurate means of probing the secrets of the ionosphere when used with high-altitude vehicles such as the V-2 or Viking rockets. The inherent accuracy of a heterodyne system is available, which is not the case with pulse-type methods. An obvious extension would be to use three or more harmonic frequencies, especially with rockets that can pierce the $F2$-layer, as is anticipated within another year.

ACKNOWLEDGMENTS

The results obtained were made possible by the continuous support and encouragement of Dr. Homer E. Newell, Jr., especially in the early phases when the data obtained looked almost hopelessly complex. The successful operation of the extensive and critical circuitry was due to the care and technical skill of Messrs. John E. Jackson and Giles H. Spaid.

Mr. Lawrence W. Gardenhire, formerly with the New Mexico College of Agriculture and Mechanic Arts, should be commended for his work in setting up the stations on the desert under extremely unfavorable circumstances.

A project involving the launching and tracking of large rockets is of such a magnitude that it could not be conducted without the active participation of many agencies. The author wishes to express appreciation for the contributions of the agencies who cooperated in the V-2 firings, such as the General Electric Company; Army Ordnance Test Station, White Sands Proving Ground; Signal Corps Engineering Laboratories, Ballistic Radar Unit, White Sands Proving Ground; Ballistic Research Laboratories, White Sands Proving Ground Annex; Naval Ordnance Missile Test Facility, White Sands Proving Ground; and the New Mexico College of Agriculture and Mechanic Arts.

References

[1] J. E. Jackson, UARR No. 13, U.S. Naval Res. Lab., Rep. No. 3909 (1952).
[2] W. W. Berning, J. Met., **8**, 175 (1951).
[3] A. V. Appleton, J. Inst. Elec. Eng., **71**, 642 (1932).
[4] D. R. Hartree, Proc. Cambridge Phil. Soc., **27**, 143 (1931).
[5] R. J. Havens, R. T. Koll, and H. E. LaGow, J. Geophys. Res., **57**, 59 (1952).
[6] H. Friedman, S. W. Lichtman, and E. T. Byram, J. Optical Soc. Amer., **41**, 292 (1951).
[7] G. Goubau, Hochf. Tech. u. Elec. Akus., **46**, 37 (1935).

JOURNAL OF GEOPHYSICAL RESEARCH VOLUME 58, NO. 3 SEPTEMBER, 1953

ELASTICITY OF OLIVINE AND CONSTITUTION OF THE EARTH'S MANTLE

BY J. VERHOOGEN

University of California, Berkeley, California

(Received February 24, 1953)

ABSTRACT

The object of this paper is to show that Birch's recent suggestions on the occurrence of phase changes in the upper mantle are based on a pressure-density relation that is not likely to be applicable to silicate minerals, and are inconsistent with the assumption that the depth-velocity curve is continuous. It is suggested that the pressure coefficient of incompressibility (dK/dP) of a homogeneous phase may increase at low pressures and go through a maximum. Bridgman's experimental data on quartz and olivine suggest that this is so; yet the accuracy of his measurements is not sufficient to warrant any definite conclusion. There is still no way of extrapolating to zero pressure the elastic properties of the lower mantle.

INTRODUCTION

Birch [see 1 of "References" at end of paper] has recently presented certain conclusions regarding the composition of the earth's mantle which may be summarized as follows. The mantle consists of three layers, the uppermost (layer B), approximately 400 km thick, consisting perhaps of eclogitic material. Immediately below layer B and grading into it is a transitional layer C in which elastic properties vary rapidly with depth. This variation may be due to two effects: There may be a change in gross chemical composition, such as a gradual decrease in proportion of alumina-bearing phases with corresponding increase in ferro-magnesians; there may be also a gradual increase in the proportion of high-pressure phases of the ferro-magnesian minerals. The transition to high-pressure phases is complete at about 900 km depth; layer D, below this level, is homogeneous in composition and consists essentially of this high-pressure material with elastic properties, particularly a high ratio of incompressibility to density, that are found only in certain oxides, such as corundum and rutile. Birch suggests that pyroxenes, for example, $MgSiO_3$, might exist in this layer with a corundum structure, or SiO_2 might exist in rutile form. Mg_2SiO_4 might transform to a spinel structure, or break down to high-pressure phases having the composition $MgSiO_3$ and MgO.

This interpretation of the structure of the mantle appears to be open to a number of objections. In the first place, it is unlikely that silicates would occur in a corundum- or rutile-type of structure, as in both these structures the cations are in sixfold coordination, that is, have six oxygen closest neighbors. It is also a

cardinal principle of crystal chemistry that silicon in silicates is invariably surrounded by four equidistant oxygens, as required by the electronic structure and relative size of the silicon ion. As it is difficult to see how this could be changed by pressures of the order of a hundred thousand bars or so, corundum and rutile structures are unlikely. Bernal and Jeffreys [2] have suggested that olivine might change to a spinel structure, spinels such as $MgAl_2O_4$ having a high density and low compressibility. Yet it is noteworthy that chrysoberyl ($BeAl_2O_4$), which has the typical formula of a spinel, similar high density and great hardness (the compressibility is unfortunately not known), also has an olivine structure, not a spinel structure. This may be taken to indicate that a high ratio of incompressibility to density is not necessarily indicative of an oxide- or spinel-type of structure.

The suggestion that notable phase changes occur in the mantle is open to the further objection that such transitions would produce sharp, not gradual, changes in elastic properties. Equilibrium between a low- and a high-pressure form is usually univariant; it occurs at a definite pressure for any given temperature, and coexistence of both modifications over a certain pressure and temperature range in the mantle would require that the temperature gradient should have precisely the value corresponding with the univariant equilibrium curve; coexistence of high and low modifications of several different minerals would be impossible because the actual temperature gradient would then have to simultaneously fit several different univariant curves. It is true that gradual transitions might occur in multi-component systems in which all components are mutually soluble, as in the case of the temperature-induced orthorhombic-monoclinic transformation of pyroxenes $(MgFe)SiO_3$, but it is not likely that variations in composition between high and low forms in the mantle could be large enough to spread the transition over an interval of several hundred thousand bars and several hundred degrees, as required by Birch; in the case of the pyroxene transformation just mentioned, the temperature interval over which the transition occurs is vanishingly small. From common petrological evidence it would appear that the mantle-forming rock probably does not consist of more than two or three minerals, excluding minor constituents present to the extent of a few per cent or less. If one or several of these main components undergo drastic crystallographic rearrangements in the mantle, there would be a corresponding number of discontinuities in the velocity-depth curve. There is perhaps no compelling seismic evidence that this is not so; the point is, however, that Birch's conclusion is inconsistent with the use of a continuous velocity distribution. As long as we adhere to the presently accepted view that this distribution is continuous we are, in the writer's opinion, committed to a homogeneous mantle, or to a mantle in which there are only gradual changes in gross chemical composition. It remains then to be shown that the elastic behavior of the mantle can be reconciled with such views.

ELASTIC BEHAVIOR OF THE MANTLE

Birch's procedure, which we now examine in greater detail, is as follows. Consider the case of hydrostatic strain of an isotropic body; if the strain f is defined in such a way as to include second-order terms, the relation between

strain and volume V is given by the exact formula

$$V_0 = V(1 + 2f)^{3/2} \quad \ldots\ldots(1)$$

where V_0 is the volume at zero pressure, f being positive for compression, negative for expansion. Birch then writes the Helmholtz free energy F under the form

$$F = af^2 + bf^3 + \cdots \quad \ldots\ldots(2)$$

where a and b depend on temperature only. Then

$$P = -\left(\frac{\partial F}{\partial V}\right)_T = -\left(\frac{\partial F}{\partial f}\right)_T \left(\frac{\partial f}{\partial V}\right)_T \quad \ldots\ldots(3)$$

Introducing the isothermal incompressibility $K = -V(\partial P/\partial V)_T = V(\partial^2 F/\partial V^2)_T$, Birch obtains finally the relation

$$P = \frac{3}{2} K_0 \left[\left(\frac{\rho}{\rho_0}\right)^{7/3} - \left(\frac{\rho}{\rho_0}\right)^{5/3}\right]\left\{1 - \xi\left[\left(\frac{\rho}{\rho_0}\right)^{2/3} - 1\right]\right\} \quad \ldots\ldots(4)$$

where $\rho = M/V$ is the density, M is molecular mass, K_0 is the incompressibility at zero pressure, and $\xi = -b/6V_0K_0$. Considering experimental results of compression of metals up to high strains, Birch finds that they are best represented by a formula of type (4) in which ξ is nearly zero; he then obtains for the pressure coefficient of incompressibility the very simple formula

$$\frac{dK}{dP} = \frac{12 + 49f}{3(1 + 7f)} \quad \ldots\ldots(5)$$

which shows that dK/dP is independent of temperature at zero pressure, and of any specific properties of the material under consideration; all materials obeying (5) have an initial $dK/dP = 4$, irrespective of composition or temperature. From this initial value of 4, the coefficient dK/dP decreases monotonically, its value being 2.87 for $f = 0.3$.

Using seismic velocities v_P, v_S at various depths, Birch first forms the quantity $\varphi = v_P^2 - 4/3(v_S^2) = K_S/\rho$, K_S being the adiabatic incompressibility. He then shows that the variation of φ with distance r from the center of the earth, which is computed from seismic data, is also given to a close approximation by the relation

$$1 - \frac{1}{g}\frac{d\varphi}{dr} = \left(\frac{dK}{dP}\right)_T - 5T\alpha\gamma - 2\tau\alpha\varphi/g \quad \ldots\ldots(6)$$

where g is gravity, T is temperature, α is the coefficient of thermal expansion, γ is Grüneisen's ratio (about 1.0 for olivine), and τ is the actual temperature gradient minus the adiabatic gradient. The two last terms on the right-hand side of (6) are probably smaller than 1, so that, to a first approximation, the function $1 - [(1/g)(d\varphi/dr)]$ represents dK/dP. The variation of this function with depth is interesting: starting from an initial value close to 4 at the top of layer B, it rises sharply to a maximum of about 9.5 at a depth of 400 km. It then decreases rapidly, returning to its initial value 4 at about 900 km, and from there on decreases slowly and regularly to a value of about 3 at the boundary of the core. It is essentially on this behavior that Birch bases his separation of the mantle

into distinct units. Since, according to him, the normal behavior of a single phase is to show a smooth monotonic decrease of dK/dP with pressure, an increase followed by a decrease in layer C can only mean that this region is not homogeneous (barring, of course, the rather unlikely case of a large decrease in temperature with depth, that is, τ negative and large). Layer D, on the contrary, must be homogeneous, since dK/dP behaves exactly as predicted by (5). The elastic properties of the materials forming this layer, extrapolated back to zero pressure by the use of (5) and (4), do not correspond with those of any known silicate; they are comparable only to those of certain oxides such as corundum or rutile. This Birch takes as further proof that phase transitions must occur higher up in the mantle.

COMPRESSIBILITY OF COMPOUNDS

It should be noted that the argument rests on the validity of equation (5) which itself implies that the free energy F is expressible in the form

$$F = af^2 \quad \ldots\ldots\ldots\ldots\ldots\ldots\ldots\ldots\ldots\ldots (7)$$

all higher terms being very small or zero. Although this relation is apparently adequate to represent experimental data for alkali metals, it is unlikely that it could have general validity. Consider, for instance, the case of a simple lattice (for example, NaCl) characterized by a single interatomic distance r. Then V is proportional to r^3, and $f = 1/2[(V_0/V)^{2/3} - 1]$, by definition. At the absolute zero of temperature, F becomes equal to U, the internal energy, which, if (7) is valid, must be of the form

$$U = -A/r^2 + B/r^4 \quad \ldots\ldots\ldots\ldots\ldots\ldots\ldots\ldots\ldots (8)$$

where A and B are constants. This represents a solid held together by attractive forces proportional to r^{-3}, the repulsive forces being proportional to r^{-5}. This would hardly apply to ionic crystals for which there should be an electrostatic energy term in r^{-1}, and for which the repulsive forces are usually proportional to r^{-8} or r^{-12}, the exact value of the exponent being determined from the initial compressibility. To obtain such rapidly varying forces one would have to introduce in (7) terms in f^4 or f^6.

If one now turns to more complicated structures, such as olivine, it is still less likely that a one-constant relation such as (7) could represent the facts. An olivine crystal, as is well known, consists of independent SiO_4 tetrahedra with interstitial Mg ions. The repulsive forces which contribute to the incompressibility may now arise from any or all of the six possible interactions: O—O, O—Si, O—Mg, Mg—Mg, Mg—Si, Si—Si. All these interactions probably have different potential functions, as shown by spectroscopic data. Matossi [3] finds, for instance, that the force constant for the O—Si interaction in zircon is about 10 times that for the O—O interaction, and judging from the similarity in infra-red absorption bands of olivine and zircon, this must be approximately true of olivine also. Not only are the force constants (a force constant measures the ratio of the restoring force acting on a particle to its displacement from the equilibrium position) different, but so are probably the anharmonic factors which express the variation of the force constant with displacement; if these anharmonic factors were zero, the particles would oscillate with a constant frequency ν depending only on the force constant and mass

of the particles; the Grüneisen factor $\gamma = -d\ln\nu/d\ln V$ would be zero, and so would the thermal expansion.

An olivine crystal, or any other similar compound, may thus be thought of in terms of a large number of springs of different types assembled in a three-dimensional network, each kind of spring having a different stiffness and a certain rate of change of stiffness with increasing deformation. That the behavior of such a complicated system could be represented by a one-constant formula of type (7) would be short of a miracle. One can imagine a very simple model consisting of just two springs assembled in series, each of these having a stress-strain relation of the type $F = ax + bx^2$, F being the force applied, x the deformation of the spring, a and b constants representing the force constant and anharmonic factor of each spring, respectively. It is easily seen that for small forces the deformation will be mostly taken up by the softer spring; but as this first spring gradually becomes stiffer, the deformation will be transferred to the second one, the elastic constants of which now determine the over-all behavior. In such a case, there would be a certain pressure range in which the incompressibility of the system would rise from a low initial value, corresponding to the elasticity of the softer spring, to a higher value corresponding to the elasticity of the harder spring; dK/dP in this case would go through a maximum. Such a simple system still only represents a rough approximation to an actual crystal; yet it is sufficient to show that there is no reason why dK/dP should necessarily decrease monotonically with increasing strain, as it might do in a monoatomic solid in which all springs are of the same type. The incompressibility of a complex compound might increase at different rates in different pressure ranges, and dK/dP might therefore have a maximum. The maximum that Birch finds in the mantle is thus physically not inconsistent with the homogeneity which must follow from the assumption that the depth-velocity curve is continuous.*

EXPERIMENTAL EVIDENCE ON COMPRESSIBILITY OF COMPOUNDS

These considerations suggest that the incompressibility of a compound such as forsterite is likely to vary with pressure in a complicated way, and there seems to

**Added in page-proof:* If we try to follow in more detail the high-pressure behavior of olivine, we first notice that the idealized structure of forsterite (Bragg [6], p. 148), in which oxygen ions lie in hexagonal close-packing, implies, for the given lattice parameters, a very short Mg–O distance and an abnormally large Si–O distance (1.81 A). The normal Si–O distance in silicates is 1.61. Hexagonal close-packing of oxygen in an olivine structure with normal Si–O spacing would require an Mg–O bond length of less than about 1.98; if it were, say, 1.9, the structure would have a remarkably high density (4.61) and presumably also a compressibility less than that of periclase. Such appears to be the explanation of the high density and great hardness of chrysoberyl ($BeAl_2O_4$), in which the Al–O distance is about 1.90 and in which the oxygen ions are correspondingly close-packed. If it were possible to reduce by pressure the normal Mg–O distance in forsterite to about 1.97 or so, it would also acquire the close-packed, high-density structure pictured by Bragg; and there would be nothing to prevent this change from being a gradual one. As it would be accompanied by a notable increase in density, there would be a pressure range in which the incompressibility K would be abnormally small; this would be followed by a further range, in which dK/dP would increase rapidly as K would rise to the high value characteristic of the more densely packed phase. The corresponding seismological picture might then be that of a low-velocity layer overlying a region with large dK/dP, in which K would rise well above its original value. The pressure range at which this would occur, of course, is not known; it might be of the order of one hundred thousand bars at room temperature, probably less at higher temperatures.

be no reason to expect that dK/dP should decrease monotonically with increasing pressure. If we turn to experimental evidence on compression of silicates, we find, indeed, a suggestion that their behavior is not as simple as postulated by Birch. Unfortunately, only very few compounds have so far been tested to 100,000 kg/cm^2 (Bridgman [4]). Of these, several show polymorphic transitions and cannot be used in this connection; others are considered by Bridgman not to be as satisfactory as desirable. Of the remaining few, some (for example, HgSe and HgTe) have volume-pressure curves that cross, and which are therefore inconsistent with any one-constant formula.

The only silicate or oxide that has been tested to 100,000 kg/cm^2 is quartz, for which there are also earlier measurements. At low pressures, experimental results are represented by the formula (Bridgman [4], p. 67)

$$Y = \frac{V}{V_0} = 1 - 2.645\ 10^{-6} P + 22.6 \times 10^{-12} P^2$$

from which we get the initial incompressibility $K_0 = -(Y'/Y')_{P=0} = 0.378 \times 10^6$, the initial rate of change of incompressibility $K_0' = (dK/dP)_{P=0} = \{[YY''/(Y')^2] - 1\}_{P=0} = 5.46$, and the second derivative $K_0'' = +2.03 \times 10^{-5}$ which is positive, indicating that K' initially increases with increasing pressure. There is also a set of measurements between 0 and 40,000 kg/cm^2, and another from 25,000 to 100,000 kg/cm^2; unfortunately they do not agree in the range where they overlap (25,000 to 40,000). From the high-pressure measurements alone, it is possible to compute numerically the value of dK/dP. If we have measurements of $Y = V/V_0$ at five points $(Y_{n-2}, Y_{n-1}, Y_n, Y_{n+1}, Y_{n+2})$ equally spaced at pressure intervals h, we can set

$$Y_n' = (Y_{n+1} - Y_{n-1})/2h$$

and

$$Y_n'' = (Y_{n+2} + Y_{n-2} - 2Y_n)/4h^2$$

Applying these formulae to experimental values of the ratio V/V_0 at 60,000, 70,000, 80,000, 90,000, and 100,000 kg/cm^2, which are respectively 0.902, 0.892, 0.883, 0.875, 0.868 (Bridgman [4], p. 68), we get at the central point

$$\left(\frac{dK}{dP}\right)_{80,000} = +11.2$$

which is about twice the value at $P = 0$. This in itself is not a decisive proof against Birch's formula (5), which predicts that dK/dP should decrease, as dK/dP is extremely sensitive to small experimental errors.

Bridgman has also determined the compression to 40,000 kg/cm^2 of an olivine of unstated composition [5, p. 78]. It is somewhat simpler to represent the data using P and T as independent variables, which is readily done by use of the Gibbs free energy G. We expand G in a Taylor series around an initial point (P_0, T_0). In particular, at constant temperature, and taking $P_0 = 0$, we have

$$G = G_0 + P\left(\frac{\partial G}{\partial P}\right)_0 + \frac{1}{2} P^2 \left(\frac{\partial^2 G}{\partial P^2}\right)_0 + \cdots$$

all derivatives being taken at constant T. Since $(\partial G/\partial P)_T = V$, we easily get by differentiation the relation

$$\frac{V}{V_0} = 1 - a_1 P + a_2 P^2 - a_3 P^3 + a_4 P^4 + \cdots \quad \text{.....(9)}$$

with

$$\left.\begin{aligned} a_1 &= 1/K_0 \\ a_2 &= (K_0' + 1)/2K_0^2 \\ a_3 &= [1 + 3K_0' + 2(K_0')^2 - K_0K_0'']/6K_0^3 \\ a_4 &= [1 + K_0'(6 + 11K_0' + 6K_0'^2 - 2K_0K_0''(2 + 3K_0') + K_0^2K_0''']/24K_0^4 \end{aligned}\right\} \quad \ldots(10)$$

where primes indicate differentiation with respect to P at constant T, and subscripts 0 indicate value at the origin. If the coefficients $a_1 - a_4$ can be determined from experiment, the corresponding values of K_0 , K_0' , etc., can be computed by use of relations (10). The incompressibility K and its pressure derivatives are then easily found, since

$$K = K_0 + K_0'P + \tfrac{1}{2}K_0''P^2 + \cdots$$

$$K' = K_0' + K_0''P + \tfrac{1}{2}K_0'''P^2 + \cdots$$

Etc.

We first try to fit Bridgman's data on olivine to a three-constant formula of type (9). This gives $a_1 = 0.8 \times 10^{-6}$, $a_2 = 1 \times 10^{-12}$, $a_3 = 0$, and the formula

$$\frac{V}{V_0} = 1 - 0.8 \times 10^{-6}P + 1 \times 10^{-12}P^2 \quad \ldots(11)$$

is found to represent the data *exactly; no other formula could give a better fit* (see Table 1).

TABLE 1.

P (10^4 kg/cm^2)	V/V_0 for olivine	
	Experimental (Bridgman)	Calculated from equation (11)
1	0.9921	0.99210
2	0.9844	0.98440
3	0.9769	0.97690
4	0.9696	0.96960

Equations (10), reduced to the case of a two-constant formula, give

$$K_0 = 1/a_1 = 1.25 \times 10^6$$

$$K_0' = \frac{2a_2}{a_1^2} - 1 = 2.125$$

$$K_0'' = \frac{2a_2}{a_1}\left[\frac{4a_2}{a_1^2} - 1\right] = +1.3 \times 10^{-5}$$

$$K_0''' = \frac{12a_2^2}{a_1^2}\left[\frac{4a_2}{a_1^2} - 1\right] = +0.98 \times 10^{-10}$$

which, as in the case of quartz, indicate that K' increases with increasing pressure. This formula, however, cannot be extrapolated very far, as it leads, beyond 400,000 kg/cm^2, to values of the volume which increase with pressure.

If we add to (11) a term $-2 \times 10^{-18} P^3$, we obtain the same value of K_0', but now K' decreases with increasing pressure. The agreement with experimental results is less good than in the previous case, but the difference at 40,000 kg/cm^2 amounts only to about one unit in the fourth decimal place (0.96947 instead of 0.9696). This is still well within the experimental error; the formula, however, now predicts a negative volume at 800,000 kg/cm^2. To remedy this, we add a term in P^4, and determine the four constants $a_1 - a_4$ by least squares. This gives

$$\frac{V}{V_0} = 1 - 0.861 \times 10^{-6}P + 5.93 \times 10^{-12}P^2 - 8.67 \times 10^{-17}P^3 + 9.32 \times 10^{-25}P^4 \ldots . (12)$$

which also fits well the experimental data, as indicated in Table 2.

TABLE 2

P (10^4 kg/cm^2)	V/V_0 for olivine	
	Experimental	Calculated by (12)
1	0.9921	0.99198
2	0.9844	0.98445
3	0.9769	0.97713
4	0.9696	0.96954

We now find $K_0 = 1.161 \times 10^6$, $K_0' = 15$, and $K_0'' < 0$, so that K' decreases with increasing pressure; the volume, however, becomes negative between 200 and 300,000 kg/cm^2.

The conclusion, then, is that experimental data for olivine are not sufficiently accurate to give the sign of K''. Best agreement is secured by use of a two-constant formula which gives a perfect fit and which predicts that K' will increase with pressure, at least in the low-pressure range in which the formula is applicable;

TABLE 3

Silicates	a_1	a_2	K_0 (kg/cm^2)	K_0'
Orthoclase	1.757×10^{-6}	4.167×10^{-12}	0.57×10^6	1.7
Labradorite	1.361	3.083	0.73	2.3
Hypersthene	1.057	4.75	0.94	7.5
Olivine	0.80	1.00	1.25	2.1
Garnet	0.73	2.167	1.37	7.1

but this again may be fortuitous as in the case of quartz. It is interesting to note, however, that the experimental data for other silicates investigated by Bridgman [5, p. 78] can also be very well represented by a two-constant formula; the values of K_0', as indicated in Table 3, range from 1.7 to 7.5, K_0'' being positive for all of them.

Formula (5) also predicts that K_0' should be independent of temperature. To find how K' varies with temperature, we now write the full Taylor expansion of G at temperature T, putting $T - T_0 = \theta$, and take the pressure derivative as before. This gives

$$\frac{V}{V_{00}} = 1 + \alpha_{00}\theta + \frac{1}{2}\theta^2\left(\alpha_{00}^2 + \frac{\partial \alpha_{00}}{\partial T}\right) + \cdots$$

$$- P\left[\chi_{00}\left(1 + \alpha_{00}\theta + \frac{1}{2}\alpha_{00}^2\theta^2 + \frac{1}{2}\theta^2\frac{\partial \alpha_{00}}{\partial T} + \cdots\right) + \theta(1 + \alpha_{00}\theta)\frac{\partial \chi_{00}}{\partial T}\right.$$

$$\left. + \frac{1}{2}\theta^2\frac{\partial^2 \chi_{00}}{\partial T^2}\right] + \frac{P^2}{2}\left[\left(\chi_{00}^2 - \frac{\partial \chi_{00}}{\partial P}\right)(1 + \alpha_{00}\theta) + 2\chi_{00}\theta\frac{\partial \chi_{00}}{\partial T} - \theta\frac{\partial^2 \chi_{00}}{\partial T\,\partial P}\right] + \cdots$$

where $\chi = 1/K$. If the development be limited to terms in θ, and setting $V_{\theta 0} = V_{00}(1 + \alpha_{00}\theta)$, we have for the volume change with pressure at temperature T

$$\frac{V}{V_{\theta 0}} = 1 - P\left[\chi_{00} + \theta\frac{\partial \chi_{00}}{\partial T}\right]$$

$$+ \frac{P^2}{2}\left[\chi_{00}^2 - \frac{\partial \chi_{00}}{\partial P} + \frac{2\chi_{00}}{1 + \alpha_{00}\theta}\frac{\partial \chi_{00}}{\partial T} - \frac{\theta}{1 + \alpha_{00}\theta}\frac{\partial^2 \chi_{00}}{\partial T\,\partial P}\right]$$

which shows how temperature affects the coefficients a_1 and a_2 in equation (9). We now form $K_{\theta 0}' = (2a_2/a_1)_{T=T_0+\theta} - 1$ and take the derivative with respect to θ, which should be zero if K_0' is independent of T. Calculations show that this can only be true for all values of θ if $\partial \chi_{00}/\partial P = \chi_{00}^2$, $2\chi_{00}(\partial \chi_{00}/\partial T) = \partial^2 \chi_{00}/\partial T\,\partial P$, in which case $K_0' = -1$ and $a_2 = 0$ at all temperatures. We conclude that if the pressure-volume relation can be adequately expressed by a two-constant formula, K_0' will not be independent of temperature. There is actually some experimental evidence that K_0' for sodium chloride at high temperature is not equal to its low temperature value. At 1000°K, which is about three times the Debye temperature for NaCl, the constant-volume specific heat C_V will be constant. We have then $(\partial C_V/\partial V)_T = -T(\partial \alpha K/\partial T)_V = 0$, from which we obtain, after some transformations

$$\left(\frac{dK}{dP}\right)_T = +\frac{2}{\alpha\chi_T}\left(\frac{\partial \chi_T}{\partial T}\right)_P - \frac{1}{\alpha^2}\left(\frac{\partial \alpha}{\partial T}\right)_P = \frac{2}{\alpha\chi_S}\left(\frac{\partial \chi_S}{\partial T}\right)_P + \frac{2}{\alpha C_P}\left(\frac{\partial C_P}{\partial T}\right)_P - \frac{1}{\alpha^2}\left(\frac{\partial \alpha}{\partial T}\right)_P$$

where C_P is the specific heat at constant pressure, χ_T and χ_S represent, respectively, the isothermal and adiabatic compressibility. The experimental values at 1000°K and $P = 0$ of the various terms to the right are listed by Birch [1, p. 250]; we get $(dK/dP)_{1000°\ P=0} = 2.1$. At ordinary temperature, the compression of NaCl can be represented in the form $V/V_0 = 1 - 4.26\ 10^{-6}\,P + 51 \times 10^{-12}\,P^2$, from which we get $K_0' = 4.6$, which is about twice the value at 1000°K.

It cannot be said, therefore, that experimental results for non-metals favor Birch's equation (5), as they can be adequately represented by a two-constant formula which gives an initial increase of dK/dP with pressure. The initial value of dK/dP is certainly not always 4, as predicted by (5) and appears to depend on temperature. Yet experimental uncertainties are too large to allow any formal conclusion; the compressibility of olivine in the pressure range of interest in the mantle will apparently not be known until its is actually measured. Clearly, Birch's extrapolation of K/ρ to its value at zero pressure by use of (5) is unwarranted, and his argument for phase changes seems to rest on insecure evidence.

It has been said that the inference that phase changes occur in layers B and C is inconsistent with a continuous velocity-depth distribution. The seismic evidence is, however, not sufficiently clear on this point; the apparent rapid increase in velocity around 400 km could perhaps be more satisfactorily interpreted as a number of small discontinuous jumps between which the velocity increases with depth at a slower rate. Small phase transitions that do not correspond with any major reorganization of the crystal lattices involved are indeed quite likely. Nor is it excluded that the composition of the mantle might gradually change with depth as, for instance, by gradual increase in the proportion of metallic iron. There is still no clear picture of the physical constitution of the mantle, no definite seismic indication as to its homogeneity or otherwise, and there is yet no way of extrapolating to zero pressure the elastic properties of its deeper parts.

In conclusion, the author wishes to express his thanks to Drs. David Griggs and Leon Knopoff for helpful discussions of the experimental data.

References

[1] F. Birch, Elasticity and constitution of the earth's interior, J. Geophys. Res., **57**, 227-286 (1952).

[2] H. Jeffreys, The structure of the earth down to the 20° discontinuity, Mon. Not. R. Astr. Soc., Geophys. Sup., **4**, 13-38 (1937).

[3] F. Matossi, Vibration frequencies and binding forces in some silicate groups, J. Chem. Phys., **17**, 679-685 (1949).

[4] P. W. Bridgman, The compression of 39 substances to 100,000 kg /cm², Proc. Amer. Acad. Arts Sci., **76**, 55-70 (1948).

[5] P. W. Bridgman, Rough compression of 177 substances to 40,000 kg cm², Proc. Amer. Acad. Arts Sci., **76**, 71-87 (1948).

[6] W. L. Bragg, Atomic structure of minerals, Ithaca, Cornell University Press (1937).

NOTES ON AURORAL GEOMETRY AND OPTICS: I—TO LOCATE AN ELEVATED POINT VIEWED FROM TWO GROUND STATIONS IN THE SAME DIAMETRAL PLANE*

By Sydney Chapman

The Queen's College, Oxford, England,
and
The Geophysical Institute, University of Alaska, College, Alaska

(Received March 2, 1953)

ABSTRACT

A simple graphical method is explained for obtaining the height and location of a point P from its elevations e and e' as observed from two points Q, Q' on the earth's surface, in the same diametral plane as P.

1. *Introduction.*

Let P denote a point at height h above the earth's surface, and Q, Q' two ground stations within view of P, and in the same diametral plane, that is, the plane PQQ' passes through the centre O of the earth, which will be regarded as spherical, of radius a (= 6,370 km).

Let e, e' denote the angles of elevation of P above the horizons of Q and Q', and c, c' the angles POQ, POQ'. Case i—If the radius OP lies outside the angle QOQ' (whether to the north or to the south), e, e', c, c' will all be reckoned as positive, and Q will be chosen so that $e < e'$ [see Fig. 1(i)]. Case ii—If OP lies within the angle QOQ', Q will be chosen so that the angle POQ exceeds the angle POQ'; c will be reckoned positive, and c' negative, so that numerically c exceeds c'; one of the elevations e, e' will be above the northern, the other above the southern horizon, but both will be reckoned positive [see Fig. 1(ii)].

The problem here considered is this: to determine h and c, given the angles e, e' and the angle QOQ' ($= c - c'$).

This is a trivial problem of trigonometry, and in no way essentially related to aurorae: but it would be helpful to auroral studies to have a simple and convenient method of solving it numerically for any of the triply infinite set of particular angles e, e', $c - c'$. After considering several alternative methods, the following is presented as being concise and practical.

2. *The formulae, graphs, and tables.*

First consider one station Q only, within view of P: the triangle OPQ has angles as shown in Figure 2. Let PT be the perpendicular from P on to OQ produced.

*From a lecture course given at the University of Alaska, December 1952.

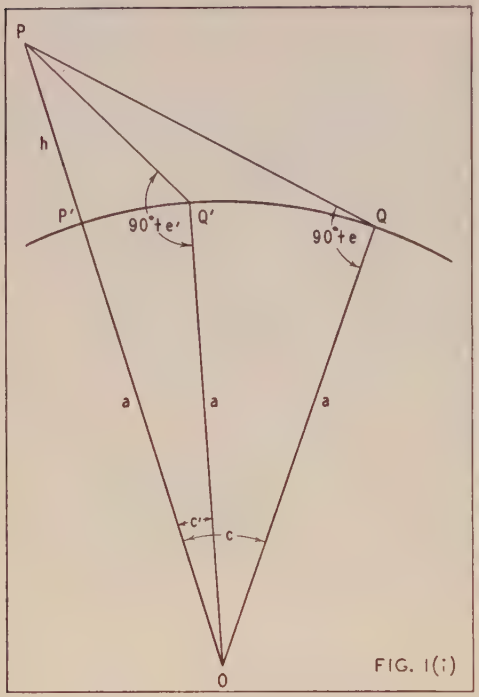

FIG. 1(i)

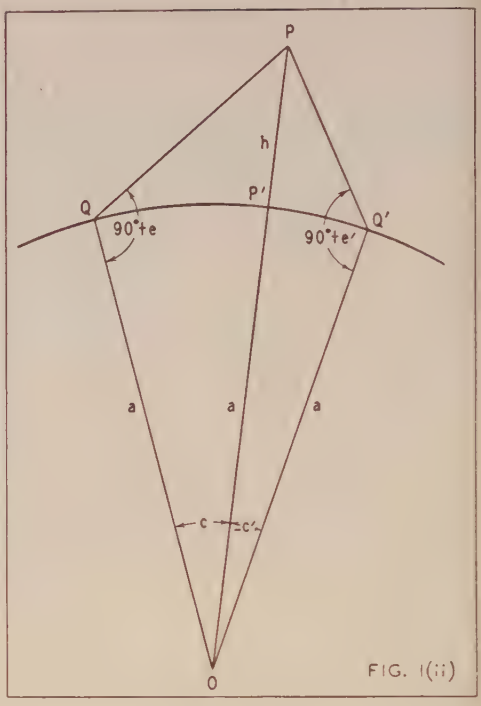

FIG. 1(ii)

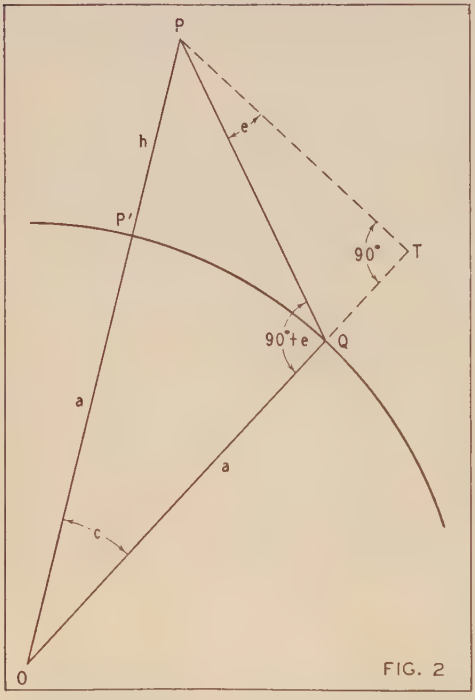

FIG. 2

FIGS. 1 AND 2—A POINT P AT HEIGHT h ABOVE THE EARTH IS SEEN FROM TWO STATIONS Q, Q′ (THE PLANE PQQ′ PASSING THROUGH THE EARTH'S CENTRE O) AT ELEVATIONS e, e′; THE ANGLES QOP, Q′OP ARE c, c′; THE POINT Q IS CHOSEN SO THAT $PQO < PQ'O$, $POQ > POQ'$

FIG. 1(i), CASE i—WHEN P LIES OUTSIDE THE ANGLE QOQ′, e AND e′ ARE RECKONED POSITIVE, AND $e' > e > 0$, $c > c' > 0$, $QOQ' = c - c'$

FIG. 1(ii), CASE ii—WHEN P LIES IN THE ANGLE QOQ′, THE LARGER ELEVATION IS TAKEN AS e′, AND THE SMALLER AS e; $e' > e > 0$; ALSO $QOP = c > 0$, $Q'OP = -c'$ AND c′ IS RECKONED NEGATIVE, $c > -c' > 0$, $QOQ' = c - c'$

Then as the elevation e is reckoned positive (§1) regardless of the sign of c,

$$\tan e = \frac{QT}{PT} = \frac{(a+h)\cos c - a}{(a+h)\sin|c|}$$

$$= \frac{(a+h)(\cos c - 1) + h}{(a+h)\sin|c|} = \frac{\cos c - 1}{\sin|c|} + \frac{h}{a+h}\operatorname{cosec}|c| \quad \ldots\ldots(1)$$

$$= \frac{h}{a+h}\operatorname{cosec}|c| - \tan\frac{1}{2}|c|$$

This is convenient for calculating e for any chosen values of h and c.

Alternatively,

$$\frac{a}{a+h} = \frac{OQ}{OP} = \frac{\sin OPQ}{\sin OQP} = \frac{\sin(90° - e - |c|)}{\sin(90° + e)} = \frac{\cos(e + |c|)}{\cos e}$$

so that

$$\cos(e + |c|) = \frac{a}{a+h}\cos e \quad \ldots\ldots(2)$$

This is convenient for calculating c for any chosen values of h and e.

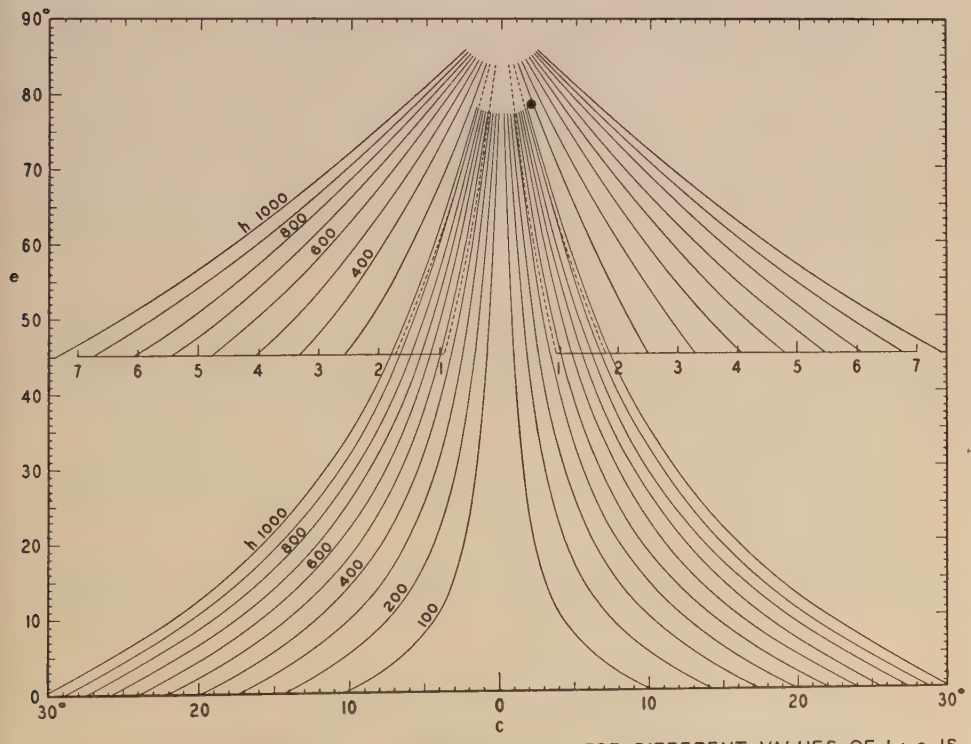

FIG. 3—THE CURVES SHOW e AS A FUNCTION OF c FOR DIFFERENT VALUES OF h; e IS THE ELEVATION OF A POINT P AT HEIGHT h, AS VIEWED FROM A STATION Q, AND c IS THE ANGLE QOP SUBTENDED BETWEEN P AND Q AT THE EARTH'S CENTRE O; THE CURVES ON THE LEFT ARE MIRROR IMAGES OF THOSE ON THE RIGHT; IN THE UPPER HALF OF THE FIGURE, THE PARTS OF THE CURVES IN THAT HALF ARE DRAWN ALSO WITH A FOURFOLD MORE OPEN SCALE OF c

As aurorae commonly lie between the heights 100 and 1,000 km, values of e have been calculated from (1) as a function of c for $h = 100n$ km, where $n = 1, 2, 3, \cdots, 10$. When c is zero, $e = 90°$ for all values of h. When $e = 0$, $c = c_0$ where $\cos c_0 = a/(a + h)$. Figure 3 shows the graphs of e as a function of c for these values of h; the curves are drawn on both sides of the axis of ordinates ($c = 0$), corresponding to Q being on one or other side of P relative to a third point Q' in the same plane. The Tables give the calculated values of c_0 and e for the points P (specified by h, c) used in plotting the curves. In the upper part of Figure 3, parts of the curves (for $e > 45°$) are reproduced on a more open scale of abscissae c.

Table 1—*Values of* c_0

h =	100	200	300	400	500	600	700	800	900	1000
c_0 =	10°.09	14°.17	17°.25	19°.79	21°.99	23°.95	25°.71	27°.32	28°.81	30°.20

Table 2—*Values of* e

h \ c	0°.5	1°	1°.5	2°	3°	4°	6°	8°	11°	14°	18°	21°	25°
100	60.50	41.25	30.01	23.05	15.07	10.58	5.46	2.36	.....	.....	.....	.....	.....
200	73.99	60.05	48.99	40.52	29.05	21.88	13.43	8.46	3.62	0.17	.....	.....	.....
300	79.02	68.73	59.61	51.81	39.80	31.38	20.70	14.21	7.94	3.61	.....	.....	.....
400	81.59	73.50	65.98	59.17	47.79	39.08	27.15	19.52	12.04	6.92	1.88	.....	.....
500	83.16	76.49	70.13	64.19	53.76	45.24	32.78	24.37	15.91	10.09	4.41	1.02	.....
600	84.21	78.52	73.02	67.79	58.29	50.17	37.64	28.75	19.53	13.12	6.85	3.14	.....
700	84.96	79.99	75.14	70.47	61.81	54.16	41.82	32.68	22.91	15.99	9.20	5.20	0.72
800	85.53	81.10	76.76	72.54	64.60	57.42	45.43	36.20	26.04	18.70	11.46	7.17	2.42
900	85.97	81.97	78.03	74.18	66.85	60.11	48.54	39.34	28.92	21.25	13.61	9.10	4.07
1000	86.32	82.66	79.05	75.51	68.71	62.37	51.24	42.15	31.58	23.66	15.68	10.94	5.68

Figure 3 is a reduced version of a large diagram on squared paper on which the scales of e and c are respectively 1 inch = 5° and 1 inch = 2°.5. On this scale the diagram enables h to be estimated easily by eye to 10 km, and c, c' to about 0°.1, if e and e' are known to 0°.2.

3. *Method of determining* h *and* c *from a set of values of* e, e', *and* $c - c'$ *for two given stations* Q, Q'.

For actual use, the base network of Figure 3 should be filled in by joining corresponding scale points on the right and left sides of the diagram, and corresponding scale points on the top and bottom; it is better to use an enlarged version of Figure 3 drawn on squared paper by use of the numerical data in Tables 1, 2.

Case i (Fig. 4): P lies on the same side of both Q and Q' (whether to the north or south), and e, e', c, c' are all reckoned as positive, and $e < e'$, $c > c'$.

Over Figure 3 lay a sheet of tracing paper on which axes Oc, Oe are drawn, horizontally to the right and vertically upwards, with scales of c and e marked along them, identical with those of Figure 3. Mark the points C, E' along Oc and Oe, such that $OC = c - c'$, $OE' = e' - e$. Place the paper so that Oc is at the level of the given value of e in Figure 3; and slide the paper along, with Oc at this level,

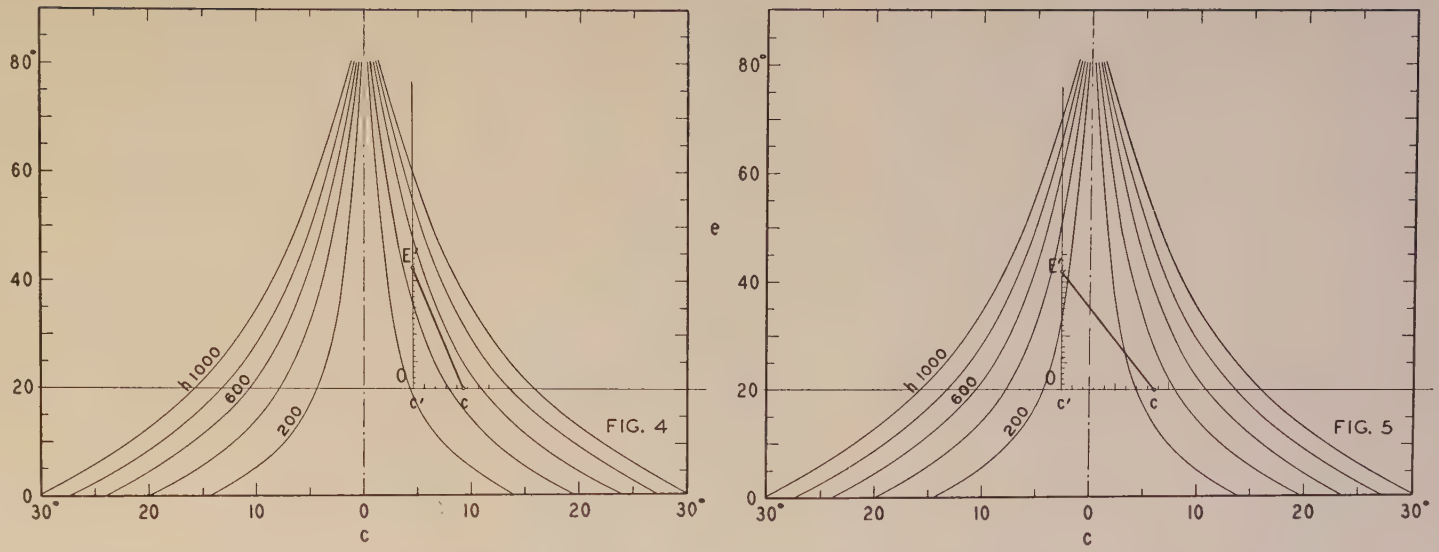

FIG. 4—METHOD OF DETERMINING h, c, AND c′ FOR A POINT P AT HEIGHT h VIEWED FROM TWO STATIONS Q, Q′, BOTH ON THE SAME SIDE OF P, FROM THE ELEVATIONS e, e′ OF P FROM Q, Q′, AND THE ANGLE QOQ′ (=c-c′); THE LINE Oc IS PLACED AT THE LEVEL e, AND OE′=e′-e, OC=QOQ′; THE TRACING PAPER IS MOVED UNTIL THE POSITIONS OF C AND E′ CORRESPOND TO THE SAME VALUE OF h

FIG. 5—METHOD OF DETERMINING h, c, AND c′ FOR A POINT P AT HEIGHT h VIEWED FROM TWO STATIONS Q, Q′, ON OPPOSITE SIDES OF P, FROM THE ELEVATIONS e, e′ OF P FROM Q, Q′, AND THE ANGLE QOQ′ (=c-c′); e IS THE NUMERICALLY SMALLER OF e AND e′, BOTH RECKONED POSITIVE; c′ IS RECKONED NEGATIVE, SO THAT OC=QOQ′=c-c′; OE′=e′-e; THE LINE Oc IS PLACED AT THE LEVEL e, WITH E′ AND C ON OPPOSITE SIDES OF THE MEDIAN VERTICAL SCALE, AND Oc IS MOVED UNTIL THE POSITIONS OF E′ AND C CORRESPOND TO THE SAME VALUE OF h

Note: In Figures 4 and 5 above, the line *OE′* is parallel to the median vertical scale, though owing to optical illusion this may seem not to be so.

until the points C and E' lie on the same h curve, either one of those actually drawn, or on an imaginary h curve envisaged by mental interpolation. This gives the value of h for P, and the abscissae of O and C give the values of c' and c. If the Oc scale is extended to the left of O, the values of c can conveniently be read on it from the position of the median axis of Figure 3.

For example, if e is 20°.7, and e' is 51°.8, and $QOQ' = c - c' = 4°$, then the points C and E' will both lie on the curve for $h = 300$ km, and the abscissa of O will be 2°, and that of C, 6°.

Case ii (Fig. 5): P lies between Q and Q'; e is smaller numerically than e'; both are reckoned positive, so that $e' > e > 0$, c' is reckoned negative and c ($> -c'$) positive, and the known angle QOQ' is $c - c'$.

Mark points C and E' along Oc and Oe so that $OC = c - c' = QOQ'$, and $OE' = e' - e$. Place the tracing paper at the level e, as before, and slide it along this level until E' lies on the left-hand curve, and C on the right-hand curve, for the same value of h. Then this is the value of h for P, and the abscissae of C and O are c and $-c'$.

For example, if $QOQ' = 5°$, and $e = 29°.05$, $e' = 40°.52$, then $h = 200$ km and $c = 3°$, $c' = -2°$.

4. *Application to aurorae.*

The above method is applicable to observations of an auroral point in the diametral plane through the stations Q and Q', for which $c - c'$ is known. The simplest case is that in which Q and Q' lie on a geomagnetic meridian, and P is the apparent summit, as viewed from Q and Q', of the lower border of an auroral arc lying at constant height along a circle of geomagnetic latitude.

Even if Q and Q' are on different geomagnetic meridians, and e and e' are the elevations of the corresponding apparent summits P, P' of the lower border of such an auroral arc, the method may still be applicable.

Auroral arcs often lie along a circle of geomagnetic latitude, and their lower borders are approximately at uniform height h; in this case, the method is applicable to the extent that the geomagnetic latitude of the arc is constant; if it varies along its length, this simple method of finding h and c will be faulty.

The need for such a method of determining h and c impressed itself upon me in connection with the study of the specially outstanding aurorae which extend to unusually low latitudes. Owing to their rarity in such regions, it is to be expected that there will usually be no provision for simultaneous *photography* of the aurora from the two ends of a suitable base-line situated there—which of course is the only really satisfactory way of determining h and c. In such a case, there is value in even a rough determination of h and c by means of the elevations e, e' measured at two points Q, Q' not too different in geomagnetic longitude—that is, if the aurora has an arc form, and particularly if the elevations refer to an identifiable point on the aurora, the same or nearly so for both stations.

5. *Acknowledgments.*

I am indebted to Anne and Joseph Cain and M. Sugiura, of the University of Alaska, for help in the preparation of this paper, and to Dan C. Wilder, of the Geophysical Institute, who has constructed the Figures.

SOME REGULARITIES OF THE IONOSPHERIC F REGION

By B. Chatterjee

Institute of Radio Physics and Electronics,
University of Calcutta, Calcutta, India

(Received March 2, 1953)

ABSTRACT

It has been shown recently by Ratcliffe that, although the behaviour of the critical frequency (and hence the maximum ionization density) of the $F2$ region is very irregular, that of its total ion content (in a column of unit cross-section) is much less so. However, the regularities observed by Ratcliffe are confined only to a few stations and disappear when the $F1$-$F2$ bifurcation is large. It is shown in the present paper that if, instead of the total ion content of the $F2$ region, that of the $F1$ *cum* $F2$ region (n_T) is considered as a whole, then the regularities become much more marked. Further, the regularities are found to persist for all the three stations considered—Slough (northern hemisphere), Falkland Islands (southern hemisphere), and Singapore (equatorial region)—even when the bifurcation is large. Certain peaks, however, are found to occur on the otherwise smooth variations of the monthly mean values of n_T. These are explained as due to tidal effects. The paper also shows that the observed regularities of the composite F region are in conformity with the recent hypothesis that $F1$ and $F2$ belong really to one ionized region, being produced by a common ionizing radiation from the sun.

1. INTRODUCTION

The $F2$ region of the ionosphere is well known for its irregular behaviour. Its maximum ionization density does not rise and fall symmetrically with the diurnal and seasonal variations of the solar zenith angle (χ), as the ionization densities of the E and $F1$ regions do, following approximately the $\sqrt{\cos\chi}$ law of Chapman [see 1 of "References" at end of paper].

However, it has been shown recently by Ratcliffe [2] that if, instead of the ionization density values (N_m), one considers the total ion content of the $F2$ region (say, in a column of unit cross-section), then the variations of the same with χ show much more regularity. Ratcliffe, however, found such regularities only in the records of a few stations. Further, the regularities were found to be practically non-existent when the bifurcation of the F region into $F1$ and $F2$ was large.

In the present paper, it will be shown that if, instead of considering the total ion content of the $F2$ region only (as done by Ratcliffe), that of the $F1$ *cum* $F2$

region is considered as a whole, then the regularities become much more marked. Further, the regularities are found to persist for all the stations considered—northern and southern—even when the bifurcation is large (after making due allowances for the effects of tides). The paper also discusses how far the observed regularities of the composite F region are compatible with the recent hypothesis that the $F2$ region is produced by a sort of bifurcation of the $F1$ region, the latter being produced by the usual Chapman process by ionizing solar rays of appropriate wavelengths.

The stations, the records of which have been considered in the investigations, are Slough, latitude 51°32′ north, longitude 0°34′ west (northern hemisphere), Falkland Islands, latitude 51°42′ south, longitude 57°51′ west (southern hemisphere), and Singapore, latitude 1°19′ north, longitude 103°49′ east (near the equator). The records analysed were in most cases for the year 1951.

2. CALCULATION OF THE TOTAL ION CONTENT

The total ion content in a column of unit cross-section of the composite F region is calculated on the assumption that it is formed of a superposition of two parabolic layers, $F1$ and $F2$ as shown in Figure 1. The dotted lines represent the two layers separately and the full line shows the over-all ionization distribution of the F region. Since for a parabolic layer of semithickness y_m and maximum

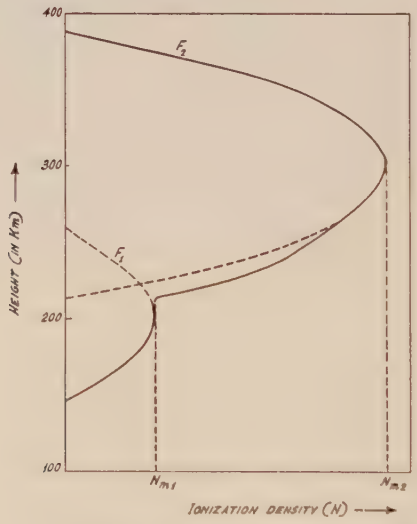

FIG. 1—PARABOLIC IONIZATION DISTRIBUTIONS OF THE F1 AND F2 REGIONS, AS ASSUMED FOR CALCULATING THE TOTAL ION CONTENT OF THE COMPOSITE F REGION MADE UP OF F1 AND F2

ionization density N_m , the total ion content (in a column of unit cross-section) is given by $4/3(y_m N_m)$, the total ion content for the composite F region is given by $4/3(y_{m1}N_{m1} + y_{m2}N_{m2})$, where the subscripts 1 and 2 refer, respectively, to the regions $F1$ and $F2$.

If the complicating effect of the terrestrial magnetic field is neglected then,

$$N_{m1} = \frac{\pi m}{e^2}(f^{\circ}F1)^2 \qquad \text{and} \qquad N_{m2} = \frac{\pi m}{e^2}(f^{\circ}F2)^2$$

where $f^{\circ}F1$ is the critical penetration frequency for the $F1$ region and $f^{\circ}F2$ is that for the $F2$ region. The total ion content for the F region (n_T), taken as a whole, is therefore given by

$$n_T = \frac{4}{3}\frac{\pi m}{e^2}(y_{m1}\overline{f^{\circ}F1^2} + y_{m2}\overline{f^{\circ}F2^2})$$

$$= \frac{4}{3} \times 1.24 \times 10^4 \times 10^5(y_{m1}\overline{f^{\circ}F1^2} + y_{m2}\overline{f^{\circ}F2^2})$$

where semithicknesses are measured in km and frequencies in Mc/s. Hence,

$$n_T = 1.653 \times 10^9(y_{m1}\overline{f^{\circ}F1^2} + y_{m2}\overline{f^{\circ}F2^2})$$

Similarly for the $F2$ region alone, the ion content n_2 is given by

$$n_2 = 1.653 \times 10^9(y_{m2}\overline{f^{\circ}F2^2})$$

In carrying out numerical computations, the semithickness of the $F1$ layer, where no data regarding its actual value are available, will be taken as 100 km, after Ratcliffe [3]. In cases where there is no bifurcation, that is, in cases where only the regular $F1$ maximum is present, the layer will be treated as a simple parabolic one and the calculations made accordingly.

Note: It has been the usual practice to call the single layer, in the absence of bifurcation, the $F2$ layer. But, according to the current theory, this single layer ought to be called the $F1$ layer. The height at which this single layer is observed is also in conformity with this nomenclature.

3. RESULTS OF ANALYSIS

The results of analysis of the three stations (Slough, Falkland Islands, and Singapore) are presented in graphical forms in Figures 2 to 5. It will be seen from the graphs that the monthly mean diurnal variations of $f^{\circ}F2$ (critical penetration frequency of the $F2$ region), n_2 ("total" ion content of the $F2$ region), and n_T ("total" ion content of the composite F region) for these three stations are more or less regular in the winter solstices and also in the equinoxes. But, with the approach of summer, when the "bifurcation" of the F region becomes prominent, variations of $f^{\circ}F2$ become "anomalous" and the n_2 variations also become irregular. But even then, the n_T variations maintain their regularity. Let us consider these variations in some detail.

Figures 2 (*a*), (*b*), and (*c*) show the diurnal variation curves of the monthly mean values for the month of March (equinox) 1951 for the three stations. The curves of n_2 and n_T are similar and show sharp primary maxima at noon and small secondary maxima at midnight. These maxima are caused by the effects of solar tides as explained later. Disregarding these maxima, all the curves of $f^{\circ}F2$, n_2 , and n_T show a more or less regular variation for the equinox month.

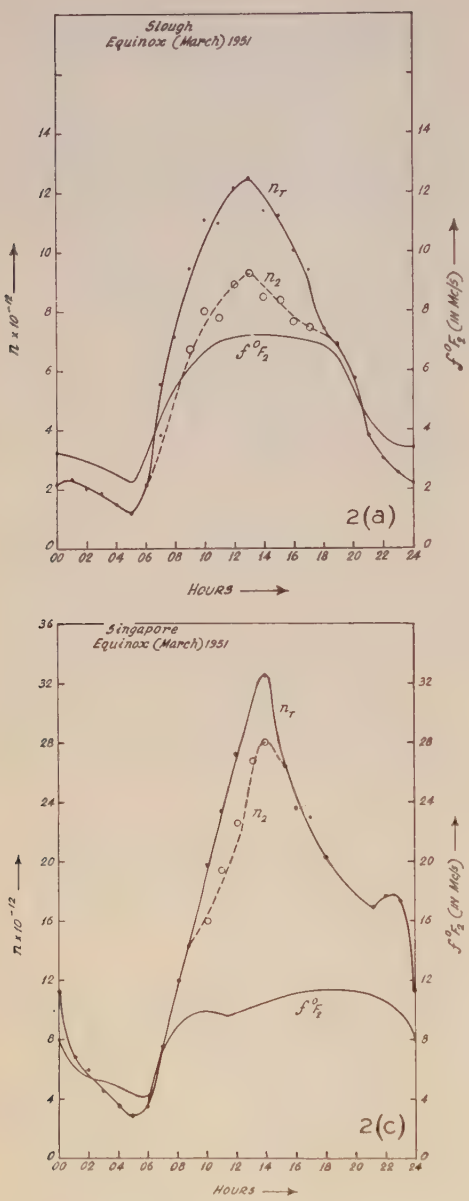

FIG. 2—DIURNAL VARIATION CURVES FOR THE MONTHLY MEAN VALUES OF $f^{\circ}F2$, n_2, AND n_T DURING EQUINOX (MARCH) 1951: (a) SLOUGH, (b) FALKLAND ISLANDS, AND (c) SINGAPORE; IT IS TO BE NOTED THAT FOR THIS SEASON, THE CURVES FOR ALL THE PARAMETERS ARE MORE OR LESS SMOOTH; n_2 AND n_T CURVES, HOWEVER, HAVE TWO PEAKS, WHICH ARE ASCRIBED TO TIDAL EFFECTS

Figures 3 (*a*), (*b*), and (*c*) depict the diurnal variation curves for the monthly mean values of the summer solstice, 1951 (that is, June in the northern hemisphere and December in the southern hemisphere). Here the variations in the values of $f^{\circ}F2$ and n_2 for Slough and for Falkland Islands show several maxima and minima and are most irregular. n_T , however, has a surprisingly regular variation for both the stations, there being only a secondary peak at midnight due to the tidal effects. For Singapore also, the values of $f^{\circ}F2$ and n_2 show some irregulari-

ties. The n_T variation, however, has none of these, and retains its regularity as in the previous cases.

Figures 4(*a*), (*b*), and (*c*) show the diurnal variation curves of the monthly mean values for the winter solstice of 1951 (that is, December in the northern hemisphere and June in the southern hemisphere). Here all the parameters vary quite normally for Slough and also for Falkland Islands. The variations are also normal for Singapore, except that the n_2 and n_T maxima are rather peaky due to the tidal effects.

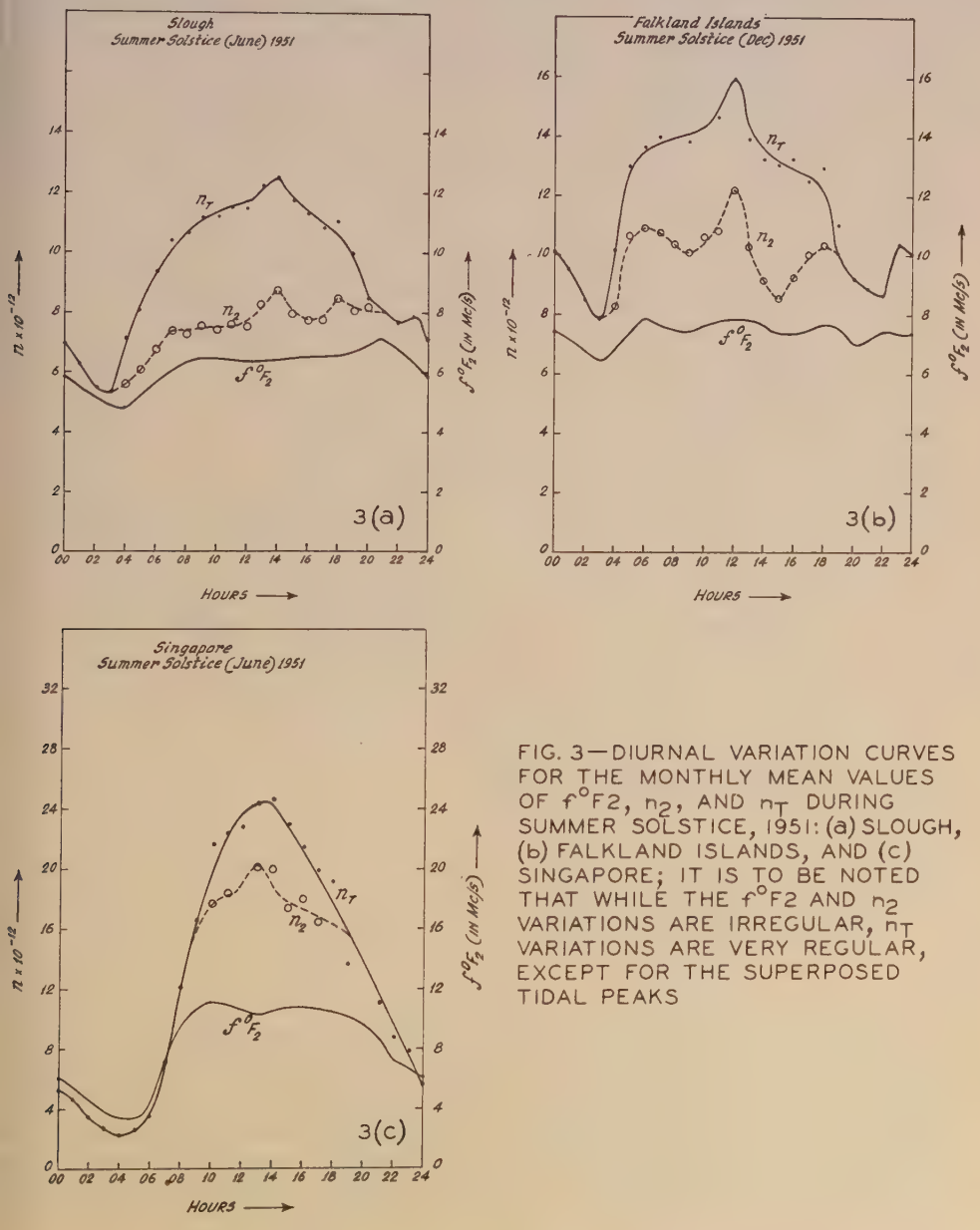

FIG. 3—DIURNAL VARIATION CURVES FOR THE MONTHLY MEAN VALUES OF $f^{\circ}F2$, n_2, AND n_T DURING SUMMER SOLSTICE, 1951: (a) SLOUGH, (b) FALKLAND ISLANDS, AND (c) SINGAPORE; IT IS TO BE NOTED THAT WHILE THE $f^{\circ}F2$ AND n_2 VARIATIONS ARE IRREGULAR, n_T VARIATIONS ARE VERY REGULAR, EXCEPT FOR THE SUPERPOSED TIDAL PEAKS

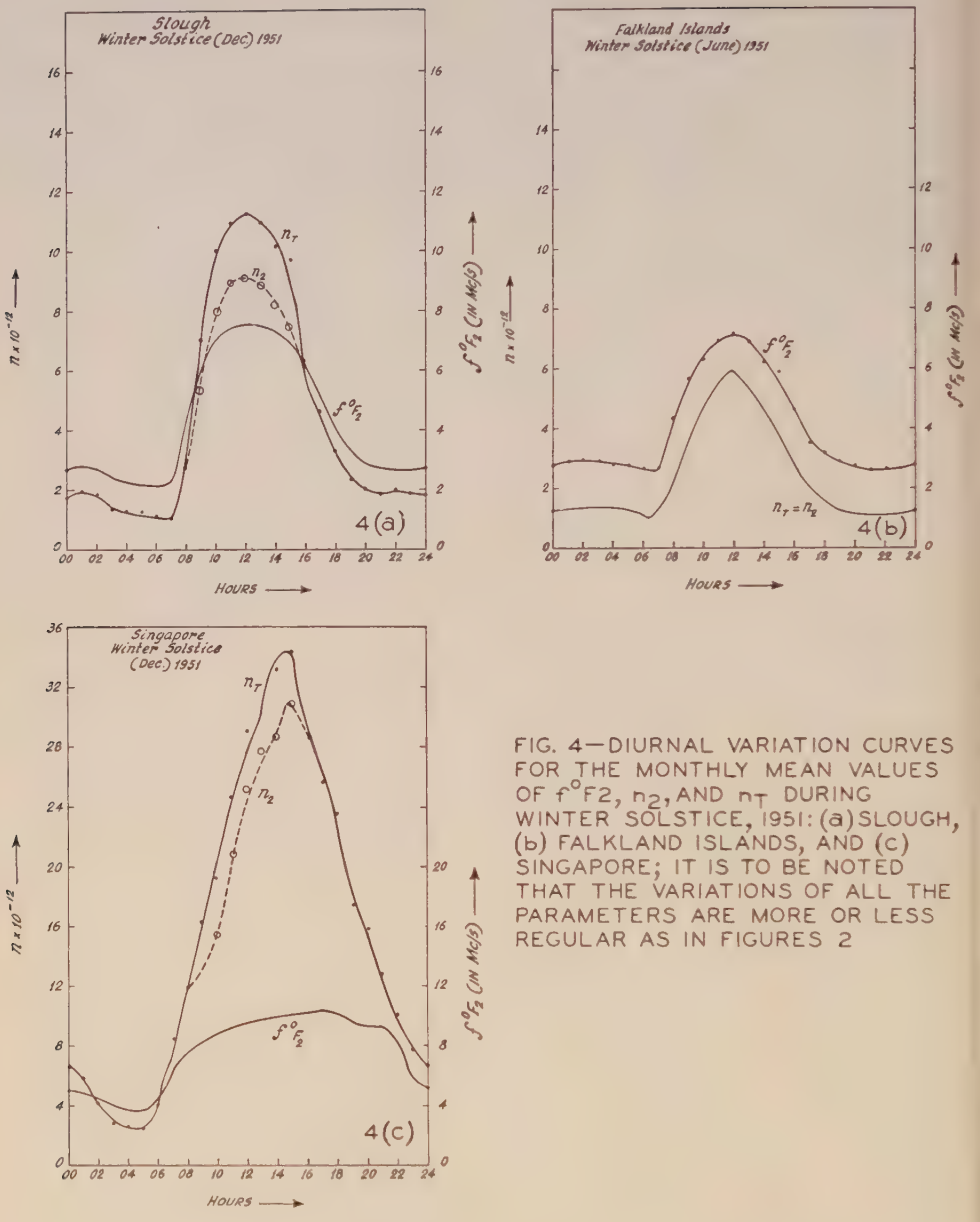

FIG. 4—DIURNAL VARIATION CURVES FOR THE MONTHLY MEAN VALUES OF f°F2, n_2, AND n_T DURING WINTER SOLSTICE, 1951: (a) SLOUGH, (b) FALKLAND ISLANDS, AND (c) SINGAPORE; IT IS TO BE NOTED THAT THE VARIATIONS OF ALL THE PARAMETERS ARE MORE OR LESS REGULAR AS IN FIGURES 2

Figures 5(*a*), (*b*), and (*c*) show the seasonal variation curves of the monthly mean noon values of $f°F2$, n_2 , and n_T for the same three stations, year 1951. For Slough [Fig. 5(*a*)], the value of n_T varies smoothly with a principal maximum in May and a secondary one in October. For Falkland Islands [Fig. 5(*b*)], on the other hand, the principal maximum is in October and a secondary during March-April. For Singapore [Fig. 5(*c*)], n_T has the principal maximum in October-Nov-

ember and a secondary during March-April. These seasonal variation effects result from solar tides and are discussed in the next section.

4. DISCUSSIONS ON THE OBSERVED RESULTS

As mentioned in the introduction, according to the current theory, the $F2$ region is produced by a sort of bifurcation process of the $F1$ region, which latter is produced in the usual manner by the Chapman process—ionization of oxygen atoms by solar rays of appropriate wavelengths. Two processes of bifurcation have been suggested, as follows:

According to the first, the rising temperature gradient and decreasing recom-

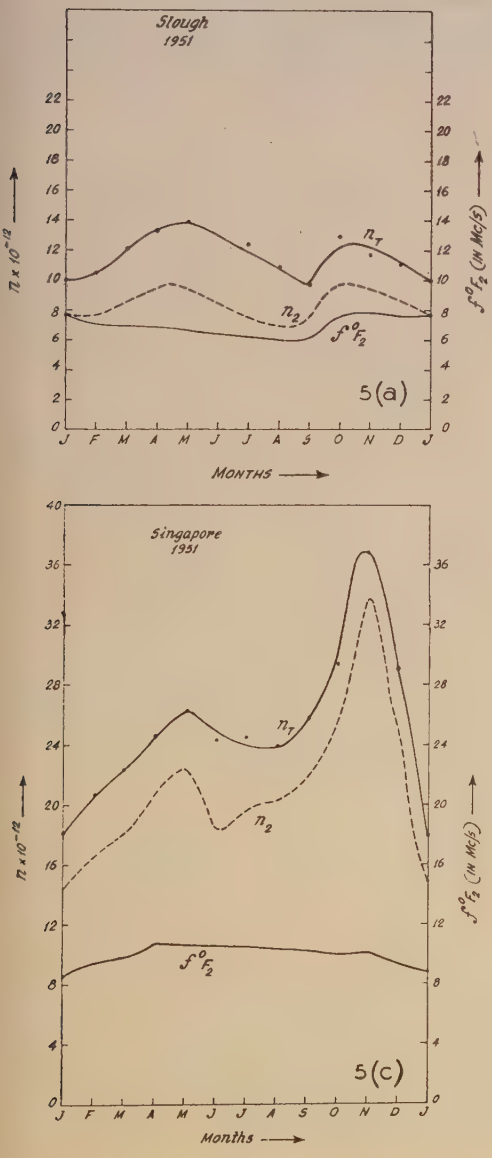

FIG. 5—SEASONAL VARIATION CURVES OF THE MONTHLY MEAN VALUES OF f^0F2, n_2, AND n_T IN 1951: (a) SLOUGH, (b) FALKLAND ISLANDS, AND (c) SINGAPORE; THERE ARE TWO MAXIMA IN ALL THE CURVES OF n_T, WHICH ARE EXPLAINED AS DUE TO TIDAL EFFECTS

bination coefficient that are known to exist above the $F1$ maximum cause a spread of $F1$ ionization to great heights, increasing the ionization density in the upper parts of this region to values much beyond what would be expected of a normal Chapman layer (that is, in an isothermal atmosphere). This causes a secondary maximum ($F2$) to appear above the $F1$ maximum [4, 5, 6]. It is clear that as there may not be sufficient time for attainment of equilibrium condition, the variation of the temperature gradient with height may not follow the zenithal position of the sun. Also, as the value of recombination coefficient depends on the temperature, the ionization will vary in a manner not simply related to the solar zenith angle.

The second hypothesis is based on Martyn's theory of tides in the ionosphere. According to this theory, though tidal motions of the neutral atmospheric particles are mainly horizontal, those of the ions have generally a large vertical component due to the electrodynamical forces developed [7, 8, 9]. There may thus be vertical transport of ions, lowering the density at one height and increasing that at others. This effect may easily be conceived as causing a secondary maximum to appear above the usual $F1$ maximum.

In connection with the tidal hypothesis, it is to be noted that, besides the proper tidal motions (due to the gravitational pull of the sun, amplified greatly by the well-known resonance effect), there are also tide-like motions due to world-wide temperature gradients developed by the diurnal heating and cooling of the atmosphere. There is, in fact, a strong semidiurnal component of this effect, as evidenced by the atmospheric pressure oscillations, the magnitude of which is nearly the same as that due to tidal motions (see ref. [1], p. 38).

Now, while the variation of the total ion content (n_T) of the composite F region depends on the variation of the total absorption of the appropriate solar ionizing radiations, that of the $F2$ maximum (or n_2) depends on the manner in which the parameters involved in the bifurcation process vary according to one or the other hypothesis. Hence, the variation of the former will be expected to follow more closely the zenithal position of the sun than that of the latter.

However, we see from Figures 2, 3, and 4 (and as also pointed out in section 3), that there are significant peaks in the n_T curves superposed on otherwise smooth diurnal variations. This means that the thermal or and tidal motions as may produce the bifurcation are not mainly vertical, but have also large horizontal components as well. This conclusion is in conformity with the results of ionospheric observations which indicate the presence of geostrophic winds in the high atmospheric regions [10].

Now, the main effect of the semidiurnal tidal movement is the production of two pressure maxima, one round noon and the other round midnight. Maxima corresponding to these are also seen to be present in all the diurnal variation curves more or less prominently, the midnight maximum being much less prominent due to the low density of ionization at such hour. Indeed, in most of such n_T curves, the midday maximum is seen much more prominently than in the $f^{\circ}F2$ curves. (It is to be noted that as the diurnal variation curves are the monthly mean values, the effect of lunar tide, if any, related to the lunar day, has been eliminated.)

Again, both the ionizing effect of solar radiation and the tidal effect of the

solar gravitational pull have seasonal components due to the tilt of the earth's axis with reference to the ecliptic. The former produces maximum ionization during local summer when the zenithal distance of the sun is minimum; the latter produces a shift in the phase of the diurnal tide, which is most marked during solstices and is absent during the equinoxes [11]. The effect of this phase shift, coupled with that of the seasonal intensity variation of the ionizing radiation, produces two maxima in the seasonal variation curve of the noon-time n_T values. One of these is between the summer solstice and vernal equinox, and the other near the autumnal equinox, as shown in Figures 5(*a*), (*b*), and (*c*). It may be noted that Singapore, which is geographically north (1°19′) but magnetically south (about 10°), shows a variation analogous to the southern station, Falkland Islands. This shows the predominant geomagnetic control on the F region ionization, as suggested earlier by Appleton [12].

5. CONCLUSION

It is to be noted that in carrying out the calculations the following approximations had to be made:

(1) Both $F1$ and $F2$ regions are assumed to have parabolic distribution of ionization.

(2) The $F1$ layer has been assumed throughout to have a semithickness of 100 km.

(3) The effects of the earth's magnetic field have been neglected. These approximations do effect the calculated results significantly, so far as the absolute values of the ion contents are concerned, even up to 20 to 30 per cent, according to Ratcliffe [2]. According to the same author, however, the nature of the relative variations of the total ion content, as obtained, is much less in error.

It may also be noted that the stations studied are only those for which the data published by Radio Research Board, Department of Scientific and Industrial Research, England, are available. This is because the semithickness values of the $F2$ region which are essential for the computation are not given in the data published by the Central Radio Propagation Laboratory, National Bureau of Standards, Washington, D.C., and other organizations. It is, however, not unreasonable to conclude that when similar computations will be possible for other stations, with the $F2$ semithickness data available, similar results will also be found for them. The regularities observed in the behaviour of n_T may thus be regarded as significant and support the hypothesis that $F1$ and $F2$ have a common origin of ionization.

6. ACKNOWLEDGMENT

My grateful thanks are due to Prof. S. K. Mitra for his constant guidance, help, and encouragement throughout the progress of the work. Thanks are also due to the Scientific Man Power Committee, Government of India, for financial help. I am also indebted to the Radio Research Board, Department of Scientific and Industrial Research, England, for providing us with their data.

References

[1] S. K. Mitra, The upper atmosphere, Calcutta, Asiatic Society of Bengal, 2nd ed., 294 (1952).
[2] J. A. Ratcliffe, J. Geophys. Res., **56**, 487 (1951).
[3] J. A. Ratcliffe, J. Geophys. Res., **56**, 463 (1951).
[4] D. R. Bates and H. S. W. Massey, Proc. R. Soc., A, **187**, 261 (1946).
[5] F. L. Mohler, J. Res., Nation. Bur. Stan., **25**, 507 (1940).
[6] A. P. Mitra, Indian J. Phys., **26**, 79 (1952).
[7] D. F. Martyn, Proc. R. Soc., A, **189**, 241 (1947).
[8] D. F. Martyn, Proc. R. Soc., A, **194**, 429 (1948).
[9] D. F. Martyn, Proc. R. Soc., A, **194**, 445 (1948).
[10] G. H. Munro, Nature, **162**, 806 (1948).
[11] A. P. Mitra, J. Atmos. Terr. Phys., **1**, 286 (1951).
[12] E. V. Appleton, Nature, **144**, 151 (1939).

RADIO NOISE FROM AURORA*

By R. P. Chapman and B. W. Currie

Physics Department, University of Saskatchewan, Saskatoon, Saskatchewan, Canada

(Received March 9, 1953)

ABSTRACT

A search for radio noise of 10-cm wavelength from aurora during 1951 and 1952 with improved equipment was unsuccessful. The failure to detect the auroral radio noise, observed previously in 1949, is attributed to the decrease of the intensity of auroral displays and of sunspot-activity.

1—INTRODUCTION

Incidental to a search during 1948 and 1949 for radio echoes of 10-cm wavelength from aurora, short pulses of radiation were observed on the receiver of the radar set even when the transmitter was off [see 1 of "References" at end of paper]. The auroral origin of these pulses was checked by adding a discriminating circuit and a counting rate meter to the receiver and attaching a remotely-controlled auroral camera to the antenna. Further observations at that time showed that the pulses were most numerous whenever the antenna was directed at bright, active types of aurora, that they came in bursts lasting only a small fraction of a second, and that each pulse was from one to five microseconds in duration.

An investigation [2] of known mechanisms conceivably responsible for radiation of this wavelength from aurora showed that only a plasma type of oscillation was likely to radiate sufficient energy to be detected by our receiver [detectable power density, 2×10^{-16} watt per (meter)^2 per cycle band-width] without assuming improbable values either for the volume of the radiating region or for ionic densities and temperatures at auroral levels. Although a plasma origin for the pulses appeared the most reasonable, it still implied that fairly regular distributions of electrons with densities of the order of 10^{11} per cm^3 existed within auroral structures for at least brief intervals of time [3,4]. For these reasons, an intensive search was made during the past year (1951-52) for radio noise of this wavelength after a number of improvements had been made in the receiving and detecting circuits to reduce noise of internal and local origin and to increase their sensitivity to pulses of a duration of a few microseconds.

2—EQUIPMENT AND PROCEDURE

The receiver was part of the British type 271 radar unit. A voltage regulator to improve the stability of the receiver and filters to eliminate external interferences were placed in the power lines to the receiver. The motor alternator

*Investigation supported financially by the Defense Research Board of Canada.

supplying the 500-cycle power for the receiver was replaced by a conventional type of power supply operating off the A.C. mains. The pulsed klystron in the receiver (effective only one-fourth of the time) was replaced by a type 417-A klystron operating continuously. The discriminator and counter circuits were modified so that the dead-time following each pulse was reduced from several milliseconds to 60 microseconds. A recording milliammeter was added to the counter. The auroral camera on the antenna was replaced by the phototube of an auroral detector of the same general type as used at this Laboratory for recording the occurrence and intensity of aurora [5]. These changes increased the power sensitivity of the receiver at least 30 times and the number of radio pulses that could be detected per unit time several hundred times.

Two different procedures were followed in the search for pulses. One consisted of setting the discriminator so that small numbers of pulse, due to the local noise, were appearing on the pulse recorder; directing the antenna alternately at auroral structures and at aurora-free sky; and comparing the numbers of pulses for the two positions. The other consisted of setting the discriminator so that only the very occasional pulse appeared on the pulse recorder; keeping the antenna in a fixed position pointing toward the north; and correlating the occurrences of pulses with changes of intensity of aurora within the angular field of the antenna. In the latter case, the pulse voltages were superimposed on the voltages from the auroral recorder so that deflections due to the two were in opposite senses. This made it possible to decide whether or not a pulse was coincident with an increase of auroral intensity to within a time limit of a second.

3—RESULTS AND DISCUSSION

Neither procedure indicated the occurrence of noise attributable to aurora. Several reasons for this result can be suggested. The original observations were faulty, noise pulses of local origin having been associated incorrectly with aurora; an unknown source of 10-cm waves was in operation during 1949, and the waves from it were either reflected or scattered by auroral structures to our receiver; the noise pulses are much weaker now than they were in 1949, and could only be picked up by a more sensitive receiver; and pulses of this wavelength are not occurring with the present auroral displays.

A re-examination of the 1949 data confirmed the original conclusions. While irregular fluctuations of amplitude in the random noise detected by a receiver are to be expected, an increase in both the number and the intensity of the noise pulses whenever the antenna is pointing toward aurora is most improbable. This happened many times during the course of 17 displays between January 17 and June 7. During this period, noise was not detected with eight other displays. Six of these were during the last week of April and May. At that time, the failure to observe noise was attributed to a decrease in the sensitivity of the equipment. In view of our later observations, it is now suggested that the aurora was not emitting noise on these occasions.

The possibility that the observed pulses were either reflected or scattered by aurora cannot be eliminated completely. Radar echoes of 10-cm wavelength (frequency, 3,000 Mc/sec) from aurora have never been observed in our search

for them, although echoes of frequencies 106 and 56 Mc/sec are regularly observed [6]. A study of the relative amplitudes and occurrences of echoes of these frequencies shows that they arise by critical reflection from highly ionized regions within auroral structures [7]. Critical reflection of 3,000 Mc/sec waves would require electron densities of the order of 10^{11} per cm^3. Since this is only about a thousand times greater than the electron densities required for echoes at the lower frequencies, it is possible that such a high electron density occurs sporadically in auroral structures, and persists long enough to give detectable 10-cm echoes from a source operating continuously. Such echoes might not be detected by a search radar because of its pulse-width and recurrence frequency (1 microsecond and 500 per second, respectively, in our case). No source of 10-cm waves is known to have been operating close to Saskatoon during the period when the auroral radio noise was observed. Also, pulses were observed in 1949 throughout the tunable range of the receiver (about 200 Mc).

If radio noise from aurora is due to oscillations within an electron plasma, the third and fourth reasons suggested for failure to observe noise at this time are not necessarily exclusive. The evidence [8,9] is now definite that protons of moderate velocity enter the atmosphere at times during auroral displays. Although their ionization efficiency is not known exactly, they are probably the primary cause for the high electron densities required for the reflection of radio waves and other ionospheric effects associated with aurora [10,11]. A decrease in the number of protons entering the atmosphere would decrease the mean electron density of the electron plasma. Changes in the uniformity and the cross-sectional area of the proton beams would alter the regularity and the volume of the electron plasma. A decrease in the velocities of the incident protons could lower their effectiveness as ionizers—the protons failing to penetrate to levels with sufficient particles to produce the required electron densities. The best estimates of particle densities show an increase from about 2×10^{11} per cm^3 at 140 km to 4.4×10^{14} at 84 km.

Substantial reasons exist for believing that changes of this type to the proton beams have occurred since 1949. Figure 1 compares the monthly mean values of

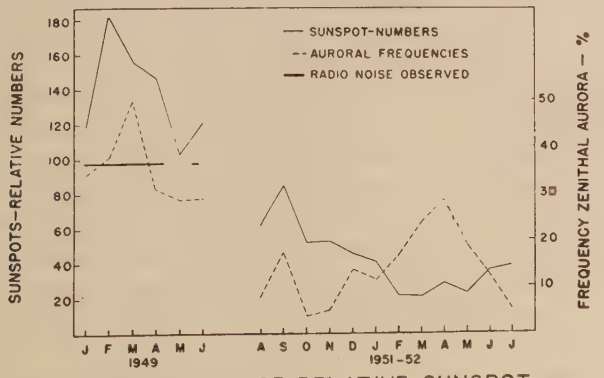

FIG. 1—COMPARISON OF RELATIVE SUNSPOT-NUMBERS AND FREQUENCIES OF ZENITHAL AURORA FOR 1949, WHEN RADIO NOISE WAS OBSERVED, WITH THE CORRESPONDING QUANTITIES FOR 1951-52, WHEN NOISE WAS NOT OBSERVED

the relative sunspot-numbers and the frequencies of occurrence of zenithal aurora at Saskatoon for January to June, inclusive, 1949, with the corresponding values for August, 1951, to July, 1952. The auroral frequencies are expressed as a percentage ratio of the number of 10-minute intervals with aurora to the corresponding number of periods when the skies were sufficiently clear for aurora to have been detected by the auroral recorder. The frequency of zenithal aurora at places to the south of the zone of maximum auroral occurrence is a particularly sensitive test of the intensity of displays, since the more intense a display the farther it usually spreads into lower latitudes. From the Figure, it is apparent that radio noise was observed only during the months with large relative sunspot-numbers and with intense auroral displays. The period in April and May, 1949, when noise was not observed is particularly interesting. Late in April the daily relative sunspot-number dropped to 122, and remained below this value for all except four days in May. Noise was observed again during the first week of June when the sunspot-number was close to or above 120. These and the later observations indicate that 10-cm radio noise from aurora does not occur until the relative sunspot-numbers are above 120.

A change in the auroral recorder in 1950 from one directed only at the zenithal sky to one scanning the sky along the geomagnetic meridian through Saskatoon from the northern to the sourthern horizon makes it impossible to compare directly the intensities of the displays for the two periods. However, since January, 1951, the fraction of the time with bright, zenithal aurora has decreased from about one-tenth to less than one-thirty-fourth. This agrees with the visual observations, the bright, active portions of displays at the present time lasting only for minutes, whereas in 1948 and 1949 they sometimes lasted for hours.

Visual observations of aurora taken at Churchill and other places in Canada close to the auroral zone indicate that the auroral zone is several hundred kilometres farther south at sunspot-maximum than at sunspot-minimum [12]. From Martyn's [13] extension of the Chapman-Ferraro theory of magnetic storms, the angular distance (θ) from the geomagnetic pole to the auroral zone may be expressed in the form

$$\sin^2 \theta = (40\pi N m u^2)^{1/6}$$

where N is the number-density and m is the mass of the particles in the solar stream approaching the earth, and u is the velocity of approach of the stream. A decrease of θ (corresponding to a movement of the auroral zone northward), requires a decrease of either N or u, or of both. This lends further support to the belief that radio noise of 10-cm wavelength was observed in 1949, and is not detectable at the present time because of the decrease in solar activity.

For anyone attempting to observe radio noise from aurora, another point is worth noting. The observations of radio echoes from aurora [6] show that centers with the highest electron densities are closest to the zone of maximum auroral occurrence. In order to reduce the inverse-square attenuation of the signals, the receiver should be placed fairly close to the auroral zone. A site directly below an auroral display reduces the probable number of pulses because of the small auroral volume within the angular field of the antenna. The largest pulse rates in 1949

were observed when the antenna was pointed at auroras less than 30° above the northern horizon.

References

[1] P. A. Forsyth, W. Petrie, and B. W. Currie, Nature, **164**, 453 (1949).
[2] P. A. Forsyth, W. Petrie, and B. W. Currie, Can. J. Res., A, **28**, 324 (1950).
[3] L. Tonks and I. Langmuir, Phys. Rev., **33**, 195 (1929).
[4] M. Ryle, Proc. Phys. Soc., A, **62**, 483 (1949).
[5] W. D. Penn and B. W. Currie, Can. J. Res., A, **27**, 45 (1949).
[6] B. W. Currie, P. A. Forsyth, and F. E. Vawter, J. Geophys. Res., **58**, 179 (1953).
[7] P. A. Forsyth, J. Geophys. Res., **58**, 53 (1953).
[8] C. W. Gartlein, Nature, **167**, 277 (1951).
[9] A. B. Meinel, Phys. Rev., **80**, 1096 (1950).
[10] W. Petrie, Scientific Report AR-1, Geophysics Research Division, Air Force Cambridge Research Center (1950).
[11] W. Petrie, Scientific Report AR-2, Geophysics Research Division, Air Force Cambridge Research Center (1951).
[12] F. T. Davies, Trans. Oslo Meeting, 1948; Internat. Union Geod. Geophys., Assoc. Terr. Mag. Electr., Bull. No. 13, 255 (1950).
[13] D. F. Martyn, Nature, **167**, 92 (1951).

Journal of Geophysical Research Volume 58, No. 3 September, 1953

MEASUREMENTS OF THE INNER ZODIACAL LIGHT DURING THE TOTAL SOLAR ECLIPSE OF FEBRUARY 25, 1952*

By Wm. A. Rense, James M. Jackson, and Barbara Todd

Department of Physics, University of Colorado, Boulder, Colorado

(Received March 12, 1953)

ABSTRACT

Photographs of the skylight in the vicinity of the eclipsed sun were taken during the total eclipse of February 25, 1952, at a point in the shadow path near the Red Sea in Saudi Arabia at an altitude of 32,000 feet.

A photometric analysis of the photographs yielded information about the intensities and degree of polarization of the zodiacal glow between 5°.5 and 13° from the sun. The data are consistent with the planetary dust-cloud theory of the origin of the light, and tie in previous observations of the glow beyond 30° of the sun with those of the solar corona within 3° of the sun.

INTRODUCTION

Although a few eclipse observers have reported at various times that the zodiacal light may be seen during a total eclipse, no measurements of the light had ever been made. Accordingly, it was proposed that a group from the University of Colorado Physics Department, under the auspices of the Air Force, undertake to photograph the sky in the region of the eclipsed sun during the solar eclipse of February 25, 1952, in the Near East, with the aim of detecting and measuring the zodiacal glow within the limits 5° to 15° of the sun. The plan was to fly high in the shadow path in a pressurized B-29 and effect the observation through a plastic astrodome. The reason for flying at a high altitude was twofold: to reduce the general sky brightness relative to the zodiacal glow, and to assure little or no interference from dust, clouds, etc., in the lower atmospheric layers. A Schmidt camera of aperture F/0.9, covering a field of radius 20°, was to be used. The sun was to be centered in the field and exposures so estimated that the whole of the sky in the neighborhood of the eclipsed sun would register with a density suitable for accurate photometric studies. A Polaroid filter was placed immediately in front of the film, so that polarizations as well as intensities could be determined later. The filter consisted of sixteen 22°.5 wedges, with points joining at the center of the film where the coronal image was to fall. Alternate strips transmitted light, the planes of polarization of which were at right-angles. The B-29 was to be based in Dhahran, Saudi Arabia, several days before the eclipse. It was scheduled to leave

*The research reported in this paper has been sponsored by the Geophysics Research Division of Air Force Cambridge Research Center under Contract W19-122 ac-9.

the base on the morning of the eclipse and fly into the path of the moon's shadow at an altitude of about 30,000 feet, at a point north of Mecca above the desert sands near the Red Sea.

OBSERVATIONS

All the above plans were successfully carried out. The photographs were taken $09^h\ 36^m.3$ GCT at 32,000 feet above sea-level, over a point indicated on the map in Figure 1. The eclipse itself as viewed from that height was a fascinating spectacle.

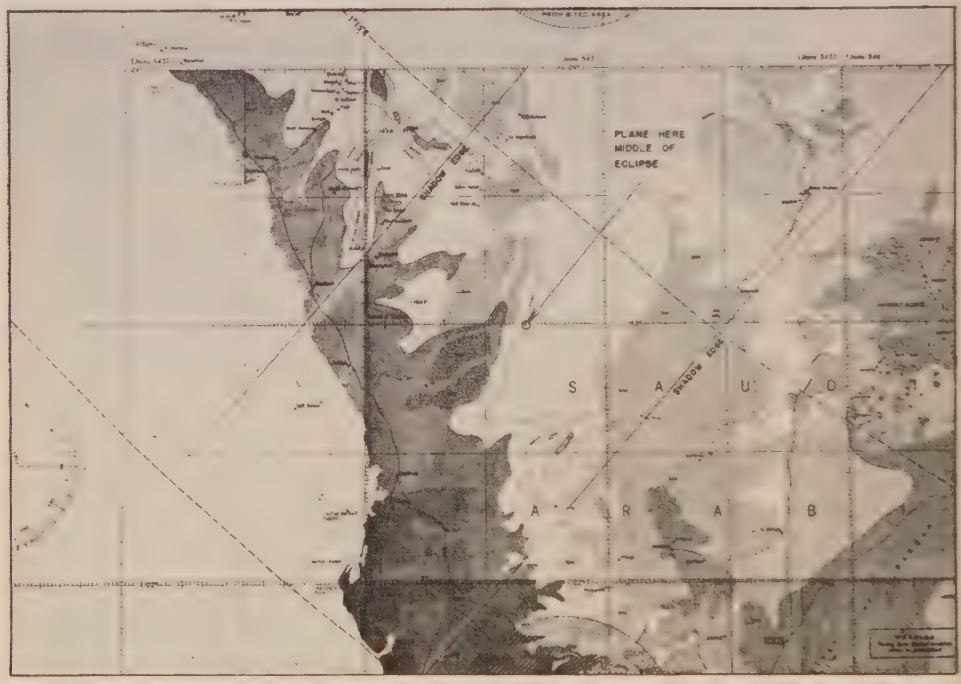

FIG. 1—MAP SHOWING WHERE OBSERVATIONS OF THE ZODIACAL LIGHT DURING THE TOTAL SOLAR ECLIPSE OF FEBRUARY 25, 1952, WERE MADE, THE PLANE FLYING AT 32,000 FEET ABOVE SEA-LEVEL AT THE TIME

The sky was perfectly clear with not a cloud above or below the plane. The ship was flying at a ground speed of 300 mi hr in the direction of the shadow, which could easily be seen on the sands below as it moved along with a relative velocity of about 1,200 mi/hr. The circular outline of the 70-mile-diameter shadow was clearly evident. Circumscribing the main shadow was a 20-mile-wide brownish rim of variable intensity. The sky near the horizon was surprisingly bright at mid-totality with an appreciable amount of light coming from the desert beyond the shadow's rim. Within 60° of the sun the sky was quite dark, yet not so dark that stars could easily be seen. The silvery corona stood out clearly and a few small prominences were visible.

No window space was available for viewing a wide angle of the sky near the sun, and this fact, plus the confinement necessitated by the manipulation of the camera, precluded any naked-eye observations of the zodiacal light. Four photo-

graphs were obtained, with exposures around 0.2 second, on Kodak Super Ortho-press film. These were returned to the United States and developed three weeks after the eclipse. Two had been overexposed because of shutter failure, so that only two were suitable for analysis.

The reductions were carried out using density-intensity calibration curves derived from step-wedge exposures made on samples of the film adjacent to the portions used for the photographs.

Intensities were corrected for intrinsic instrumental variations and scattering. The scattering corrections were negligible, but the former, which depend on distance from center of field, were considerable for large angles. The polarized wedge junctions prevented good readings for angles less than 5° from the sun, while edge effects restricted the maximum angle to 13°.

RESULTS

The results for film No. 1 are summarized in Table 1. Column 1 lists the angular distances from the sun for which calculations of zodiacal light intensities were made. Column 2 lists, in arbitrary units, the brightness of the sky for each angle, both for light polarized with electric vector parallel to the plane of incidence and for light polarized with electric vector perpendicular to the plane of incidence. The plane of incidence is determined by the line from the sun to the small cone of the sky under observation and the line along the cone to the observer.

TABLE 1

Angular distance from sun (1)	Sky brightness in arbitrary units (2)		Total sky brightness (3)	Total brightness zodiacal light (4)	Ratio, ρ, polarized components of zodiacal light (5)
	∥	⊥			
°			*ergs/cm²/sec/steradian*	*ergs/cm²/sec/steradian*	
5.5	297	353	0.342	0.144	0.80
7.0	285	337	0.328	0.116	0.79
8.5	271	317	0.309	0.086	0.79
10.0	271	315	0.308	0.071	0.78
11.5	270	311	0.305	0.055	0.77
13.0	271	312	0.305	0.040	0.74

The intensities were obtained from a graph of the photometric data in polar coordinates. Intensity was plotted against azimuth with respect to the sun for each elongation angle. The isophotes were not far from circles in the vicinity of the sun, showing definite ellipticity only at the larger distances from the sun (solar elongations). This is consistent with the belief [see 1 of "References" at end of paper] that the zodiacal light is not a narrow band here but extends well around the sun in all azimuths. Nevertheless, in finding the figures for Column 2, the position of the main axis of the glow was estimated from the graph and corre-

sponding readings on either side were taken and averaged. Final results proved to be almost independent of the choice of this axis.

The total brightness of the sky is given in Column 3 and that of the zodiacal light alone in Column 4, the units being ergs/cm^2/sec/steradian. These figures were found in the following way: The total brightness of the sky was assumed to have two components—sunlight scattered in the earth's atmosphere and the zodiacal light. Regarding the first, little quantitative information is available. But in order to determine the contribution of the zodiacal glow in an independent way, it is necessary to estimate or compute the general sky brightness caused by the first-mentioned component. Hulburt [2], in connection with observations of the variation of sky brightness at a given point with time during the total eclipse of October 1, 1940, set up a method whereby he was able to compute sky brightness caused by direct sunlight scattered from the upper atmosphere into the umbra, and by sunlight indirectly scattered into the umbra from the surrounding atmosphere illuminated by light in the penumbra. His equations were adopted here to calculate the relative variation of the sky brightness close to the eclipsed sun. Here the first of his constituents is negligible so that only the second need be calculated. This was done using the equation

$$b_u = \int_d^e \sigma n i_u \, dx$$

where b_u is the sky brightness, σ is the light scattering coefficient per molecule n is the molecular density of the atmosphere, i_u is the illumination in the umbra due to light scattered from the surrounding atmosphere, and x is the distance from the observer to a point in the atmosphere along the line of sight. The integration was performed from the center of the umbra to its edge for various elongations from the sun.

The fact that the plane was flying at 32,000 feet at the time of the observations had to be taken into consideration in finding the integral. Using Hulburt's values for σ, n, and i_u , the integration was performed graphically.

Absolute values of brightness obtained by the integration were not used because these, as Hulbert found, are consistently much less than the observed brightness. It is assumed here that the integration does enable one to obtain the correct relationship between *relative* brightness and angular distance from the sun. One reason Hulburt's values may have been low is that he had neglected at higher levels direct illumination of the umbra by radiation from the sunlit ground outside the moon's shadow. Ignoring of this factor may have, however, little effect on relative brightness.

With the results on relative brightness of scattered sunlight available, it was necessary to arrive at an absolute value of the scattered light component for only one point. This was accomplished after first finding, from the eclipse photograph, the total sky brightness at 10° from the sun. Density measurements, camera constants, and film characteristics were available. Using the value of 1.25 as the average sensitivity of the film (Kodak Super Ortho-press), the value of 0.308 erg/cm^2/sec steradian was arrived at as the total brightness of the sky at 10° from the sun. The

zodiacal light brightness at this angular distance was found by extrapolating the averaged results of Elvey and Roach [3] for the region of the glow between 30° and 90° of the sun. This gave, after a conversion of units, 0.071 erg/cm^2/sec/steradian. Subtracting this value from the total brightness, one obtains 0.237 erg/cm^2/sec/steradian as the contribution to sky brightness due to scattered light in the earth's atmosphere for a region 10° from the eclipsed sun. With the information obtained from Hulburt's equation, absolute brightness of the scattered light component for each angle was then found and subtracted from the absolute brightness (Column 3, Table 1) computed from that of the known value at the 10° point and the relative values (sum of polarized parts) of Column 2 (Table 1). The result is Column 4 (Table 1), the zodiacal brightness in ergs/cm^2/sec/steradian for each elongation. The intensities of the zodiacal light components having vibrations parallel and perpendicular to the plane of incidence, respectively, were next computed. This was accomplished after allowing for the polarization of the scattered light constituent of the total light. The polarization of the scattered light was assumed to be uniform over the region of sky considered and to have a value of 0.89 for the ratio of the parallel and perpendicular components. This fraction was arrived at by plotting a curve of the ratio of components in Column 2 and extrapolating to longitudes ($> 20°$) where the zodiacal light intensity is a negligible fraction of the whole. The ratio of parallel to perpendicular components, ρ, is given in Column 5.

In Table 2 are shown the results obtained from film No. 2, using the same basic assumptions as for film No. 1. Because the two photographs were taken at different times and analyzed independently, the differences between Tables 1 and 2 provide a fair indication of the accuracy and reliability of the photometric techniques used. The probable errors of the absolute values of the intensities are nevertheless quite large, about 25 per cent. Considerable error is therefore expected in the polarization values. The results are regarded as correct only to a first-order approximation.

TABLE 2

Angular distance from sun (1)	Sky brightness in arbitrary units (2)		Total sky brightness (3)	Total brightness zodiacal light (4)	Ratio, ρ, polarized components of zodiacal light (5)
	∥	⊥			
°			*ergs/cm²/sec/steradian*	*ergs/cm²/sec/steradian*	
5.5	341	391	0.343	0.147	0.82
7.0	328	380	0.333	0.123	0.78
8.5	312	358	0.314	0.090	0.77
10.0	312	345	0.308	0.071	0.77
11.5	312	346	0.308	0.057	0.78
13.0	297	330	0.295	0.033	0.74

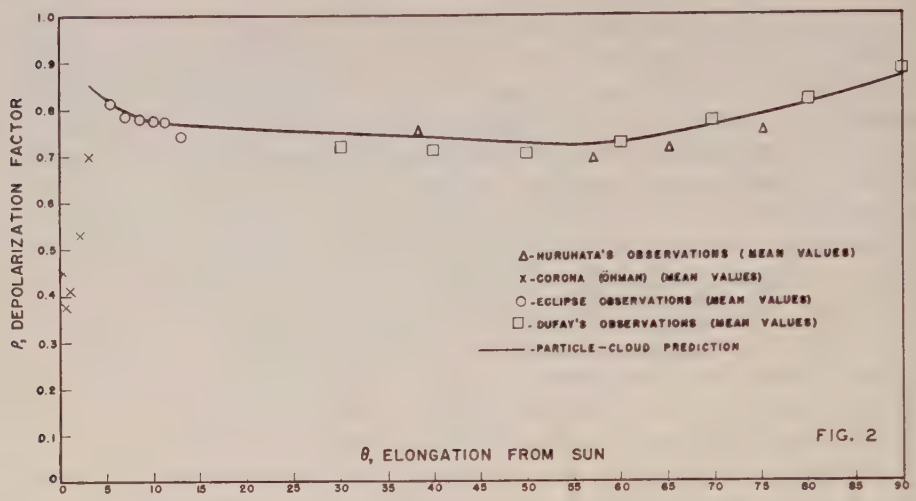

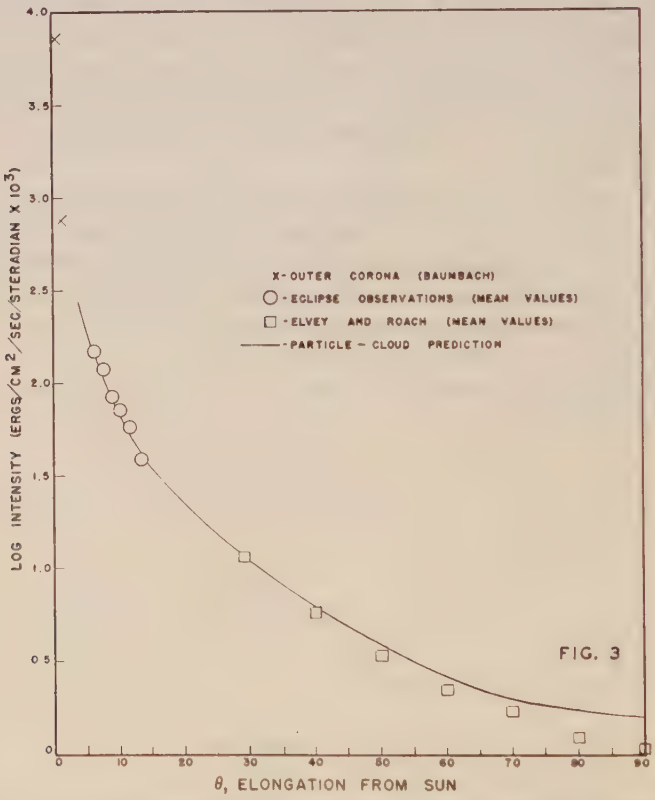

FIG. 2—THE RATIO, ρ, OF PARALLEL TO PERPENDICULAR ELECTRIC COMPONENTS OF LIGHT FROM ZODIACAL GLOW AS A FUNCTION OF θ, THE ANGULAR DISTANCE FROM SUN; THE LINE ROUGHLY REPRESENTS PREDICTED VARIATION ON THE BASIS OF THE PARTICLE-CLOUD THEORY

FIG. 3—THE GRAPH SHOWS HOW THE INTENSITY OF THE ZODIACAL LIGHT VARIES WITH θ, THE ANGULAR DISTANCE FROM SUN; THE LINE REFERS TO PREDICTION BY PARTICLE-CLOUD THEORY

SUMMARY AND CONCLUSIONS

Information about the brightness of the sky in the vicinity of the sun during a total solar eclipse is given in Tables 1 and 2. Each Table results from an independent analysis of a different photograph taken at 32,000 feet through the plastic dome of a B-29 during the total eclipse of February 25, 1952. The photographs were taken near the time of central eclipse. The sun's altitude was about 56°. In particular, for elongations between 5°.5 and 13° of the sun, relative and absolute values of the total sky brightness have been measured (Columns 2 and 3). Absolute values of zodiacal light have been computed (Column 4) with a minimum of assumptions. Polarization of the zodiacal light has also been expressed by computing the depolarization factor, ρ, which is the ratio of the components having electric vector parallel and perpendicular, respectively, to the plane of incidence (Column 5). The assumptions included the use of Hulburt's equation for finding relative sky intensity due to scattered light during an eclipse, and the extrapolation of known values of zodiacal light brightness at large solar elongations (30° to 40°) to obtain one value at smaller elongations (10°).

Expected values of the depolarization factor, ρ, and relative intensities of the zodiacal glow for various elongations from the sun, θ, have been computed by Rense [4] on the basis of the planet-dust theory and meteoritic reflection constants. These predicted values are shown by lines in Figures 2 and 3. The circles refer to the observed values obtained for smaller elongations (5° to 13°) by the writers during the eclipse of February 25, 1952. These values are the simple averages of Tables 1 and 2. Polarization data by Dufay [5], Öhman [6], and Huruhata [7], and intensity data by Elvey and Roach [3] (beyond 30°) and Baumbach [8] (corona) also appear in Figures 2 and 3. The eclipse data seem to be consistent with predictions of the planet-dust theory. The results also tend to confirm a point of view adopted by Van der Hulst in his discussion of the theory of the solar corona, namely, that the *F*-component of the corona is a continuous part of the cloud giving rise to the zodiacal light. Dust and solid chunks of material, which apparently cause the zodiacal glow for elongations greater than 5° by diffusely reflecting sunlight, must also contribute to the corona light (since the dust cloud scatters light along most of the line of sight), although diffraction effects treated by Van der Hulst [8] here become important. Because of the rise in temperature of the particles, the cloud must change its character at sufficiently small distances from the sun (about 0.1 astronomical unit) becoming, after evaporation is complete, an electron and molecular-like cloud, scattering light in a way (such as free electron scattering) different from that which prevails in other parts of the cloud. These facts help explain why the polarization in the corona is very great at points within 2° of the sun, but decreases rapidly for points $>3°$. For within 2°, the small but dense electron and molecular-like cloud would be very influential in determining intensity and polarization along the line of sight, whereas outside this limit its effect would rapidly diminish. At about 0.1 astronomical unit from the sun, solid particles once more can exist and the character of the scattering all along the line of sight is entirely that appropriate for a particle cloud. As shown in Figures 2 and 3, the eclipse results help fill the gap in the data on corona and zodiacal light intensities and polarizations. The coronal polarizations are for both components (*F* and *K*).

The *F*-component alone, however, according to Öhman [6] has little or no polarization, a fact which is consistent with the extension of the reflection curve in Figure 2.

Huruhata [7] finds evidence that the variations in brightness of the zodiacal light from season to season and from year to year are a result of the presence of meteoric particles along the orbit of the Comet Encke. His data on intensity and polarization of the zodiacal light point to a comet origin of the particles of the interplanetary cloud.

ACKNOWLEDGMENTS

The writers are greatly indebted to Dr. W. B. Pietenpol, of the Upper Air Laboratory, University of Colorado, and to the personnel of the Air Force Cambridge Research Center and the personnel of the 6531st Flight Test Squadron, Rome Air Development Center, Griffiss Air Force Base, Rome, New York, for their active cooperation in all phases of the work concerned with the preparation and carrying out of this research project.

References

[1] H. N. Russell, R. S. Dugan, and J. Q. Stewart, Astronomy, Boston, Ginn and Co., rev. ed., Vol. 1, 358 (1945).
[2] E. O. Hulburt, Nation. Geog. Soc., Contrib. Tech. Papers, Solar Eclipse Ser., No. 2, 78 (1942).
[3] C. T. Elvey and F. E. Roach, Astroph. J., **85**, 213 (1937).
[4] W. A. Rense, Astroph. J., **115**, 501 (1952).
[5] J. Dufay, J. Phys. Radium, **10**, 219 (1929).
[6] Y. Öhman, Pop. Astr. Tidskr., **27**, 133 (1946).
[7] M. Huruhata, Pub. Astr. Soc. Japan, **2**, 156 (1951).
[8] Cf. H. C. van der Hulst, Astroph. J., **105**, 471 (1947).

Journal of Geophysical Research Volume 58, No. 3 September, 1953

AURORAL RADIO-ECHO TABLE AND DIAGRAM FOR A STATION IN GEOMAGNETIC LATITUDE 56°

By Joseph C. Cain

Geophysical Institute of the University of Alaska, College, Alaska

(Received March 18, 1953)

ABSTRACT

Chapman has computed the echo geometry of radio signals reflected from auroras for the transmitter-receiver sites at geomagnetic colatitudes, $\alpha = 30°$, 45°, 60°, and 90°. This paper computes the echo geometry for $\alpha = 34°$, which is the geomagnetic colatitude of the Jodrell Bank Radio Experimental Station, of the University of Manchester, and is very close to that of the stations in northern United States which are concerned with radio echo work.

In a recent paper [see 1 of "References" at end of paper], Chapman has discussed the geometry of normal radio echoes from auroral ionized sheets, on the assumption that the reflecting elements are ionized rays lying along lines of force of the geomagnetic field. Numerical results were calculated for points in the geomagnetic meridian plane and also for points east and west of this plane. The meridian calculations gave the height h, distance d, and geomagnetic colatitude θ of an auroral reflecting point returning echoes at angular elevations e to a transmitting station in geomagnetic colatitude α. These quantities were determined for values of α ranging from 24° to 40° at 2° intervals, and for values of e ranging upwards at 2° intervals from 0° (signals transmitted and reflected horizontally) to the highest elevation possible at the station (this elevation does not, in general, fall in the series 0°, 2°, 4°, $\cdots$). These numerical results were shown graphically in a diagram from which values of h, d, and θ could be interpolated for intermediate values of e and α.

More extensive calculations were made for echoes not confined to the meridian plane, giving for any one station Q at geomagnetic colatitude α, the positions of echo points P higher than 60 km at 20-km intervals from which reflection occurs for beams of elevation e ranging from the horizon upwards at 2° intervals. Such points on the echo curves were specified both by their Cartesian coordinates x (northward horizontal), y (eastward or westward horizontal) and z (vertical from the horizon plane through Q), and alternately by the spherical coordinates e (elevation), ψ (azimuth east or west of geomagnetic north) and d (distance from Q to P). Also given were the geomagnetic colatitude θ of P and the horizontal distance R ($= d \cos e$) from Q to the projection P' of P on the horizontal plane through Q. To obtain for the given station Q any quantity u such as x, y, ψ, h, R, and θ for intermediate values of e and d by interpolation, it is convenient to con-

struct from the table a diagram showing lines of equal u as a function of e and d. But to represent the general distribution of reflecting points for beams of different elevation and azimuth, it seems most convenient to draw the plan diagram for these points. This diagram is obtained by projecting the points P on the horizontal plane through Q, and gives for each value of e the locus of the projection points P', the actual reflecting point P corresponding to P' being at a height R tan e above the plane. Such tables and diagrams were given by Chapman for values of geomagnetic colatitude $\alpha = 30°$, 45°, 60°, and 90° (the geomagnetic equator). Since these values are too widely spaced to permit accurate interpolation for intermediate values of α, any station undertaking the investigation of discrete radio echoes from aurora should have available a table and diagram computed and drawn for its own value of α.

TABLE 1—*Computed values for auroral radio-echo station at geomagnetic colatitude 34°*

Elevation and azimuth	h	R	x	$\pm y$	ψ	θ
	km	*km*	*km*	*km*	°	°
$e = 0°$	60	876	557	676	50.5	29.6
$\psi_0 = 90°$	80	1013	754	676	41.9	27.9
	100	1133	957	606	32.4	26.0
	120	1242	1166	428	20.2	23.9
	134	1311	1311	0	0	22.4
$e = 2°$	60	681	407	547	53.3	30.7
$\psi_0 = 84°.0$	80	814	570	581	45.5	29.3
	100	932	742	564	37.3	27.8
	120	1039	920	483	27.7	26.2
	140	1138	1105	272	13.8	24.3
	147	1170	1170	0	0	23.6
$e = 4°$	60	537	321	430	53.3	31.4
$\psi_0 = 78°.0$	80	660	458	476	46.1	30.2
	100	771	603	481	38.6	28.9
	120	873	756	437	30.0	27.6
	140	968	914	317	19.1	26.0
	154	1028	1028	0	0	24.9
$e = 6°$	60	432	272	336	51.0	31.7
$\psi_0 = 71°.8$	80	543	389	379	44.3	30.7
	100	645	514	390	37.2	29.6
	120	740	647	359	29.0	28.4
	140	828	786	260	18.3	27.1
	154	887	887	0	0	26.1
$e = 8°$	60	356	244	260	46.9	31.9
$\psi_0 = 65°.3$	80	455	346	295	40.5	31.0
	100	547	456	301	33.4	30.1
	120	633	574	268	25.1	29.0
	140	716	699	158	12.8	27.9
	147	745	745	0	0	27.4
$e = 10°$	60	300	226	198	41.2	32.0
$\psi_0 = 58°.5$	80	388	319	221	34.8	31.2
	100	470	418	215	27.2	30.3
	120	549	524	163	17.2	29.4
	134	602	602	0	0	28.7
$e = 12°$	60	258	215	143	33.7	32.1
$\psi_0 = 50°.9$	80	335	300	150	26.4	31.4
	100	409	392	120	17.0	30.5
	114	460	460	0	0	29.9
$e = 14°$	60	225	202	98	25.8	32.2
$\psi_0 = 42°.3$	80	294	282	84	16.6	31.5
	87	318	318	0	0	31.2

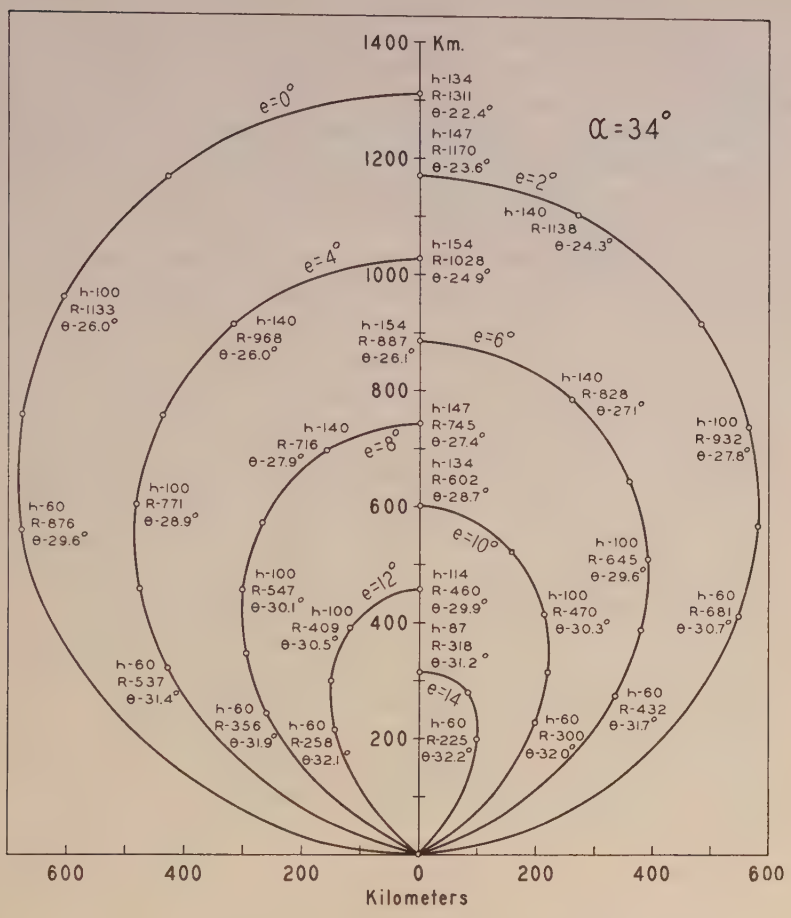

FIG. 1—PLAN DIAGRAM FOR AURORAL RADIO-ECHO STATION AT GEOMAGNETIC COLATITUDE 34°

As the geomagnetic colatitude of the Jodrell Bank Radio Experimental Station of the University of Manchester is 34°, and as the station has already accumulated an important body of echo observations, it was judged desirable to compute a table and draw a plan diagram for $\alpha = 34°$. This is also very nearly the value of α corresponding to the northern United States where much radio work in connection with the aurora is in progress.

The values computed for this geomagnetic colatitude are given in Table 1. For each value of e ranging from 0° upward at 2° intervals, values of R, x, y, ψ, and θ are given for values of h from 60 km upwards at 20-km intervals. Also shown are the limiting azimuths ψ_0 giving the direction of the tangent at Q to the plan curves, and the value for the meridian echo point, the height of which, in general, does not fall within the series 60, 80, 100, $\cdots$ km.

In the diagram (Fig. 1), half of each curve is drawn on alternate sides of the geomagnetic meridian, giving the locus of P' for $e = 0°, 2°, 4°, \cdots 14°$. The values of h, R, and θ are shown alongside each meridian point and also for points off the

meridian at heights 60, 100, and 140 km. The scale of distance is given along the base of the diagram. By drawing a radius from the origin at any desired azimuth, it is possible to infer the range of elevation for the beams in that azimuth which can be reflected back to the origin. The limiting value of e is 18.6°, but the curves for $e = 16°$ and $e = 18°$ have been omitted from the diagram, as the corresponding points lie below the lowest auroral height ever observed (65 km) and are therefore unlikely to be of physical interest.

I wish to acknowledge the helpful suggestions of S. Chapman and the assistance of D. C. Wilder and A. B. Cain in the preparation of this paper.

Reference

[1] S. Chapman, The geometry of radio echoes from aurorae, J. Atmos. Terr. Phys., 3, 1-29 (1952).

JOURNAL OF GEOPHYSICAL RESEARCH VOLUME 58, NO. 3 SEPTEMBER, 1953

STATISTICAL STUDY OF WAVES FROM BLASTS RECORDED IN THE UNITED STATES

BY E. H. VESTINE AND S. E. FORBUSH

Department of Terrestrial Magnetism, Carnegie Institution of Washington, Washington 15, D. C.

(Received March 30, 1953)

ABSTRACT

Computational methods are described for analyzing a time series into two new time series, these comprising one having systematic quality and stationary autocorrelation, and the other having the properties of random noise. The methods are illustrated by application to seismic records. When a spike signal is expected in a certain interval of record, a significance test for the reality of an observed spike signal is applied.

It is shown that seismic records obtained many kilometers from the source have a remarkably stationary autocorrelation over considerable intervals of time. The random noise level is also high. After analysis, in one case a spike signal due to the reflection of a compressional wave from the Mohorovičić discontinuity was probably found, although it was not distinguishable among other similar pulses in the record.

I. INTRODUCTION

The interpretation of seismic records of explosions and earthquakes is often difficult because of unfavorable signal-to-noise ratio conditions. Preliminary to such interpretation, identification and timing of various phases of the explosion records are desired. The satisfactory timing of the first arrival of the compressional (P) and shear (S) waves ordinarily affords little difficulty. With respect to other phases, the timing of the interval of record is less precise and often impossible by usual methods.

The present study is concerned with the separation of the various phases of the record when these phases have mutually distinguishable statistical properties. For instance, each phase may have a different autocorrelation function with time. An autocorrelation of the entire record at an observing station may then permit the timing of the arrival of the various phases one by one, by noting the time intervals of successive stationary conditions of autocorrelation. In much the same way, changes in the energy spectrum from one interval of record to the next may be helpful. With respect to energy of ground motion, the mean square departure in ground motion averaged over suitable intervals of time may show significant differences in various parts of the record. Such departures may be of

special interest when parts of the record autocorrelated in time can be removed from the record.

Hurley [see 1 of "References" at end of paper] has recently studied the waves from explosions some miles from the source. The present paper gives results of somewhat similar studies made for larger explosions observed at greater distances. These records were obtained with velocity meters by the Carnegie Institution of Washington and cooperating agencies. While the methods of statistical analysis used here probably do not differ in fundamental particulars from those of Hurley and his coworkers, the details of numerical procedure more closely follow those used previously by one of us in geomagnetic applications, and subsequently included by Wiener [2] in his treatment of practical applications of his theory of prediction in improved form.

In order that statistical methods be applied intelligently to the recorded waves from blasts, it is first necessary to mention very briefly some existing ideas respecting the theory of propagation of seismic waves.

II. THEORY OF SEISMOLOGY

At the present time, the theory of seismology of the crust is in a state of flux. On the experimental side it is not quite clear just what precisely is observed, and from the theoretical side it is by no means obvious how these observed results should be explained. The further elaboration of this statement is best left to the experts, and present remarks refer only to those ideas which motivated the present statistical study.

On the experimental side, it appears clear at any rate that the times of arrival of P and S waves are satisfactorily defined in shot records, in reasonable accord with simple theory. It is also proper, when recording at suitable distances from the explosion, to identify a pronounced pulse following the onset of P waves with a P-wave reflection from the Mohorovičić discontinuity or layer. This result accords well with simple ray theory, and provides one of the most direct experimental determinations on the deeper portions of the earth's crust. Unfortunately, for reasons not yet fully understood, this P-wave reflection is sometimes weak or missing. When it is weak, the certainty of its identification, in the presence of other signals, may be rendered more secure by statistical methods. This is true if rigorous statistical tests can be devised and applied to the suspected signal.

The remaining signals usually found in the records are not well understood. They probably are to be explained, in part, in terms of processes such as dispersion, "wave-guide" effects, reverberation, and scattering phenomena, as well as the P- and S- and Rayleigh-type surface waves predicted by theory [4, 5, 6, 7, 8]. The S and Rayleigh surface waves have been identified many times in the earthquake records, but claims that they have been identified in explosion records have not been strongly pressed, although the S phase is often seen.

III. IDENTIFICATION OF PHASES OF SHOT RECORDS BY STATISTICAL TECHNIQUES

It can be shown that when a time series is stationary its self-correlation or autocorrelation is likewise stationary [2]. Hence various phases of a record can

be examined for changes to other stationary levels, if any, indicating changes in physical phase. For instance, if there be imagined a pulse in energy from a shot in the form of a wave front, this signal is received at the recording station by direct transmission. However, if the medium is layered, either locally or more extensively, or if there are parts of the crust which by virtue of inhomogeneities act as scattering centers, there may appear in sequence a series of signals in time following the initial pulse. The indirectly propagated signals may not closely resemble the initial pulse, but their character depends on the initial pulse, the geometry, and the distribution of density in the crust. Accordingly, they may be correlated in time with the amplitude and character of the initial pulse in some way. This yields an autocorrelation function

$$\phi(\tau) = \sum^{N} f_n f_{n-\tau} / \sum^{N} f_n^2 \quad \ldots\ldots\ldots\ldots\ldots\ldots\ldots\ldots\ldots\ldots (1)$$

where the time series f_n represents the observed record, at the time t_n , and N is large.

The part of the record systematic in time which gives rise to a stationary autocorrelation can be removed under certain conditions by the use of prediction techniques. A suitable prediction formula for the purpose is

$$f_n = \sum k_\nu f_{n-\nu} \quad \ldots\ldots\ldots\ldots\ldots\ldots\ldots\ldots\ldots\ldots (2)$$

where the constants k_ν are weights related to the autocorrelation according to the scheme

$$\phi(j + l) = \sum k_\nu \phi(l - \nu) \quad \ldots\ldots\ldots\ldots\ldots\ldots\ldots\ldots\ldots\ldots (3)$$

From the form of (2) it is clear that it is not necessary to know the autocorrelation function in order to find the weights k_ν in (2), because they can be found such that the mean square error in the predicted values f_n shall be a minimum simply by regarding (2) as a set of observational equations, which can then be solved by the usual method of least squares. In this way, a selected number s of the values k_ν can be found from a total of S observational equations. However, it is desirable to know something about the type of the autocorrelation present because one might otherwise pick the values k_ν for intervals τ such that the autocorrelation might be very small or zero; in such event the derived function (2) would be unsatisfactory. Moreover, the number of constants s of k_ν required is dependent on the complexity of the autocorrelation function, as is readily seen from inspection of (3). It is also apparent from (3) that the best values of k_ν are likely to be forthcoming for values ν such that $| \varphi(\tau) |$ is large, or at displacements τ corresponding to the maxima and minima of the autocorrelation function.

IV. APPLICATION OF STATISTICAL TECHNIQUES TO WAVES FROM BLASTS

(*A*) of Figure 1 shows the first four seconds of record of a vertical velocity meter as measured by Tatel and colleagues at Grand Marias, Minnesota, at a distance of 173.7 km from an explosion at Eveleth, Minnesota. The values were scaled as the departures from the mean of the four-second interval, and comprise

a time series f_n at discrete times 1/50th of a second apart. In (*B*) of Figure 1, the residue of (*A*) remaining after removing the predicted function

$$f_n = k_3 f_{n-3} + k_6 f_{n-6} + k_9 f_{n-9} + k_{12} f_{n-12} \quad \ldots\ldots\ldots\ldots\ldots (4)$$

is shown. The weights k were obtained from 50 values of the third second of record, by the method of least squares, the interval of three units of time being approximately that from inspection of the autocorrelation function throughout the first, third, and fourth second of record. This gave $k_3 = -0.886$, $k_6 = -0.105$, $k_9 = 0.021$, and $k_{12} = -0.075$. It will be noted that the noise level is high, although there may be an indication of a reflection from the Mohorovičić discontinuity in the early part of the second second of record. The square of the departures in (*B*) have been meaned in successive groups of ten values as running means

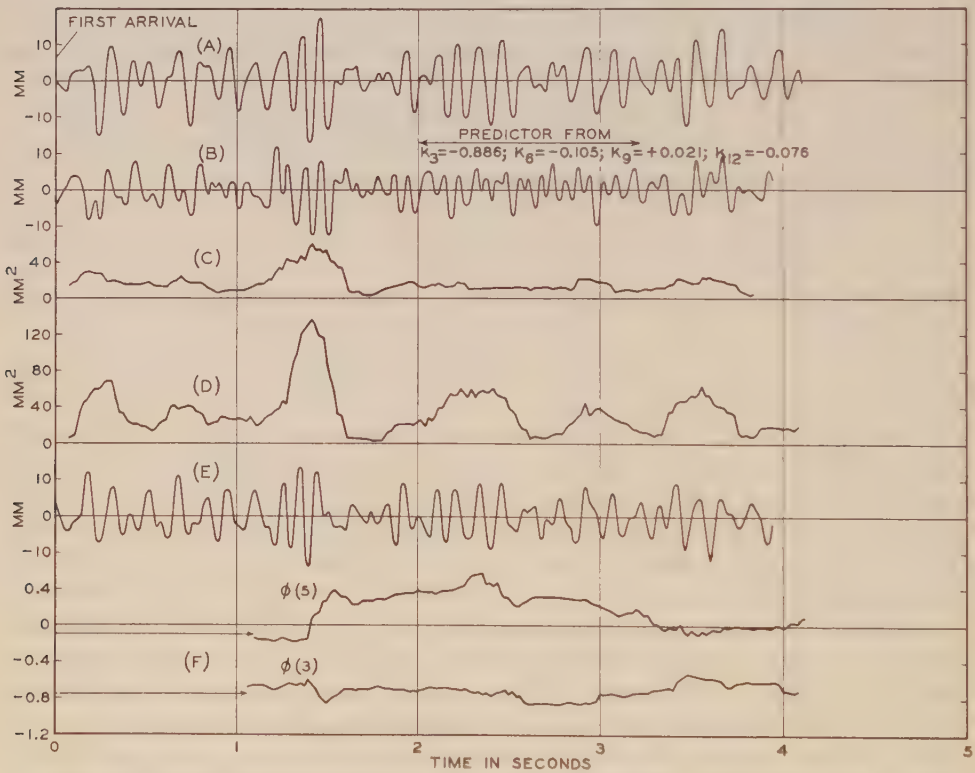

FIG. 1—(A) DEPARTURES IN VELOCITY OF VERTICAL MOTION AT GRAND MARIAS, MINN., 173.7 KM FROM SHOT; (B) OBSERVED MINUS PREDICTED MOTION; (C) SMOOTHED MEAN SQUARE DEPARTURES OF (B); (D) SQUARED DEPARTURES OF (A); (E) PREDICTED VALUES FROM (A); AND (F) AUTOCORRELATIONS FOR VARIOUS VALUES OF τ (UNIT 1/50 SECOND), JULY 2, 1951

in (*C*) of Figure 1, which may be compared with the unsmoothed squared departures of (*D*) obtained directly from (*A*). An outstanding departure in these values appears at about the time of the supposed reflection from the Mohorovičić discontinuity, which will be discussed with respect to its statistical significance later in this paper.

Also shown in (F) of Figure 1 is $\phi(3)$, as given by (1) taking N to be 50. It remains large in magnitude and in general less than -0.6, whereas $\phi(5)$ is smaller and may have about three stationary levels, with an abrupt change from a negative to a positive sign near the time of supposed Moho reflection. Similar results were obtained for $N = 25$ (not shown) for $\phi(2)$, $\phi(3)$, $\phi(5)$, and $\phi(8)$. These showed that the contribution to the autocorrelation when derived for only 25 intervals is subject to considerable systematic variability, which on an average is not nearly so prominent for $N = 50$. This is further clarified from Figure 4, where the autocorrelation function for $N = 50$ is shown for values of τ up to 10, for the four seconds of the record taken separately. There is evidently a remarkable systematic quality of the record which is common to the entire four seconds of time, but it is not clear why this should be so. A physical phase such as surface P waves might be one possibility, but it is difficult to understand why these should have a dominant period of about six time units. The fluctuations in the contribution to the autocorrelation given by $N = 25$ would then be explicable on the basis of more or less discrete signals arriving in such a way that their net contribution to the autocorrelation is greatly diminished when added for a longer period. This con-

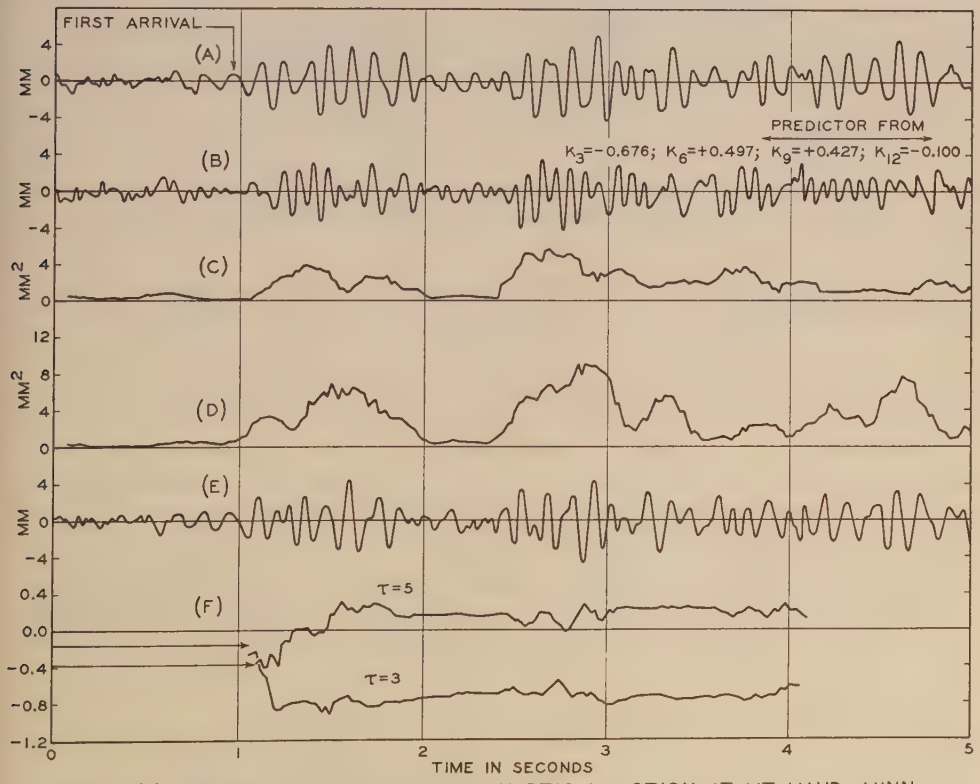

FIG. 2—(A) DEPARTURES IN VELOCITY OF VERTICAL MOTION AT MT. MAUD, MINN., 216.6 KM FROM SHOT; (B) OBSERVED MINUS PREDICTED MOTION; (C) SMOOTHED MEAN SQUARE DEPARTURES OF (B); (D) SQUARED DEPARTURES OF (A); (E) PREDICTED VALUES FROM (A); AND (F) AUTOCORRELATIONS FOR VARIOUS VALUES OF τ (UNIT 1/50 SECOND), JULY 2, 1951

ception is perhaps supported by the squared departures of the values f_n plotted in (D) of Figure 1, which suggest that energy was received in several instalments, transferred to the predicted function, leaving only the energy distribution shown in short-term averaged form in (C) of Figure 1. In other words, much of the incoming energy becomes converted into the systematic and predictable function or phase.

Figures 2 and 3, respectively, for Mt. Maud, for shot at Eveleth, Minnesota, at a distance of 216.6 km, for the same shot, and Gainesville, Virginia, at a distance of 111.9 km, for a different shot (in Tennessee), show similar results. In each of the three records analyzed there are stationary levels in the autocorrelation, especially to be noted in the values $\phi(2)$ or $\phi(3)$.

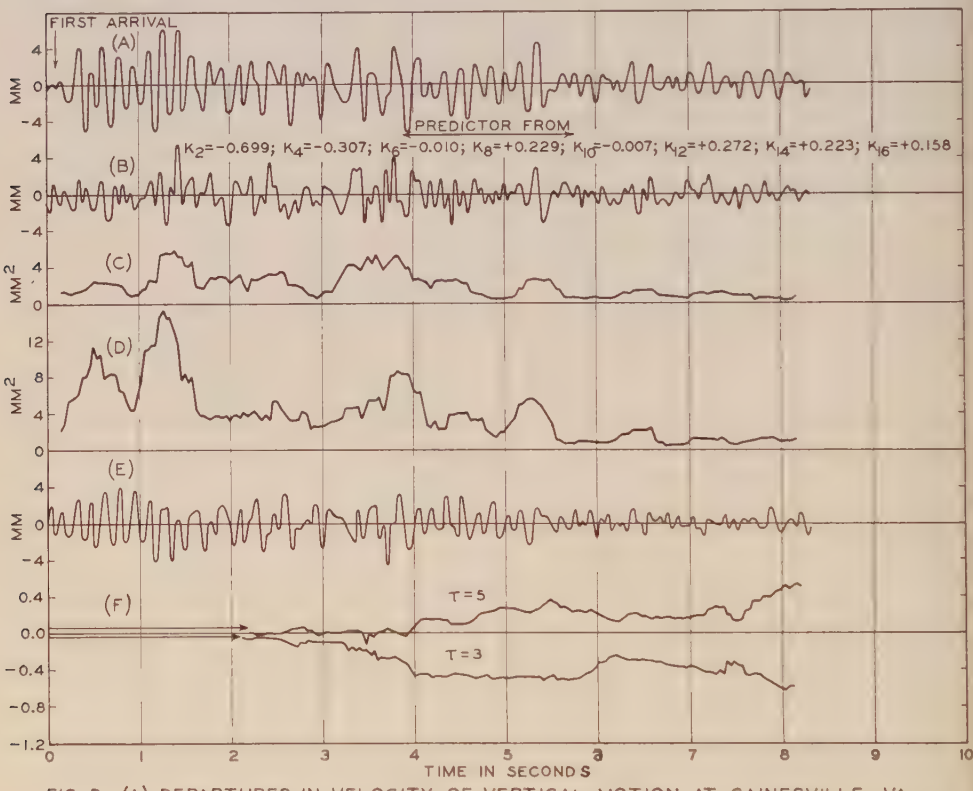

FIG. 3—(A) DEPARTURES IN VELOCITY OF VERTICAL MOTION AT GAINESVILLE, VA., 111.9 KM FROM SHOT; (B) OBSERVED MINUS PREDICTED MOTION; (C) SMOOTHED MEAN SQUARE DEPARTURES OF (B); (D) SQUARED DEPARTURES OF (A); (E) PREDICTED VALUES FROM (A); AND (F) AUTOCORRELATIONS FOR VARIOUS VALUES OF τ (UNIT 1/25 SECOND), DECEMBER 20, 1950

In Figure 1, for Grand Marias, Minnesota, the autocorrelation function $\phi(\tau)$ is rather similar in the first, third, and fourth second of record, but is different, for example, for $\phi(5)$ in the second showing the supposed Mohorovičić reflection, presumably because the latter may be accompanied by a slight increase in signal frequency. At Mt. Maud, the autocorrelation function for the second to fifth second, inclusive, is about the same, but during the first second the autocorrelation

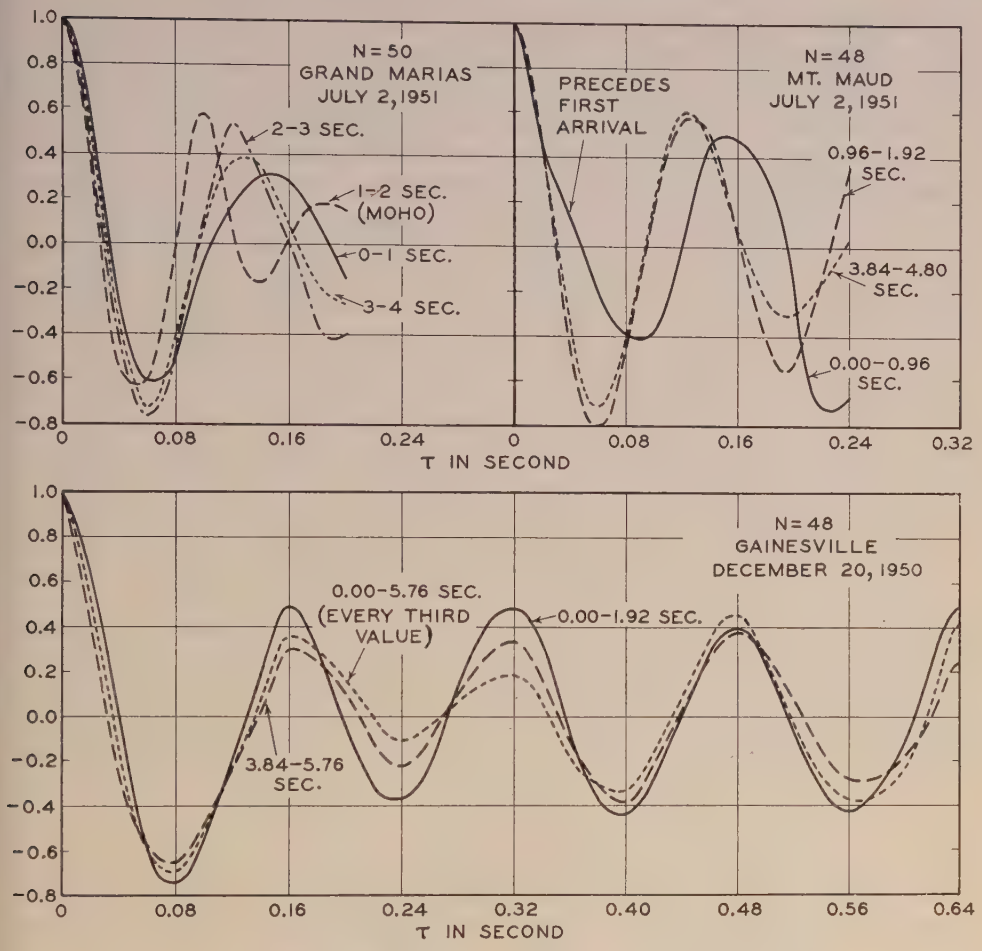

FIG. 4—AUTOCORRELATIONS AT THREE STATIONS FOR VERTICAL VELOCITY METERS DURING THE FIRST FEW SECONDS FOLLOWING FIRST ARRIVAL OF P WAVES

of the ground unrest preceding the first arrival shows an obviously notable difference. At Gainesville (Fig. 3), for a different shot, the autocorrelation appears similar in the first and second seconds, and in the fifth and sixth. The Mohorovičić reflection is expected in the second second, because there was a strong reflection at the neighboring station of Wilderness, Virginia, only about ten miles away.

Figure 5 shows for Grand Marias a sample curve of the autocorrelation function for the observed minus computed signals. If the autocorrelated part of the record has in fact been removed, by the prediction, the remaining signal should show a low autocorrelation, and should appear more or less random, unless more than the one autocorrelated phase appears in the record. The original justification for the removal of a single systematic function from the record was, of course, the similarity in the autocorrelation function from one second of record to the next, throughout the record at each of the three stations. It would appear from Figure 5 that the prediction of the autocorrelated part has been only partially successful,

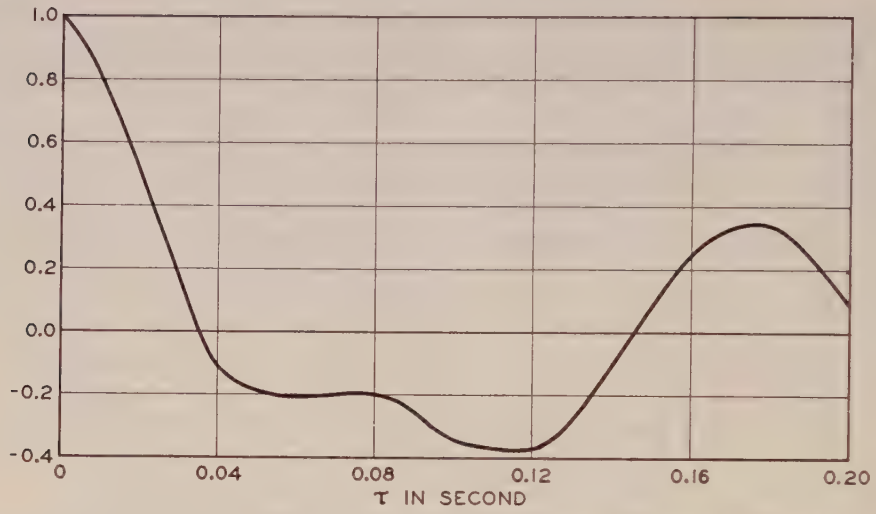

FIG. 5—AUTOCORRELATION OF RESIDUALS (B) OF FIGURE 1, INTERVAL FIRST SECOND

though it is clear that the greater part of the autocorrelated signal has been removed.

Figure 6 shows the result of a simple statistical test of the random quality of the observed minus computed signals from (*B*) of Figures 1, 2, and 3. The standard deviations of successive sums, taken for h residuals at a time throughout the

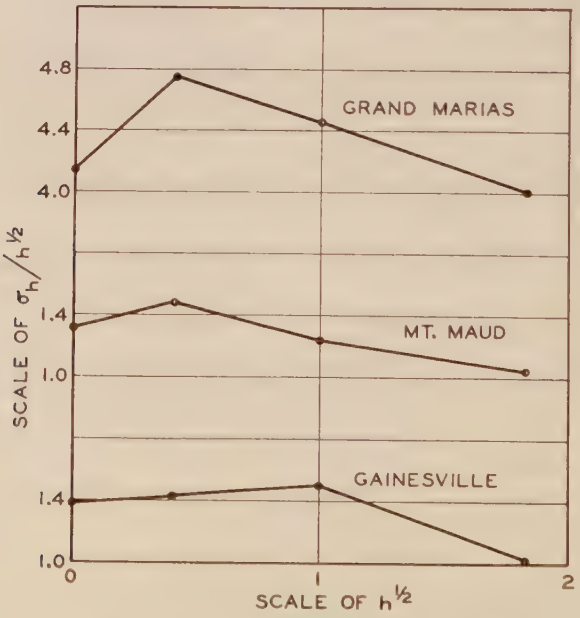

FIG. 6—TEST FOR APPROXIMATE NUMBER OF REPETITIONS h IN RESIDUALS OF (B) OF FIGURES 1, 2, AND 3, RESPECTIVELY

record was found for $h = 1, 2, 3, \cdots$. If adjacent residuals are correlated, the characteristic $\sigma_h/(h)^{1/2}$ with increasing h may approach a limit independent of $(h)^{1/2}$, according to Bartels [9]. When this limit is reached, the residuals for greater values of h are no longer correlated. For values of h less than that for which this limit is attained, the ratio of the characteristic to $(h)^{1/2}$ is expected to increase with increasing h. From Figure 6, this increase persists apparently to about $h = 2$, but this is only a rough estimate. This means that if the residuals shown in (B) of Figures 1, 2, and 3 are replaced by successive means of these residuals taken in pairs, the resulting residuals will on the average be mutually independent.

It is of physical interest to determine whether or not the residuals so found have the properties of random noise, when $h = 2$. In the first place, the mean of the residuals is about zero, and hence compatible with this supposition. The next attribute amenable to simple examination is the sequence in which the signs of the residuals appear, and whether the sequence noted is compatible with expectations based on random numbers. If random, the probability that r successive positive residuals appear followed by a negative value is $(1/2)^r \cdot (1/2)$, and will be the same for negative residuals in sequence followed by a positive value. For (B) of Figure 1, it is found that the observed and theoretical frequencies, respectively, for such sequences taken for $r = 1, 2, 3, \cdots$ become: 29(28), 17(14), 9(8), and 2(2). Thus $\chi^2 = 1$, and since there are four degrees of freedom, from tables it is found that the probability $P = 0.8$ of getting a fit as bad as or worse than this [10]. In other words, the numbers of observed sequences the same in sign are indistinguishable from those expected for heads and tails in successive flips of a coin. For (B) of Figure 2, with $h = 1.5$, the frequencies are 46(40), 23(20), 4(10), 6(5), 1(2), $\chi^2 \sim 5$, giving $P \sim 0.3$. For (B) of Figure 3, taking $h = 2$, the frequencies are 29(30), 21(15), 5(7), 4(4), 0(2), 1(1), $\chi^2 \sim 5$, $P = 0.3$.

1. *Statistical test for reality of extraneous signals or residuals*—The residuals (observed minus predicted) in (B) of Figure 1 have been divided into ten successive groups of ten residuals each, except for the last which includes only nine residuals. The means of group were as follows:

Group	1	2	3	4	5	6	7	8	9	10
No. in group	10	10	10	10	10	10	10	10	10	9
Group mean	−1.2	−0.0	−0.4	−0.2	+0.2	+0.8	+0.5	+0.3	−0.2	+0.7

(The mean of all the residuals was zero.)

From previous tests of independence of successive residuals, it was found that means of successive pairs (non-overlapping) could safely be regarded as independent. Thus, in the above table, each group comprised ten means of two residuals.

While the means of the groups may be homogeneous, the variances may be non-homogeneous, that is, the variance from one or more of the groups may differ significantly from that for the remainder of the groups. To test this, the variance was computed for each of the ten groups, so that a test [11] might be made of the hypothesis that the ten sets of variance came from populations with the equal variances. The variances from the ten groups of ten deviations each are given in

the following table. The samples correspond to those in the preceding table showing the means. As before, each sample comprises ten means, each individual mean being the average of two successive non-overlapping deviations (observed minus predicted). From tables [11], the observed F is found to be just equal to that for the five per cent level of significance.

Variance for single deviations from sample means

Sample No. . . .	1	2	3	4	5	6	7	8	9	10
No. in sample . .	10	10	10	10	10	10	10	10	10	9
S_i^2	18.2	11.8	9.5	33.4	4.6	9.3	6.3	11.8	8.7	10.0

Thus, at the five per cent level of significance, one would reject the hypothesis that the ten populations have the same variance. That is, if there were drawn many sets of ten random samples comprising ten each from a normal population (with the variance estimated from all ten of the experimental groups), then about five per cent of such sets would result in a value of F as big or bigger than that found from the actual set of data. This is rather weak evidence for rejecting the hypothesis that the ten samples came from populations with the same variance. Thus, one would not have very much confidence that the variance in any one or more of the samples was significantly different from the others. This is particularly so because the samples of residuals were definitely selected sequentially so that one of them would have the maximum variance for a sample of ten. An inspection of the ten individual deviations in sample 4 shows that three of these values contribute about 70 per cent of the sample variance. Moreover, these three values are of a size such that in sampling from a normal population (with the variance derived from the 99 samples) the probability of obtaining deviations as great or greater than the smallest of the three values (actually all three were nearly the same) is about 0.025, so that it is not surprising to obtain three or four in a sample of 99.

Similarly, a test of the hypothesis of homogeneity for the variances from the first five samples of residuals (instead of all ten) was acceptable at the ten per cent level, which in the light of the above remarks is not convincing evidence that the variance of the fourth sample is really different from the others. Thus the evidence for ascribing a real departure to sample 4 on the basis of tests so far made is very weak. This is even intuitively evident when the conclusion would be determined by a couple of values.

If now the variance in sample 4 is compared with that in the other nine samples, it will be found that the hypothesis that these two variances came from the same sample would be rejected (with $P < 0.01$). However, account must be taken of the selection made before applying the test. If, however, it were known *a priori* (before examining the data) that a large variance was expected only in the particular interval covered by sample 4 (or in some particular part of the time series), then the above test would be definite evidence for a significantly larger variance there.

Similar tests were made for homogeneity of the sample variances for the stations Mt. Maud, Minnesota, for which the homogeneity hypothesis was acceptable at the ten per cent level, and for Gainesville, Virginia, acceptable at the three per cent level. In these two cases, no attempt was made to select the samples

in such a way as to insure maximum variance in any one of them. The variances of individual deviations from the sample means for these cases are shown in the following tables.

Variance from sample means, Mt. Maud, Minnesota

Sample No. . . .	1	2	3	4	5	6	7	8	9	10
No. in sample . .	10	10	10	10	10	10	10	10	10	10
S_i^2	1.01	1.55	0.71	1.32	1.99	2.17	2.70	1.31	0.36	0.98

Variance from sample means, Gainesville, Virginia

Sample No. . . .	1	2	3	4	5	6	7	8	9	10
No. in sample . .	10	10	10	10	10	10	10	10	10	10
S_i^2	0.70	1.65	1.08	1.30	2.19	1.03	0.78	0.31	0.40	0.61

In reference [1], running averages of the squares of the differences between observed and predicted values are suggested as a measure of the error of prediction. Such a measure is shown in (*C*) of Figure 1. However, no statistical tests exist to determine the significance of peaks on such curves. Tests for this purpose could, of course, be constructed empirically by drawing random samples of single deviates, which would then be squared and running means computed. A few hundred repetitions of the sampling would provide approximate estimates of the probability for the occurrence of peaks of a given amplitude or greater which arise solely from sampling, when no signal is present. With signals of given magnitude present, the same empirical procedure could be used to determine the probability of not finding any indication of the signal when it was present.

2. *Use of power spectrum*—It can be shown that the power spectrum of a time series and the autocorrelation are in fact related, each being the cosine Fourier transform of the other [12]. The foregoing analyses of seismic records on the basis of the autocorrelation accordingly will have an equivalent treatment based on the use of Fourier analysis. This equivalence is illustrated in Figure 7, where the power spectrum obtained from 48 ordinate Fourier analyses is given in (*A*) for three overlapping intervals in the record of the vertical component at Grand Marias, each 48/50th of a second in duration. It will be noted that the amplitude of the spectrum in the second second, in which the reflection from the Mohorovičić layer may appear (as shown by Fig. 1), is greater at the higher frequencies. In (*B*) of Figure 7 is shown the autocorrelation function for the first interval of Figure 1, the plotted points being obtained from direct application of (1), fitted by the theoretical curve

$$\phi(\tau) = e^{-|\tau|/\tau_0} \cos \omega_0 \ldots\ldots\ldots\ldots\ldots\ldots\ldots\ldots\ldots\ldots (5)$$

where $\omega_0 = 6.375$ cycles in 48/50 sec, and $\tau_0 = 6.5/50$ sec. In (*C*), the power spectrum obtained in the usual way, using the cosine transform together with (5), is compared with that for the corresponding interval in (*A*), from Fourier analysis. It is clear that the agreement is reasonably close. When machine methods are available for Fourier analysis, it may accordingly be more convenient to make use of the power spectrum method in the analysis of seismic records.

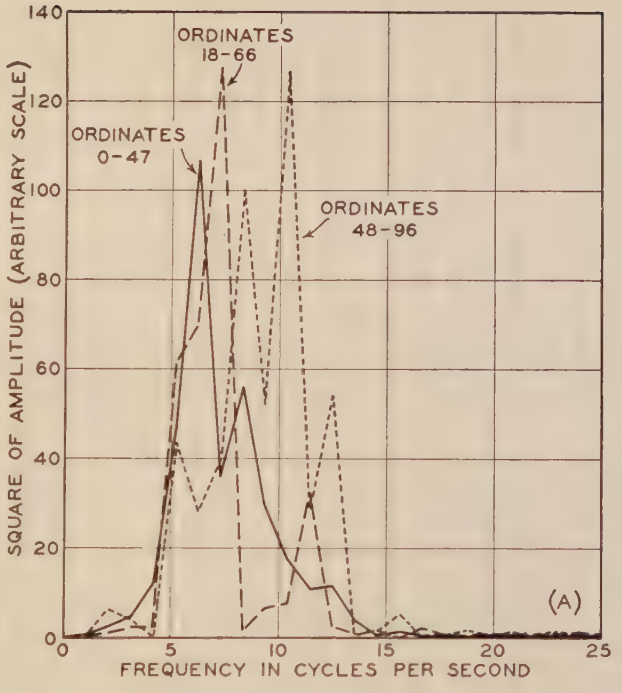

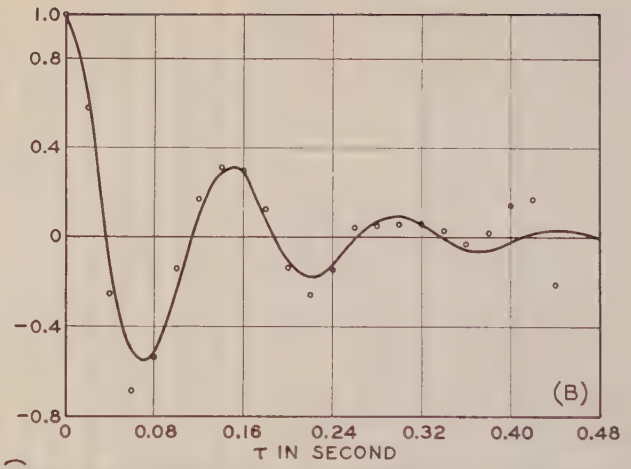

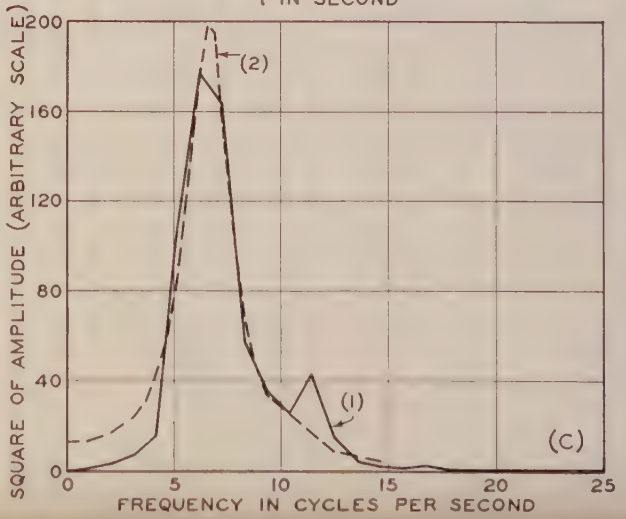

FIG. 7—(A) ENERGY SPECTRA FROM ORDINATES 0-47, 18-66, AND 48-96 OF OBSERVED SIGNAL OF FIGURE 1(A); (B) AUTOCORRELATION FOR 0-47; AND (C) COMPARISON OF SPECTRA FROM (1) AUTOCORRELATION AND (2) FOURIER ANALYSIS ORDINATES 0-47, GRAND MARIAS

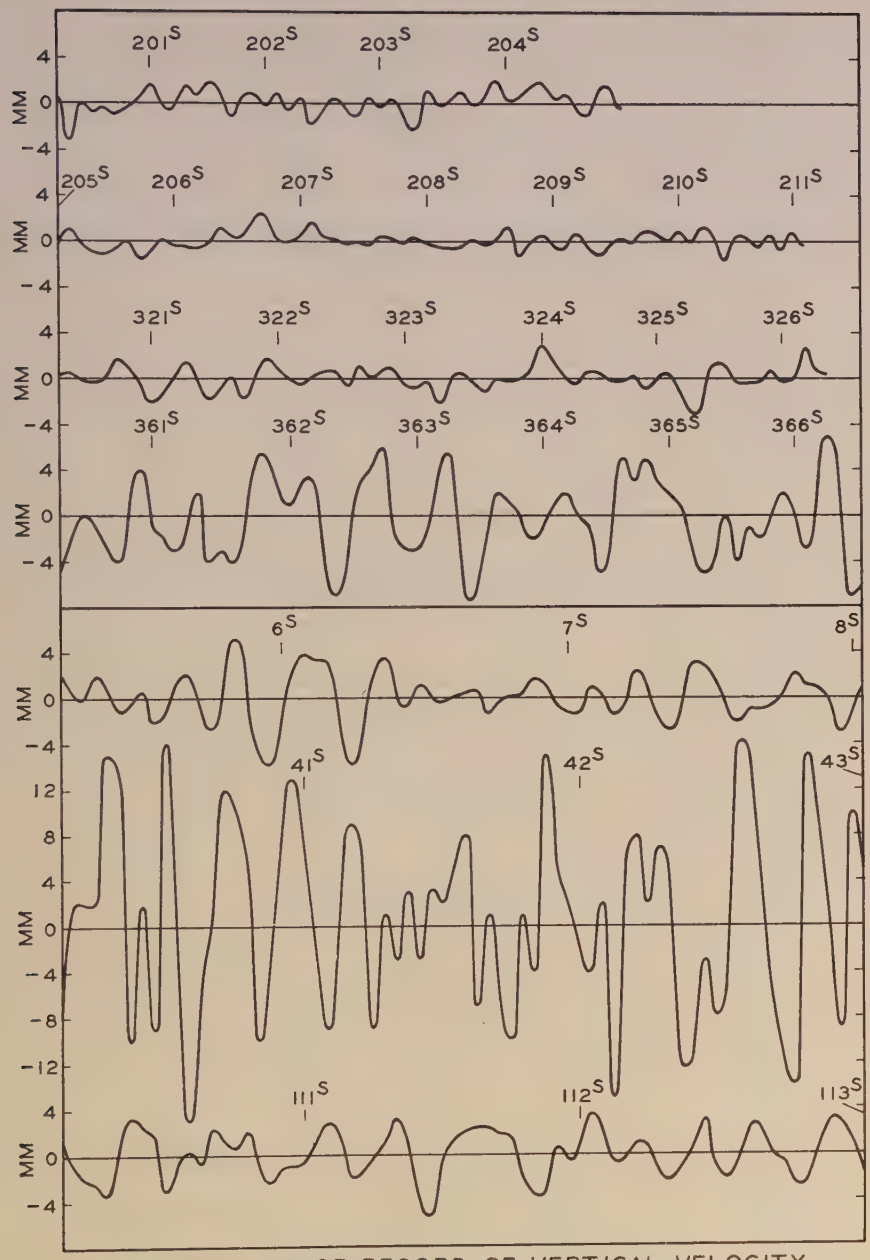

FIG. 8—SCALINGS OF RECORD OF VERTICAL VELOCITY SEISMOMETER AT (A) LITTLETON, N.H., FEBRUARY 5, 1949, X=1,220 KM, AND AT (B) BRISTOL, VA., JULY 8, 1950, X=9 KM, TVA BLASTS

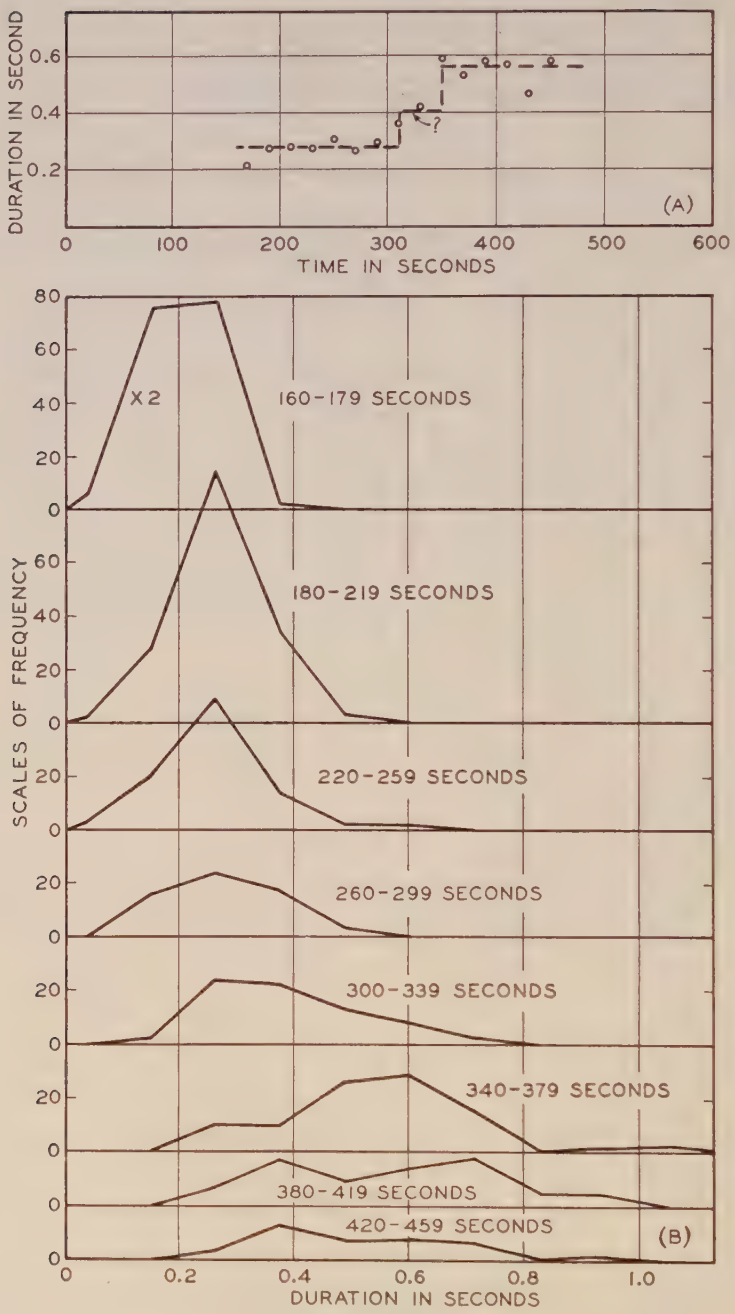

FIG. 9—(A) AVERAGE DURATIONS OF FLUCTUATIONS BY 20-SECOND INTERVALS, AND (B) FREQUENCY DISTRIBUTIONS OF VARIOUS DURATIONS BY 40-SECOND INTERVALS, LITTLETON, N. H., X=1,220 KM, TVA BLAST, FEBRUARY 5, 1949

The most interesting feature brought out by the analyses of Figure 7 is the pronounced peak in frequency between 6 and 7 cycles. This is not a real periodicity but an important quality of the data.

3. *The spectrum and autocorrelation very near and very far from the shot*—The spectrum and autocorrelation in the V component have been considered for the first few seconds of record at stations 100 to 200 km from the blast. One of the most striking features noted was the rather marked similarity in the autocorrelation in each second of record, at each station, following the first arrival of P waves. Since it is by no means clear why this should be so, the autocorrelation was derived for a few sample intervals of the V-component record observed at a great distance, and also at a station very close to the shot point. The records conveniently available for this purpose were those for the great South Holston blast in Tennessee, February 5, 1949, recorded by M. A. Tuve at Littleton, New Hampshire, 1,220 km away; also, those for the Tennessee shot of July 8, 1950, recorded by J. N. Nanda and W. F. Steiner at Bristol, Virginia, 9 km away. Unfortunately, the tapes are much too long and full of detail to reproduce here, so that it has been necessary to show (Fig. 8) but little more than the intervals of record actually analyzed, as drawn from scalings of the original records. In Figure 8 there is included (A) partial record at Littleton, N.H., of P phase, 201^s to 211^s; S phase, 321^s to 326^s; and R phase, 361^s to 366^s: also (B) partial record at Bristol, Va., of P phase, 6^s to 8^s; and record 41^s to 43^s, 111^s to 113^s.

The intervals analyzed were selected in the following way: It will be recalled that the various physical phases of a record might be identified by the intervals in which their autocorrelation or spectrum remains stationary, and knowing this autocorrelation a prediction technique may permit the probable isolation and identification of individual pulses which rise sufficiently above the general noise level. This is a laborious procedure, so that the durations of fluctuations during 20-second intervals were merely scaled off and averaged (from about 60 to 100 fluctuations per interval), with the result shown in Figure 9. It is apparent that these averages remained remarkably stationary in various intervals of record. The average duration is relatively stationary following the onset of P waves, again following the arrival of S waves, and finally the average duration of the fluctuations becomes considerably longer and again highly stationary. This result is in itself probably more interesting than the autocorrelations shown for this station, covering intervals well centered in the intervals of stationary duration, shown in Figure 10. It is apparent that (A) and (B) of Figure 10, following first arrivals of P and S waves, show little autocorrelation, the result being nearly similar to that expected for random noise, whereas (C) shows slightly higher autocorrelation. The curve (C) corresponds roughly to the interval in which Rayleigh waves are sometimes observed in earthquake records [13, 14], with periods of 20 seconds or so and outside the response range of the equipment operated in obtaining the present record.

A careful search by rigorous methods [9] for a periodic component of period equal to the average duration appropriate to the interval providing the autocorrelation revealed that any such component was insignificant in either the V or H record. This was done in the hope that a real periodicity, differing 90° in phase,

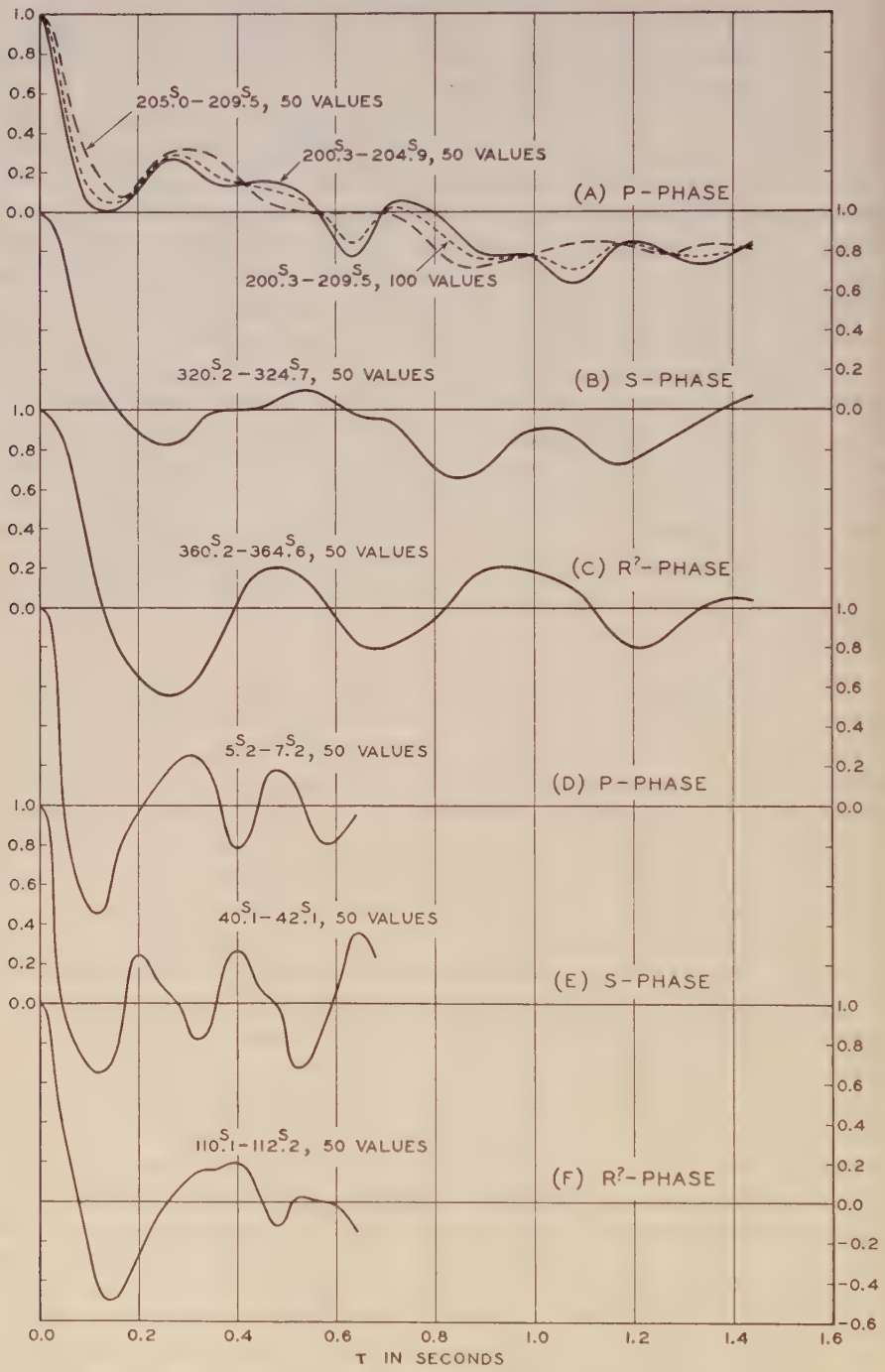

FIG. 10—AUTOCORRELATION AT LITTLETON, N.H. (A,B,C), X=1,220 KM, AND AT BRISTOL, VA. (D,E,F), X=9 KM, TVA SHOTS

as in Rayleigh waves, might be found in the V and H components. This result is also given support by the autocorrelation curves, which do not indicate compatibility with a substantial persistent wave of this or other period.

According to theory [3], the P and S signals should decrease in amplitude with distance x as $(1/x^p)$, where it also seems clear observationally that p is greater than one. On the other hand, surface waves should diminish only as $(1/x^{1/2})$. For this reason, the record at Littleton, New Hampshire, would be expected to include a relatively greater preponderance of signal due to surface waves than at stations closer to the shot. In fact, almost the entire record may consist of P, S, and Rayleigh surface waves propagated at the surface without much loss in energy, as suggested by the work of Nakano [5] and Lapwood [6]. This might help explain the three stationary levels in the duration of fluctuations shown in Figure 10, which together with inspection of the record suggests also the existence over considerable intervals of time of three remarkably stationary levels of energy manifestation. The noisy characteristics of the record at Littleton would then be explicable on the basis of the propagation of surface waves of three types over a rough surface. This also recalls a paper by Jeans [7] discussing surface waves, which seems to have escaped much notice, possibly because most seismographs recording earthquake signals are sensitive at lower frequencies.

The autocorrelations in the V component at a station only 9 km from the shot are shown following the onset of P, S, and later phases of record in (D), (E), and (F) of Figure 10. It is apparent that the autocorrelation is higher than at the distance of 1,220 km (for a different shot). However, it is characteristic of signals, including considerable noise as before. There is no evidence of a persistent periodic component, and inspection of the record reveals that stationary levels of energy manifestation noted at Littleton would exist only during relatively short intervals of record. Accordingly, it cannot be maintained that the autocorrelations shown here for this station are necessarily typical, and they are included only as a matter of interest. It is also understood that Hurley and his coworkers are undertaking detailed studies of records of this kind, obtained at stations close to the shot. A valuable study dealing with the spectrum of such records has been made by Jakosky and Jakosky [15].

4. *Remarks on response of velocity seismometers*—Detailed but as yet unreported studies of the response characteristics of the instruments have been made by Tuve and Tatel of this laboratory. The writers are informed that, in general, the response cut-off is at about 3 cps, and again at roughly 30 cps, with a relatively flat intermediate response covering the greater part of the frequency range. In normal practice, the seismometers are mounted in the field on rock outcrops of formations, the site being picked by a geologist, but this ideal is not always realized. The degree to which the local ground site participates in the response of the instrument is not precisely known, but is not thought to be dominant in the case of the present records [16].

V. GENERAL CONSIDERATIONS

The present study has been concerned mainly with autocorrelation and curve fitting techniques. It was found by this means that the record at a single station

can be separated into an autocorrelated time series and a random time series. It has been noted that there may be short intervals of record in which extraneous and transitory signals appear. In the case of each of the three records analyzed here, inspection of the original records by eye failed to reveal a reflection from the Mohorovičić region. After analysis, one of the three records (that for Grand Marias) shows a possible reflection of dubious statistical significance. However, (*A*) of Figure 7 shows that the energy spectrum derived for the interval (ordinates 48–96), including the possible reflection, indicates more energy at higher frequencies than for the other two intervals. Also, (*A*) of Figure 4 shows that the autocorrelation function for this interval apparently differs from that for the others. These facts make it more probable that the reflection is real. Although in this case the statistical evidence for a real reflection was uncertain, it would be quite definite for cases with a slightly greater signal-to-noise ratio, in which the signal might escape visual detection.

If instead of a single station, several stations close together had been used, the technique of analysis would be similar. In this case, the cross-correlated signal would be fitted by a predictor function. If these stations are too close together, it is likely that the cross-correlation will be nearly equivalent to the autocorrelation at a single station. If they are too far apart, the cross-correlation may be so small that the predicted signal removed will be small. In this event, little gain will again be expected. Accordingly, it is for intermediate spacings of stations that this alternative procedure is likely to be helpful, where special circumstances may warrant considerable extra expenditure of effort.

The techniques applied here afford another approach to the study of the propagation of elastic waves in an inhomogeneous medium. It is possible that statistical methods may be of considerable assistance here. It has been noted that by this means correlated and random time series can be approximately separated in the record. A possible short spike signal from the explosion should not appear in the autocorrelated signal, but there is at least a threefold uncertainty in interpretation of the latter nevertheless. It is easy to see that the autocorrelation can arise from surface waves generated by reflections, as suggested by Nakano [5]. On the other hand, the autocorrelation, for example, Figure 7(*B*), is not unlike that frequently found in other scattering problems. It may also appear when "waveguide" interference and augmentation result [8]. Now, it is not unlikely that all three effects are present in the data—it is mainly a question of degree. It is expected that surface waves predicted by theory may dominate at greater distances. At any rate, surface waves presumably proceed without much loss in energy, whereas scattering and multiple reflection processes require a high degree of transparency of the medium, or high reflection coefficients, in order that the energy loss be kept low.

Although the nature of the autocorrelated signal and its stationary condition in various parts of a record may be suggestive, it is only a phenomenological aspect of the wave propagation. If this aspect is mainly due to surface waves, the surface distribution of sources might then be found from the autocorrelation by known methods.

VI. CONCLUSION OR SUMMARY

Statistical techniques are applied in the study of waves from blasts recorded at distances at which reflections from the Mohorovičić region of the crust might be expected, and also at a station a great distance from the blast. It was found that relatively stationary levels of autocorrelation exist, sometimes for considerable intervals of time, in various phases of the record. Under these conditions, the record is successfully analyzed into an autocorrelated part and a randomly disposed part closely described by the normal error law in the records examined here. The pulse from the Mohorovičić region is normally detectable by eye in the original record, but when it is weak its identification and timing may be in doubt. In the latter event, a statistical test based on sampling is applied.

It is shown that the average durations of fluctuations in vertical ground velocity at a great distance from the shot, as recorded at Littleton, New Hampshire, in the case of a TVA blast, fell into three stationary levels, nearly stationary also in energy exhibited. If these stationary levels are ascribed mainly to three sets of surface waves, proceeding without large loss in energy, it is shown that these supposed surface waves evince no significant periodicity in time. They would then necessarily be badly broken up or scattered, because the autocorrelation closely resembles that for random noise at this station.

It is suggested that the source distribution of surface waves can be found from the autocorrelation function, using methods analogous to those used in the theory of scattering and turbulence in fluids [17].

Finally, it is a pleasure to express indebtedness to Isabelle Lange, who skilfully carried out most of the numerical computations, and to W. C. Hendrix, who drew the diagrams. The writers also wish to thank Dr. P. M. Hurley and his coworkers, Department of Geology and Geophysics, Massachusetts Institute of Technology, for various helpful discussions, which led to the undertaking of the present investigation. Grateful acknowledgment is also made to colleagues at the Department of Terrestrial Magnetism for helpful suggestions, criticisms, and interest, and for making numerous seismograms available for use in the formulation of procedures of analysis.

References

[1] G. P. Wadsworth, E. A. Robinson, and P. M. Hurley, A prospectus on the applications of the linear operators to seismology, Massachusetts Institute of Technology, Dept. of Geology and Geophysics, Geophysical Analysis Group (Nov. 5, 1952).

[2] N. Wiener, The extrapolation, interpolation, and smoothing of stationary time series, New York, John Wiley and Sons, Inc. (1942).

[3] Sir Harold Jeffreys, The earth, Cambridge, University Press, 3rd ed. (1952).

[4] Sir Horace Lamb, Phil. Trans. R. Soc., A, **203**, 1-43 (1904).

[5] H. Nakano, Jap. J. Astr. Geophys., **2**, 233-326 (1925).

[6] E. R. Lapwood, Phil. Trans. R. Soc., A, **242**, 63-100 (1949).

[7] Sir James Jeans, The propagation of earthquake waves, Proc. R. Soc., A, **102**, 554-574 (1923).

[8] K. E. Burg, M. Ewing, F. Press, and E. J. Stulken, A seismic wave guide phenomenon, Geophysics, **16**, 594-612 (1951).

[9] J. Bartels, Random fluctuations, persistence, and quasi-persistence in geophysical and cosmical periodicities, Terr. Mag., **40**, 1-60 (1935).
[10] R. A. Fisher, Statistical methods for research workers, Edinburgh, Oliver and Boyd, Ltd., 9th ed. (1944).
[11] W. J. Dixon and F. J. Massey, Introduction to statistical analysis, New York, McGraw-Hill Book Co., Inc. (1951).
[12] J. L. Lawson and G. E. Uhlenbeck, Threshold signals, New York, McGraw-Hill Book Co., Inc. (1950).
[13] B. Gutenberg (Ed.), Internal constitution of the earth, New York, Dover Publications, Inc., 2nd ed. (1951).
[14] J. B. Macelwane, Introduction to theoretical seismology, Part I, New York, John Wiley and Sons, Inc. (1936).
[15] J. J. Jakosky and J. J. Jakosky, Frequency analysis of seismic waves, Geophysics, **17**, 721-738 (1952).
[16] M. A. Tuve and H. E. Tatel, Annual Report of Director, Department of Terrestrial Magnetism, Carnegie Institution of Washington, for the year 1951-1952, 69-73 (issued Dec. 12, 1952).
[17] F. N. Frenkiel, Phys. Rev., **75**, 1263-1264 (1949).

NOTE ON ANALYTICAL TESTS FOR DISTINGUISHING TYPES OF SEISMIC WAVES

By E. H. Vestine

Department of Terrestrial Magnetism, Carnegie Institution of Washington, Washington 15, D. C.

(Received March 31, 1953)

ABSTRACT

It is pointed out that surface gradients of ground displacements should prove of assistance in identifying and distinguishing the nature of seismic signals. Several theoretical relationships expected for surface disturbances are noted. These can be tested experimentally.

In the interpretation of seismograms, the various types of seismic waves are labeled and distinguished by noting their relative times of incidence, and some indications of amplitude. A theoretical conception of the geometry and density distribution it is hoped to establish is of assistance, when found to work more than once. Procedures of this kind can be very successful in simple circumstances. However, they succeed in spite of the fact that the mechanics of wave propagation in the earth's crust are not well understood.

It is the purpose here to call attention to a possible opportunity for further clarification of seismic records, especially those from explosions.

One of the most elementary difficulties relates to the possible presence of surface waves in the recorded signal. In general, the usual tests do not reveal evidence of a very persistent periodic component in the horizontal and vertical displacements of ground motion, until at a late stage of record, when Rayleigh waves sometimes appear with periods of seven seconds, say, or more. At higher frequencies, it is not unlikely that this propagation is accompanied by distortion of the waves, with loss of signal energies by leakage in the form of diffusion scattering, both laterally and downwards. Apparently, the surface structure may be such that it is only for long wave-lengths, with periods of some seconds and longer, that the ordinary ideal theory of Rayleigh waves for a homogeneous medium becomes successful [see 1 of "References" at end of paper].

Now it could well be that surface waves are mainly generated by an earthquake or shot in the manner suggested by Nakano [2] and Lapwood [3]. Since progressive trains of waves are noted on multiple seismograms at distances such as 200 km or so from the shot, apparently moving over the surface of the ground [4], it would be of some interest to know whether at times the observed signal strength increased or decreased with depth. If it could be shown that both horizontal and vertical displacements, u and w, say, decreased in signal strength with depth, the presence of surface waves might be inferred, especially if the effect persisted for some time.

This inference would be the natural and simple one to draw, but it would not necessarily be unique. A similar result might arise through interference, as noted experimentally in a special case for underwater sound [5]. On the other hand, if the downward vertical gradients of u and w were positive, at a time when the surface values of u and w were also positive and persistent in time, the result would be unfavorable to the hypothesis of surface waves, during the interval of time considered.

In order to test these possibilities, a simple qualitative test for the sign of the vertical gradients was devised for application to the multiple seismograms. It was noticed that the usual elastic equations applicable at the boundary or the free surface of the ground in the static case would permit estimates of the vertical gradients of the displacements, when the horizontal gradients of these displacements can be found from the experimental data. If the origin O of right-handed rectangular axes x, y, z be taken at the surface of the medium, such that the Ox-axis is directed away from the shot, with Oz vertically downwards, for the respective displacements u, v, w along these axes at the free surface $z = 0$, at a given instant of time t,

$$\left.\begin{aligned} \frac{\partial u}{\partial z} + \frac{\partial w}{\partial x} &= 0 \\ \frac{\partial v}{\partial z} + \frac{\partial w}{\partial y} &= 0 \\ \lambda\left(\frac{\partial u}{\partial x} + \frac{\partial v}{\partial y} + \frac{\partial w}{\partial z}\right) + 2\mu\frac{\partial w}{\partial z} &= 0 \end{aligned}\right\} \quad \ldots\ldots\ldots\ldots\ldots\ldots (1)$$

where λ and μ are the usual elastic constants [1]. If there be taken $\lambda = \mu$, and on physical grounds the horizontal gradients transverse to the shot line be neglected, there results the pair of equations

$$\left.\begin{aligned} \frac{\partial u}{\partial z} &= -\frac{\partial w}{\partial x} \\ \frac{\partial w}{\partial z} &= -\frac{1}{3}\frac{\partial u}{\partial x} \end{aligned}\right\} \quad \ldots\ldots\ldots\ldots\ldots\ldots\ldots\ldots\ldots\ldots (2)$$

where the first equation is exact, and the second assumes the horizontal gradient $\partial v/\partial y$ is negligible, in comparison with the other quantities involved. It will be seen that when $\partial w/\partial x$ is negative, at the time when u is also negative, then $|\, u \,|$ decreases with depth. Similarly when $\partial w/\partial x$ is positive, at the time when u is also positive, then $|\, u \,|$ again decreases with depth. Accordingly, the necessary condition for surface waves may be the displacement-strain relations

$$\left.\begin{aligned} \frac{u\partial w}{\partial x} &> 0 \\ \frac{w\partial u}{\partial x} &> 0 \end{aligned}\right\} \quad \ldots\ldots\ldots\ldots\ldots\ldots\ldots\ldots\ldots\ldots (3)$$

and, in any event, when both conditions are satisfied, it can be said that the amplitude of the displacement, whether in the form of waves or otherwise, diminishes with depth, to all first-order terms. However, it is also necessary that the wave equation be satisfied.

If Rayleigh waves are present, which of course satisfy the wave equation, a result quoted by Jeffreys is roughly

$$\left.\begin{aligned} u &= (e^{-0.85kz} - 0.58e^{-0.39kz}) \sin k(x - ct) \\ w &= (0.85e^{-0.85kz} - 1.47e^{-0.39kz}) \cos k(x - ct) \end{aligned}\right\} \quad \ldots\ldots\ldots\ldots (4)$$

where k gives the frequency and c the velocity. Then

$$\left.\begin{aligned} \frac{u\partial w}{\partial t} &= 0.26k \sin^2 k(x - ct) > 0 \\ \frac{w\partial u}{\partial x} &= -0.26k \cos^2 k(x - ct) < 0 \end{aligned}\right\} \quad \ldots\ldots\ldots\ldots\ldots (5)$$

Thus, the first condition satisfies (3) but the second does not, even though w tends to zero as z tends to ∞. The incompatibility arises because $| w |$ at first increases with depth to a maximum (at $kz = 0.52$) before it finally diminishes continuously with depth z. However, the signs in (5) are independent of frequency or wave-length.

From (5), a frequency dependent result is

$$u(\partial w/\partial x) - w(\partial u/\partial x) = 0.26k$$

and since k is positive, when $\partial w/\partial x$ and $\partial u/\partial x$ are available from multiple seismograms in the case when Rayleigh waves are present, there would be expected the displacement-strain inequality

$$u(\partial w/\partial x) - w(\partial u/\partial x) > 0 \quad \ldots\ldots\ldots\ldots\ldots\ldots (6)$$

a result again independent of frequency.

The interesting question arises as to whether or not an inequality such as (6) might not also be satisfied by a P-wave. For an incident P-wave, suppose [1]

$$\left.\begin{aligned} u &= A(z) \exp [ik(x - ct)] \\ w &= -B(z) \exp [ik(x - ct)] \end{aligned}\right\} \quad \ldots\ldots\ldots\ldots\ldots\ldots (7)$$

Then

$$u\partial w/\partial x = -ikA(z)B(z) \exp [2ik(x - ct)]$$

$$w\partial u/\partial x = -ikA(z)B(z) \exp [2ik(x - ct)]$$

so that the expected result for a P-wave is

$$u(\partial w/\partial x) - w(\partial u/\partial x) = 0 \quad \ldots\ldots\ldots\ldots\ldots\ldots (8)$$

and is again independent of frequency.

It would be interesting to attempt an evaluation of $u(\partial w/\partial x) - w(\partial u/\partial x)$ at a time of arrival of reflection from the Mohorovičić region, at which time (8) should be nearly satisfied. If at a series of neighboring subsequent times this difference increased, possibly remaining fairly stationary, it might suggest that Rayleigh-type waves were generated by the P-wave reflection, at points closer to the shot.

It may well be that the most useful inequality will prove to be $u\partial w/\partial x > 0$ (3), as this in no sense depends on ideal theory as an indicator of surface disturbance to the first order. It is clear that $| u\partial w/\partial x |$ will be large when u and $\partial w/\partial x$ are both large, in which case it may be well determined in the presence of noise. From the ideal theory, it is encouraging to note that u and $\partial w/\partial x$ should be in phase for Rayleigh waves. Accordingly, if in general u is large in magnitude when $\partial w/\partial x$ is large in magnitude, the signal may consist mainly of surface waves of true or scattered Rayleigh type, with $u\partial w/\partial x > 0$. Otherwise a P-wave (or an S-wave) may be inferred, especially when this value oscillates in sign with time.

It may also be noted that the boundary conditions (1) must be satisfied, in the case of a multiple seismograph which does not use automatic gain control, if its constituents are suitably mounted and spaced, and working properly.

References

[1] Sir Harold Jeffreys, The earth, Cambridge, University Press, 3rd ed. (1952).
[2] H. Nakano, Jap. J. Astr. Geophys., **2**, 233-326 (1925).
[3] E. R. Lapwood, Phil. Trans. R. Soc., A, **242**, 63-100 (1949).
[4] M. A. Tuve and H. E. Tatel, Annual Report of Director, Department of Terrestrial Magnetism, Carnegie Institution of Washington, for the year 1951-1952 (issued Dec. 12, 1952).
[5] K. E. Burg, M. Ewing, F. Press, and E. J. Stulken, A seismic wave guide phenomenon, Geophysics, **16**, 594-612 (1951).

GEOMAGNETIC AND SOLAR DATA

FINAL RELATIVE SUNSPOT-NUMBERS FOR 1952

Table 1 contains the final sunspot-numbers for 1952 for the whole disk of the sun, based on observations made at the Zurich Observatory, supplemented by series furnished by other cooperating observatories. Table 2 gives the number of sunspot-groups on each day for the year 1952. The yearly mean of the group-

TABLE 1—*Final relative sunspot-numbers for the whole disk of the sun for 1952*

Day	Jan.	Feb.	Mar.	Apr.	May	June	July	Aug.	Sep.	Oct.	Nov.	Dec.
1	66	21	0	28	30	12	59	62	89	20	14	13
2	63	7	0	16	18	19	55	42	75	23	12	12
3	58	7	0	21	9	14	39	35	55	22	7	14
4	40	15	0	26	22	7	31	44	36	42	0	16
5	32	27	9	37	32	7	26	46	35	33	9	29
6	18	31	10	33	34	6	12	43	38	37	13	32
7	27	28	10	37	30	26	13	51	35	37	32	38
8	35	26	23	40	27	21	19	49	14	23	30	43
9	47	30	20	32	23	8	44	57	16	26	30	38
10	43	18	30	30	7	17	52	59	17	24	26	28
11	55	0	38	46	7	10	70	43	7	16	23	31
12	57	16	28	28	6	18	66	54	0	15	16	42
13	61	23	35	22	8	20	72	66	7	15	18	47
14	65	35	25	19	15	22	93	50	0	14	22	63
15	72	44	22	7	14	46	90	44	8	11	23	71
16	70	44	18	8	8	36	85	45	10	10	15	67
17	55	53	20	7	10	45	53	50	11	0	28	70
18	53	52	15	17	18	45	43	43	23	0	35	66
19	44	54	9	33	22	55	23	30	17	12	43	66
20	38	35	0	53	36	57	30	22	20	15	47	50
21	33	28	0	62	26	50	25	28	27	25	42	40
22	12	20	0	52	25	55	9	30	29	27	39	35
23	24	26	0	40	32	70	9	54	42	35	35	35
24	30	17	0	27	31	58	9	69	45	33	30	29
25	32	0	23	20	17	56	17	80	38	37	28	18
26	31	0	30	26	10	56	11	74	38	40	17	30
27	27	0	46	16	43	52	19	90	37	34	14	15
28	19	0	60	17	57	66	23	85	31	33	8	0
29	15	0	71	32	49	63	26	89	28	32	0	0
30	22		75	42	36	76	36	83	19	26	7	9
31	17		66		23		60	85		22		16
Mean	40.7	22.7	22.0	29.1	23.4	36.4	39.3	54.9	28.2	23.8	22.1	34.3

numbers is 2.7 against 5.4 in 1951. The yearly mean of the relative numbers is 31.5 against 69.4 in 1951. Twenty-three spotless days have occurred in 1952, against none in 1951. Therefore, sunspot-activity in 1952 was at a much lower level than in 1951. The large drop of solar activity started in the second half of 1951 and ended in a prolonged series of spotless days at the beginning of March. Solar activity was reactivated from June to August. At the end of the year, solar activity was about at the same level as at its beginning. Figure 1 gives a graphical representation of the daily relative sunspot-numbers for 1952, the times being plotted as abscissas and the relative numbers as ordinates. The limits of the successive solar rotations are indicated by vertical arrows in the upper edge of Figure 1.

TABLE 2—*Daily number of sunspot-groups for 1952*

Day	Jan.	Feb.	Mar.	Apr.	May	June	July	Aug.	Sep.	Oct.	Nov.	Dec.
1	5	3	0	3	4	2	5	4	5	2	1	1
2	5	1	0	2	3	2	5	3	4	3	1	1
3	6	1	0	2	1	2	4	2	3	2	1	1
4	5	2	0	2	2	1	2	4	3	5	0	2
5	3	4	1	2	3	1	2	5	3	3	1	2
6	2	4	1	1	4	1	1	5	4	3	1	2
7	3	3	1	2	3	3	2	5	5	3	2	2
8	3	3	3	3	3	3	2	5	2	2	2	2
9	5	3	3	3	3	1	3	5	2	2	2	3
10	6	2	4	2	1	2	4	6	2	2	2	2
11	6	0	4	4	1	1	4	4	1	1	2	2
12	5	2	3	1	1	2	3	5	0	1	2	4
13	4	2	3	1	1	2	4	6	1	1	2	5
14	5	2	2	1	2	3	6	3	0	1	2	6
15	6	2	2	1	2	5	6	3	1	1	3	6
16	5	3	2	1	1	4	6	4	1	1	2	6
17	4	3	2	1	1	5	4	4	1	0	1	5
18	4	3	2	2	1	6	3	4	2	0	2	5
19	4	3	1	2	2	6	2	4	2	1	1	5
20	3	3	0	3	3	6	3	2	3	2	1	4
21	3	3	0	5	3	5	3	2	3	1	1	3
22	1	2	0	4	3	6	1	2	3	1	1	3
23	2	3	0	3	4	7	1	5	4	1	2	2
24	3	2	0	3	4	7	1	5	4	2	2	3
25	3	0	2	2	2	7	2	7	3	2	2	1
26	2	0	2	2	1	6	1	6	4	3	2	4
27	2	0	3	2	4	6	2	7	4	2	2	2
28	2	0	5	2	5	6	2	6	4	2	1	0
29	1	0	5	4	4	4	2	5	3	2	0	0
30	2		6	5	3	5	2	5	2	2	1	1
31	2		5		2		4	5		2		2
Mean	3.6	2.0	2.0	2.4	2.5	3.9	3.0	4.5	2.6	1.8	1.5	2.8

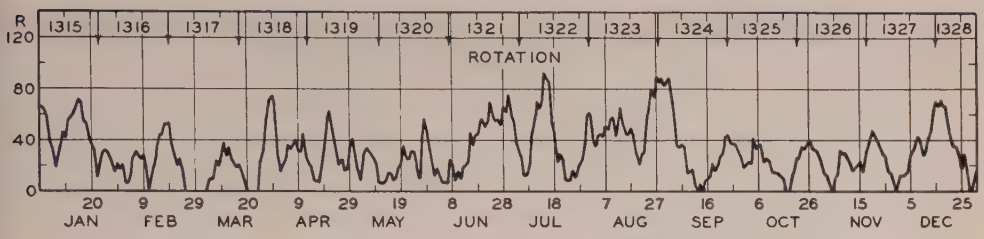

FIG. 1—DAILY RELATIVE SUNSPOT-NUMBERS FOR 1952

More details about the solar activity and the distribution and development of the individual spot-groups will be given in "Die Sonnenaktivität im Jahre 1952" (Astron. Mitt. der Eidgen. Sternwarte, Zürich, Nr. 184) and in "Heliographische Karten der Photosphäre für das Jahr 1952" (Publ. Eidgen. Sternwarte, Zürich, **10**, Fasc. 2).

M. WALDMEIER

SWISS FEDERAL OBSERVATORY
Zurich, Switzerland, June 10, 1953

INTERNATIONAL DATA ON MAGNETIC DISTURBANCES, FIRST QUARTER, 1953

The following new geomagnetic observatories are now collaborating: IK, Istanbul Kandilli (41° 02′ north, 29° 02′ east); Ba, Bangui (4° 36′ north, 18° 35′ east; MB, M'Bour (14° 24′ north, 343° 02′ east); Bi, Binza (4° 16′ south, 15° 22′ east); HI, Heard Island (53° 01′ south, 73° 21′ east); and MI, Macquarie Island (54° 30′ south, 158° 57′ east).

Preliminary Report on Sudden Commencements

S.c.'s given by five or more stations are in italics. Times given are mean values, with special weight on data from quick-run records.

Sudden commencements followed by a magnetic storm or a period of storminess (s.s.c.)

1953 January *05d 05h 46m*: twenty-seven.—25d 08h 17: Wi Ci.
1953 February: None.
1953 March 02d 04h 29m: Va Ta.

Sudden commencements of polar or pulsational disturbances (p.s.c.)

1953 January 02d 18h 17m: Eb Ta.—05d 17h 42: Ci Ta.—*06d 14h 58*: five.—07d 21h 52: Le So.—*09d 00h 31*: thirteen.—*09d 19h 31*: six.—*10d 21h 15*: six.—11d 00h 13: Ci Eb.—11d 00h 36: Eb SM.—11d 19h 37: So Wn.—15d 21h 47: Fu Eb.—16d 22h 59: Le So Eb.—*17d 22h 10*: twelve.—*20d 00h 06*: fourteen.—20d 19h 35: So Wn IK.—22d 21h 00: Le So Eb Tr.—*23d 00h 27*: thirteen.—*24d 00h 36*: six.—24d 22h 17: So Tr.—*25d 23h 50*: seven.—26d 02h 47: SF Ta.—27d 11h 45: Am Ta.—*28d 22h 02*: twelve.—*29d 18h 40*: eleven.

1953 February 01d 21h 02m: Eb Ta.—03d 01h 40: Eb SM.—03d 22h 28: Eb Ta.—04d 13h 39: Ka To.—04d 18h 18: Le So CF Wn.—05d 18h 30: Tl So Wn.—06d 17h 01: So Ka CF.—08d 01h 26: CF Bi Eb Va.—*09d 00h 23*: nine.—09d 04h 42: CF Eb SM Ta.—*09d 21h 10*: thirteen.—*09d 21h 39*: seven. —*10d 20h 57*: six.—10d 21h 20: Es CF.—11d 20h 13: So CF Tr. 12d 17h 20: So CF.—13d 21h 00: CF Eb.—*14d 00h 40*: five.—*14d 19h 01*: eleven. *15d 23h 07*: thirteen.—*15d 23h 54*: five.—*16d 16h 11*: eight.—17d 03h 12: MB CF Eb Va.—18d 07h 51: MB CF Eb.—*18d 17h 46*: seven.—18d 22h 40: Fu CF Eb. —19d 23h 19: CF Ta.—19d 23h 51: Fu Ta.—20d 17h 25: Fu So CF Wn.—*21d 00h 37*: thirteen.—21d 00h 57: Le IK.—*21d 19h 05*: nine.—22d 00h 36: MB CF.—22d 00h 45: Ta Eb Wn.—*22d 23h 28*: seven.—23d 19h 24: Wn Ta.—23d 23h 40: CF Ci Ta.—*24d 19h 36*: six.—25d 00h 38: Ci Ta.—26d 17h 58: So CF Ta.—27d 20h 58: So Tr.—*27d 21h 46*: thirteen. —28d 04h 12: Bi Ci SF.

1953 March 01d 20h 24m: Fu Hr.—*01d 20h 55*: five.—*03d 19h 27*: five.—03d 20h 12: Ma Ta.—03d 21h 45: Eb Ma Ta.—05d 03h 54: Ka Bi.—05d 20h 20: Fu So Ta.—*05d 20h 42*: eight.—06d 23h 50: Hr Eb Ta SM.—*07d 18h 04*: eight.—08d 19h 37: So Tr.—08d 22h 15: Hr Tn Ta.—08d 23h 52: Ci Ta.—09d 11h 07: Ka To.—*09d 20h 00*: five.—12d 00h 46: Tl SF Bi El.—*13d 21h 27*: six.—14d 00h 06: Fu Wn.—14d 00h 19: SF Hr Bi.—16d 12h 35: Ka To.—*16d 21h 00*: thirteen.—

Geomagnetic planetary three-hour-range indices Kp, preliminary magnetic character-figure C, and final selected days, January to March, 1953

	January 1953								
E	1	2	3	4	5	6	7	8	Sum
1	3+	4o	3o	3+	3o	3o	4−	3o	26+
2	2o	2+	4−	3+	4o	4+	4+	3o	27o
3	3−	3o	1+	1o	2+	3−	2o	2−	17−
4	3−	1−	1−	1−	1−	2+	2+	2−	12−
5	2−	3+	7−	6o	6−	5o	5−	5−	38−
6	3−	2−	2+	3o	3−	5−	3−	2+	22o
7	2o	1+	2+	2o	3o	2+	2o	1+	16+
8	3+	3+	2+	2−	1+	1−	2o	2o	17−
9	4o	0+	1+	2−	2o	3−	3−	3o	18−
10	2+	1o	1−	1−	2−	1+	1+	3−	12−
11	4−	3o	2−	2−	2−	1o	1+	2−	16−
12	2+	2o	1+	1o	3−	2o	1o	1−	13o
13	0+	1+	1o	3−	3+	2−	4−	3+	17+
14	3−	3o	3−	1+	1+	2−	2−	2+	17−
15	2−	0+	0+	1+	1+	1o	0+	2o	8+
16	1+	0+	0+	1o	1+	2o	1−	1+	8+
17	1−	0+	1−	2−	1o	0+	1+	3−	9−
18	1o	2o	2−	3−	4−	3+	3o	2o	19+
19	3−	5+	5o	5−	4−	3−	3o	3o	30o
20	5−	4o	4−	3+	2o	1+	2+	2−	23o
21	2+	2+	2+	3−	3o	2−	2−	2+	18+
22	2o	3o	2+	2o	2−	1−	1o	2o	15−
23	4o	3−	1+	1−	1−	0+	1+	0+	11+
24	1o	1o	3−	4−	3−	3+	3o	1+	19−
25	0o	1o	2+	6−	5o	3+	3o	4o	24+
26	5o	5+	4o	5−	5−	4+	6−	5o	39−
27	5o	3+	3+	5+	5−	5−	5o	2+	34−
28	3o	4−	4o	3+	3+	5−	4+	5o	31+
29	5o	4o	4−	3+	4o	4−	4+	2+	30+
30	4−	4−	4o	3+	3o	4−	3+	2−	26+
31	4−	4o	2+	3+	3o	1o	2−	1+	20+

	February 1953								
	1	2	3	4	5	6	7	8	Sum
	1o	1+	2−	1−	1o	1−	1+	2o	10−
	2o	2+	2o	2−	1+	3−	1+	1o	14+
	3−	2o	1+	2+	1o	1+	1+	1+	13+
	1+	2o	1−	2o	3o	2+	2o	0+	14−
	0o	0o	0+	1+	1o	2−	2o	0+	7−
	0o	0o	1−	1o	1o	2−	1+	0+	6o
	0+	0+	0+	1−	0o	0o	0+	1−	3−
	1−	1o	1o	2−	2−	1+	1o	2o	10+
	3−	4−	2o	2+	2+	3−	2+	4o	22o
	2o	0+	0+	1+	3o	3o	3+	5−	18o
	4−	3−	3o	3−	2−	1−	2o	2o	18+
	1o	1+	1+	2−	2−	2o	2−	0+	11o
	0o	0o	1−	0+	0+	0+	1−	2o	4+
	3o	2o	4−	3o	1+	2+	3+	1+	20o
	3−	3−	3−	2o	3−	1o	1+	4−	19−
	4+	2−	3−	3−	2+	5−	3o	2−	23o
	2+	3+	3−	3o	1+	2−	2−	1o	17o
	0+	0+	2o	2−	1+	2−	1+	3−	11+
	2+	3o	3−	3−	2+	3−	2o	3o	21−
	3o	1−	1o	1o	1+	2+	2o	1−	12o
	4o	3+	3+	2−	1o	2o	2o	2+	20−
	3o	2o	2+	2+	3−	4+	5−	6o	27+
	5+	4o	5+	5o	4o	5o	5−	4o	37+
	6−	6o	6o	4−	5−	5o	5+	5o	41+
	6−	5−	5+	5o	4+	4o	4−	5o	38−
	4+	4+	5+	4+	5+	5o	5+	5−	39−
	4o	2+	4+	5o	3+	4o	3−	5o	31−
	3o	6o	3+	2−	2+	3+	3+	2+	25+

	March 1953								
E	1	2	3	4	5	6	7	8	Sum
1	2−	2+	4−	4o	2o	2o	3o	3o	22−
2	4+	5+	6−	6−	6+	6+	6o	5+	45o
3	5−	5+	4+	5−	3o	2+	3o	4−	31o
4	4o	2+	1−	2−	2o	2+	2o	1o	16o
5	1−	3−	1o	1−	2o	2+	3+	3+	16o
6	0+	1−	2−	2o	2−	2−	1+	4o	13+
7	5o	3+	4−	3o	2+	1o	4−	1+	23+
8	2o	3−	1+	3−	3−	4+	5o	7−	27+
9	7−	4o	4−	4+	4o	3+	5−	5−	35+
10	5−	4+	4−	3−	3o	3o	2+	3−	26+
11	3+	2o	1+	1+	1o	1−	2−	1+	13−
12	3−	1+	1−	1o	1−	1−	1o	1−	9−
13	0+	0+	0+	1−	0+	1−	1−	3o	6+
14	4−	3−	1+	1+	2+	2−	3o	3o	19o
15	2o	1+	3+	4+	4o	2o	2−	1o	20−
16	3o	4o	2+	2o	2o	2−	1+	3+	20−
17	2o	2−	2+	1o	0+	1+	2−	0+	11−
18	1−	1−	1−	2−	1o	1o	2−	1o	8+
19	4o	4o	2+	3+	3+	3o	4−	4−	27+
20	4−	1−	1+	2o	1−	1+	4−	4−	17o
21	5o	4+	4+	4+	3−	3+	6o	3o	33o
22	5+	4+	3+	3−	3o	2o	4−	4+	29−
23	4+	5+	5−	4o	4o	6o	6−	3o	37o
24	5−	5+	6−	5+	4+	5o	7−	6+	43+
25	5−	5o	5o	4o	5o	5−	5+	4o	38−
26	3−	4−	3+	4−	4o	3+	5−	5−	30o
27	4o	5o	4−	4+	3+	3−	3o	4−	30−
28	4o	4o	3+	3+	4−	4o	4−	2+	28+
29	4−	3o	3−	1+	1o	1+	3o	3+	19+
30	4−	5−	2o	1o	2+	2o	4o	3o	23−
31	1+	2−	1o	1+	3−	1o	3−	3+	15o

Preliminary *C*, 1953		
Jan.	Feb.	Mar.
0.9	0.2	0.7
1.0	0.2	1.8
0.5	0.2	1.3
0.3	0.4	0.5
1.7	0.0	0.6
0.9	0.0	0.5
0.6	0.0	0.9
0.3	0.2	1.3
0.6	0.9	1.5
0.4	0.8	1.0
0.4	0.5	0.3
0.1	0.1	0.2
0.8	0.1	0.2
0.3	0.7	0.7
0.1	0.7	0.7
0.1	1.0	0.7
0.4	0.4	0.1
0.8	0.2	0.0
1.2	0.6	1.0
0.9	0.3	0.7
0.4	0.7	1.4
0.2	1.3	1.1
0.4	1.5	1.4
0.8	1.5	1.8
1.2	1.3	1.5
1.6	1.5	1.1
1.5	1.2	1.0
1.3	1.0	1.1
1.3		0.8
1.0		0.9
0.7		0.6

Final selected days		
Jan.	Feb.	Mar.
Five quiet		
4	1	11
10	5	12
15	6	13
16	7	17
17	13	18
Five disturbed		
5	22	2
19	23	9
26	24	23
27	25	24
28	26	25
Ten quiet		
4	1	4
7	3	5
10	5	6
11	6	11
12	7	12
15	8	13
16	12	17
17	13	18
22	18	20
23	20	31

19d 00h 33: Wn Ta.—19d 20h 10: SM Ta.—20d 00h 25: SM Ta.—21d 02h 11: SM Bi Ta.—*21d 19h 15*: nine.—*22d 01h 19*: five.—22d 20h 48: Fu So Wn Ta.—22d 21h 42: Tr Ta.—24d 03h 50: Va Hu.—24d 21h 10: SF Ci Ta.—*25d 18h 02*: seven.—26d 11h 17: Am Ta.—*28d 19h 32*: eight.—*29d 19h 32*: six.—29d 21h 50: Hr Wn Ta.—30d 04h 23: SM Hu.—31d 23h 42: Hr Ta.

Sudden impulses found in the magnetograms (s.i.)

1953 January 05d 16h 55m: Eb Tn Hr.—18d 11h 54: Hr Ta.—*19d 07h 37*: seven.—19d 12h 40: Le Es.—*25d 09h 18*: six.—*25d 10h 43*: seven.—*26d 19h 30*: twelve.

1953 February 06d 22h 36m: Eb Tr.—08d 14h 41: Es Ci SM.—22d 15h 30: Tn MB.—*22d 15h 40*: five.—22d 16h 20: Le MB.—22d 19h 58: Es Wn Ta SM.—24d 15h 58: MB CF Ci Eb.—24d 18h 00: CF Ta.

1953 March 01d 20h 02m: Ci Wn.—02d 13h 04: Hr Wn Ta.—02d 16h 10: Eb Ci IK Ta.—*14d 00h 35*: nine.—15d 08h 45: Es Le Wn.—23d 02h 42: Ci Ta.—*24d 18h 05*: nine.—26d 12h 35: Es Le.

Preliminary Report on Solar-flare Effects

Effects confirmed by ionospheric or solar observations are in italics.

1953 January *07d 02h 16m-03h 48m*: Ka.—09d 00h 29-01h 30: Tu (p.s.c.?).—*09d 13h 55*: Hu.—*09d 15h 45*: Hu.—10d 16h 12-16h 18: Tu.—*13d 14h 46*: Hu.—*14d 15h 30*: Hu.—*16d 02h 36-02h 48*: Ka.—24d 00h 35-00h 43: Tu (p.s.c.?).—29d 18h 48-19h 05: Ch (p.s.c.?).

1953 February 04d 11h 42m-11h 51m: SM.—10d 21h 06-21h 11: Tu.—20d 16h 04-16h 10: Tu Hu.—21d 22h 08-22h 15: Tu.

1953 March 05d 03h 53m: El.—06d 13h 17-13h 39: Tu.—06d 15h 36-15h 42: Tu.—13d 14h 50-14h 58: SM.—13d 15h 50: Hu.—13d 21h 09-22h 00: Tu.—14d 00h 34-00h 36: Tu (s.i.?).—14d 13h 30-13h 38: SM.—15d 13h 25-13h 32: SM.—30d 00h 15-00h 32: Tu.—*31d 12h 20-12h 40*: CF.

Ionospheric or solar disturbances without clear geomagnetic effect

None.

Minor disturbances reported by one station only are listed in the De Bilt quarterly circular, but omitted here.

Committee on Characterization of Magnetic Disturbances

J. Bartels, *Chairman*
University
Göttingen, Germany

J. Veldkamp
Kon. Nederlandsch Meteorologisch Instituut
De Bilt, Holland

PROVISIONAL SUNSPOT-NUMBERS FOR APRIL TO JUNE, 1953

(Dependent on observations at Zurich Observatory and its stations at Locarno and Arosa)

Day	April	May	June
1	37	46	15
2	48	40	28
3	48	35	23
4	58	26	53
5	31	9	35
6	31	8	32
7	38	8	36
8	43	0	30
9	30	0	28
10	21	0	24
11	12	0	18
12	0	0	7
13	0	0	0
14	0	0	12
15	0	0	24
16	0	7	33
17	0	8	33
18	7	14	20
19	7	10	25
20	0	10	26
21	0	11	22
22	9	11	20
23	27	11	10
24	33	13	11
25	45	18	10
26	57	11	17
27	66	10	21
28	63	18	7
29	57	23	8
30	49	18	7
31		17	
Means.....	27.2	12.3	21.2
No. days.....	30	31	30

Mean for quarter: 20.1 (91 days)

M. Waldmeier

Swiss Federal Observatory
Zurich, Switzerland

CHELTENHAM THREE-HOUR-RANGE INDICES *K* FOR APRIL TO JUNE, 1953

[$K9 = 500\gamma$; scale-values of variometers in γ/mm: $D = 5.4$; $H = 2.5$; $Z = 4.3$]

Gr.	April 1953		May 1953		June 1953	
day	Values *K*	Sum	Values *K*	Sum	Values *K*	Sum
1	5434 2222	24	1122 1312	13	1221 1122	12
2	4333 1233	22	3201 1111	10	3455 3455	34
3	4322 1233	20	1011 1222	10	5463 3343	31
4	5433 3333	27	2323 1122	16	5543 3233	28
5	3122 1122	14	3423 2123	20	2442 2242	22
6	2323 1121	15	4355 4335	32	3442 3332	24
7	1010 1223	10	4554 3233	29	3232 2222	18
8	1322 1123	15	5553 3344	32	3222 1322	17
9	2411 1122	14	4453 3334	29	1121 1223	13
10	1444 3333	25	3233 2242	21	2352 2233	22
11	1543 3433	26	3323 2121	17	2232 2223	18
12	3244 3222	22	1321 2122	14	2222 3344	22
13	4234 3332	24	2212 1021	11	4322 2233	21
14	2321 2122	15	2211 1123	13	3332 2233	21
15	4323 2133	21	1332 4565	29	1211 1133	13
16	4543 3445	32	5555 5456	40	1021 2122	11
17	5143 3232	23	6431 2333	25	3131 3233	19
18	4342 1233	22	3333 2234	23	2221 0132	13
19	3433 4333	26	4544 3234	29	2220 1212	12
20	4554 3334	31	4342 2233	23	2223 3354	24
21	4342 3454	29	3321 2232	18	2343 1333	22
22	4333 3444	28	3421 2343	22	2233 2233	20
23	5543 3333	29	2134 1133	18	2110 1123	11
24	3122 2433	20	1121 2233	15	2321 1133	16
25	3222 2234	20	2111 1223	13	3211 1222	14
26	3342 3223	20	2221 1133	15	0000 0222	6
27	4232 3223	21	4455 2333	29	0111 1133	11
28	3333 3212	20	3322 1222	17	2301 0133	13
29	2222 3222	17	1122 2222	14	2235 5454	30
30	3332 2243	22	2211 1122	12	5555 3343	33
31			2122 2232	16		

Ralph R. Bodle
Observer-in-Charge

Cheltenham Magnetic Observatory
Cheltenham, Maryland, U.S.A.

PRINCIPAL MAGNETIC STORMS

(Advance knowledge of the character of the records at some observatories as regards disturbances)

Observatory (Observer-in-Charge)	Greenwich date	Storm-time GMT of begin.	Storm-time GMT of ending[1]	Sudden commencement Type[2]	Sudden commencement Amplitudes[3] D	H	Z	C-figure, degree of activity[4]	Maximal activity on K-scale 0 to 9 Gr. day	Gr. 3-hr. period	K-index	Ranges D	H	Z
(1)	(2)	(3)	(4)	(5)	(6)	(7)	(8)	(9)	(10)	(11)	(12)	(13)	(14)	(15)
	1953	*h m*	*d h*		′	γ	γ					′	γ	γ
College	Apr. 16	04 00	17 23	.....	....	....	....	ms	16	3	7	250	1470	12
(M. L. Cleven,	Apr. 19	09 00	23 16	.....	....	....	....	ms	19	6	7	260	1560	6
to June 22;	May 6	01 00	9 20	.....	....	....	....	ms	6	4	7	230	1400	9
C. L. Beers,									7	4	7			
from June 22)	May 15	12 00	17 06	.....	....	....	....	s	16	5,6	8	410	2650	18
	June 1	02 00	5 11	.....	....	....	....	ms	3	5	7	210	1500	9
	June 29	07 30	4 13	.....	....	....	....	ms	1	4	7	200	1540	11
Sitka	Apr. 3	23 45	5 00	.....	....	....	....	ms	4	2	7	32	618	4
(T. L. Skillman)	Apr. 16	03 00	17 15	.....	....	....	....	ms	16	3	7	49	649	4
	Apr. 19	22 35	23 20	.....	....	....	....	ms	20	2	7	59	729	4
	May 6	01 31	10 01	.....	....	....	....	s	6	4	8	93	905	6
	May 15	12 00	20 18	.....	....	....	....	s	16	2,4	8	120	1552	8
	May 26	22 30	27 23	.....	....	....	....	ms	27	3,4	7	58	752	5
	June 2	05 00	4 22	.....	....	....	....	ms	2	3,4,5	7	81	943	4
									3	3	7			
	June 29	07 27	1 14	.....	....	....	....	ms	29	4	7	51	603	6
Witteveen	Jan. 5	05 46	5 24	s.c.*	−3	19	0	ms	5	3,7,8	6	30	205	
(D.van Sabben)	Jan. 19	03 00	20 12	.....	....	....	....	m	19	2	5	20	115	
									20	1	5			
	Jan. 25	08 17	30 21	s.c.	−2	10	−2	ms	26	7	7	45	260	
	Feb. 22	15 00	28 24	.....	....	....	....	ms	22	8	6	40	200	
									23	6,7	6			
									24	6,7	6			
									26	7	6			
									27	8	6			
									28	2	6			
	Mar. 1	20 00	4 03	.....	....	....	....	ms	2	6,7	6	50	195	1
	Mar. 8	15 00	10 07	.....	....	....	....	ms	8	8	6	35	240	1
									9	7	6			
	Mar. 21	18 00	28 24	.....	....	....	....	ms	24	7	7	45	265	
Cheltenham	Apr. 4	00 ..	4 23	.....	....	....	....	m	1	4	5	22	68	
(R. R. Bodle)	Apr. 10	04 ..	12 14	.....	....	....	....	m	11	2	5	26	74	
	Apr. 16	01 ..	17 03	.....	....	....	....	m	17	1	5	17	103	
	Apr. 19	03 ..	24 01	.....	....	....	....	m	20	2	5	25	111	
	May 5	21 ..	9 01	.....	....	....	....	m	8	1,2,3	5	30	104	
	May 15	13 ..	17 07	.....	....	....	....	ms	16	8	6	32	200	1
	May 18	21 ..	20 07	.....	....	....	....	m	19	2	5	18	83	
	May 27	02 ..	28 05	.....	....	....	....	m	27	3,4	5	20	87	
	June 2	02 ..	6 08	.....	....	....	....	ms	3	3	6	40	102	
	June 29	07 ..	3 11	.....	....	....	....	m	30	1,2	5	38	126	
Tucson	Apr. 14	18 ..	23 15	.....	....	....	....	m	16	1,2	5	18	96	
(J. B. Campbell)									19	2	5			
									20	3	5			
									21	7	5			
	May 5	21 16	10 01	s.c.	−2	+15	....	m	6	1,3,4	5	12	99	
									7	1,2,3	5			
									9	2	5			

(*Note:* Tucson continued on next page)

[1]Approximate time of ending of storm construed as the time of cessation of reasonably marked disturbance movements in t traces; more specifically, when the *K*-index measure diminished to 2 or less for a reasonable period.

[2]s.c. = sudden commencement; s.c.* = small initial impulse followed by main impulse (the amplitude in this case is that of t *main impulse only*, neglecting the initial brief pulse); .... = gradual commencement.

[3]Signs of amplitudes of *D* and *Z* taken algebraically; *D* reckoned positive if towards the east and *Z* reckoned positive if vertica downwards.

[4]Storm described by three degrees of activity: *m* for moderate (when *K*-index as great as 5); *ms* for moderately severe (wh *K* = 6 or 7); *s* for severe (when *K* = 8 or 9).

PRINCIPAL MAGNETIC STORMS—Continued

bservatory (Observer-n-Charge)	Greenwich date	Storm-time GMT of begin.	Storm-time GMT of ending[1]	Sudden commencement Type[2]	Amplitudes[3] D	H	Z	C-figure, degree of activity[4]	Maximal activity on K-scale 0 to 9 Gr. day	Gr. 3-hr. period	K-index	Ranges D	H	Z
(1)	(2)	(3)	(4)	(5)	(6)	(7)	(8)	(9)	(10)	(11)	(12)	(13)	(14)	(15)
	1953	*h m*	*d h*		′	γ	γ					′	γ	γ
:son— *'ontinued*	May 15	03 ..	17 07	.....	.....	.....	.....	ms	17	1	6	18	166	34
	(*Note:* Considerable activity followed until 08h GMT, May 21)													
B. Camp-ell)	May 26	20 ..	28 12	.....	.....	.....	.....	ms	27	3	6	15	109	12
	June 2	00 ..	5 10	.....	.....	.....	.....	ms	2	3	6	15	124	20
	June 29	07 ..	.. ..	.....	.....	.....	.....	m	29	4,6,8	5	17	154	18
									30	1,2,3	5			
									1	3,4	5			
	(*Note:* Storm in progress at end of month)													
n Juan G. Ledig)	May 15	04 11	17 07	.....	.....	.....	.....	m	15	7,8	5	13	137	46
									16	1,7,8	5			
									17	1	5			
	June 2	01 18	3 08	.....	.....	.....	.....	m	2	3,4	5	11	116	22
									4	3	5			
nolulu F. White)	May 5	21 16	7 13	.....	.....	.....	.....	m	6	4	5	8	89	41
	May 15	04 00	17 08	.....	.....	.....	.....	ms	15	7	6	11	149	40
	June 2	01 18	4 15	.....	.....	.....	.....	ms	2	3,4	6	9	158	40
	June 29	07 27	1 13	.....	.....	.....	.....	m	30	1,3	5	7	112	30
tituto ofisico de ancayo A.Giesecke Casaverde)	Jan. 5	05 46	5 23	s.c.	−1	−34	−5	ms	5	6,7	6	16	413	34
	Jan. 25	09 13	27 20	.....	.....	.....	.....	m	26	5,6	5	6	209	56
	Feb. 22	14 02	27 02	.....	.....	.....	.....	m	22	6,7	5	6	335	31
	Mar. 1	23 07	3 09	.....	.....	.....	.....	m	2	5,6	5	10	176	27
	Mar. 8	08 58	10 05	.....	.....	.....	.....	m	9	1	5	3	263	34
	Mar. 24	03 50	25 21	s.c.	−1	+55	−12	m	24	6	5	4	214	27
ssouras lio I. Gama)	Jan. 5	05 45	6 02	s.c.	+1	+25	+7	ms	5	6	7	24	153	38
	Feb. 22	14 03	27 02	.....	.....	.....	.....	ms	22	7	7	12	207	54
	Mar. 2	04 29	3 06	s.c.?	0	+15	+4	ms	2	8	6	11	143	55
sabethville Alexandre)	Apr. 21	11 46	22 09	s.c.	.....	+30	+2	ms	21	5,6	.....	7	277	35
	May 7	02 46	8 13	s.c.	.....	+9	.....	m	7	6,7	.....	8	178	19
	June 29	19 34	30 13	s.c.	.....	+22	.....	m	30	2	.....	17	166	20
	(*Note:* Juillet, Août, et Septembre: Pas d'erage important)													
	Oct. 21	10 10	22 10	s.c.	−1	+41	+3	m	21	5,6	.....	8	189	21
	(*Note:* Novembre et Décember: Pas d'erage important)													
ia C. Stan-y, quarter; J. Gill, l quarter)	Jan. 5	05 46	6 03	s.c.	0	15	−5	ms	5	4	6	8	171	38
	Jan. 18	23 ..	19 16	.....	.....	.....	.....	m	19	2	5	8	148	16
	Jan. 25	08 ..	28 12	.....	.....	.....	.....	m	25	4	5	7	75	21
	Feb. 22	14 ..	28 10	.....	.....	.....	.....	m	22	7,8	5	7	110	27
									24	7	5			
									27	8	5			
	Mar. 1	19 ..	3 14	.....	.....	.....	.....	m	2	5,8	5	9	146	23
	Mar. 8	14 ..	10 14	.....	.....	.....	.....	m	8	8	5	5	75	29
	Apr. 3	19 ..	4 21	.....	.....	.....	.....	m	4	1	5	3	111	27
	May 5	21 15	9 13	s.c.	0	11	−2	m	6	4	5	3	106	28
	May 14	16 40	20 12	s.c.?	0	4	−1	m	15	7	5	.....	.....	.....
									16	3,8	5			
	(*Note:* Ranges for storm of May 14 not known owing to break in recording)													
	May 26	07 20	27 12	s.c.	0	7	−2	m	27	2,3,4	5	2	141	17
	June 2	02 ..	4 14	.....	.....	.....	.....	ms	2	3	6	4	146	30
rmanus M. an Wijk)	Apr. 16	12 ..	17 02	.....	.....	.....	.....	m	16	6,8	5	17	100	91
	May 6	00 ..	7 15	.....	.....	.....	.....	m	6	4	5	13	109	68
	May 15	04 ..	17 07	.....	.....	.....	.....	ms	15	7	6	29	154	124
									16	7,8	6			
	May 18	20 ..	19 15	.....	.....	.....	.....	m	19	1	5	13	56	64
	June 2	02 59	4 18	s.c.	.....	.....	.....	m	2	3,7	5	18	111	83
	June 5	19 15	5 21	s.c.	.....	.....	.....	m	5	7	5	(Large bay)		
	June 29	07 ..	.. ..	(Storm still in progress at end of month)										

PRINCIPAL MAGNETIC STORMS—Continued

Observatory (Observer-in-Charge)	Greenwich date	Storm-time GMT of begin.	Storm-time GMT of ending[1]	Sudden commencement Type[2]	Amplitudes[3] D	H	Z	C-figure, degree of activity[4]	Maximal activity on K-scale 0 to 9 Gr. day	Gr. 3-hr. period	K-index	Range D	Range H
(1)	(2)	(3)	(4)	(5)	(6)	(7)	(8)	(9)	(10)	(11)	(12)	(13)	(14)
	1953	*h m*	*d h*		′	γ	γ					′	γ
Watheroo	Apr. 3	23 50	5 00	.....	.....	.....	.....	m	4	1,5,7	5	14	88
(J.E. Webb)	Apr. 16	00 00	17 20	.....	.....	.....	.....	m	16	5,6	5	14	87
	Apr. 19	02 30	23 20	.....	.....	.....	.....	m	20	2,8	5	16	120
	May 6	01 40	9 20	.....	.....	.....	.....	ms	6	4	6	11	110
	May 15	03 00	17 07	.....	.....	.....	.....	ms	15	8	6	31	121
	May 26	17 20	27 17	.....	.....	.....	.....	m	27	4	5	10	121
	June 2	02 20	4 23	.....	.....	.....	.....	m	2	3,4,5,7	5	20	107
									3	3,5	5		
	June 29	07 24	.. ..	.....	.....	.....	.....	m	29	4,5,6	5	.....	.....
									30	1,4	5		
		(*Note:* Storm still in progress at end of month)											
Toolangi	Apr. 3	15 05	5 05	.....	.....	.....	.....	m	4	5,7	5	17	110
(R. E. Ervin)	Apr. 16	00 ..	17 16	.....	.....	.....	.....	m	16	3,5,6	5	17	101
	Apr. 19	02 10	24 02	.....	.....	.....	.....	m	19	5	5	19	143
									20	2	5		
									21	3	5		
	May 15	03 00	17 11	.....	.....	.....	.....	ms	16	5	6	43	179
	May 26	07 24	27 18	s.c.	−1	9	1	m	27	3,4	5	14	132
	June 2	05 40	5 12	.....	.....	.....	.....	ms	3	3	6	28	163
	June 29	07 12	1 16	.....	.....	.....	.....	ms	1	4	6	30	134
Amberley	Apr. 4	00 ..	5 00	.....	.....	.....	.....	m	4	2	5	20	110
(H. F. Baird)	Apr. 16	00 ..	17 15	.....	.....	.....	.....	m	16	3	5	16	97
	Apr. 20	01 ..	23 21	.....	.....	.....	.....	m	20	2,3	5	22	116
	May 6	01 ..	9 15	.....	.....	.....	.....	m	6	4	5	21	105
									7	2	5		
	May 15	13 ..	17 09	.....	.....	.....	.....	m	15	5,6,7	5	27	218
									16	1-3,5,6,8	5		
	May 19	01 ..	20 12	.....	.....	.....	.....	m	19	4	5	14	83
	May 26	23 ..	27 18	.....	.....	.....	.....	ms	27	3	6	20	121
	June 2	03 ..	4 15	.....	.....	.....	.....	m	2	3	5	18	168
									3	3	5		
									4	3	5		
	June 29	07 26	.. ..	.....	.....	.....	.....	m	29	4	5	.....	.....
									30	1,3,4	5		
		(*Note:* Storm still in progress at end of June)											
	1952												
Heard Island	Mar. 3	07 29	12 24	.....	.....	.....	.....	s	8	8	9	.....	.....
(L. N. Ingall)		(*Note:* No record during large part of storm period)											
	Mar. 15	14 00	17 19	.....	.....	.....	.....	s	15	7,8	8	104	845
	Mar. 21	04 00	26 04	.....	.....	.....	.....	s	22	8	9	130+	1558
	Mar. 30	13 00	10 06	.....	.....	.....	.....	s	30	8	9	174	1672
									2	7	9		
		(*Note:* Incomplete record on April 10)											
	Apr. 18	16 00	20 01	.....	.....	.....	.....	ms	19	8	7	61	860
	Apr. 21	12 00	23 14	.....	.....	.....	.....	s	21	5,6	8	148	1176
		(*Note:* Incomplete record on April 21)											
	Apr. 28	00 00	8 22	.....	.....	.....	.....	s	4	1	9	166	1490
	May 17	23 59	19 20	s.c.*	−4	+32	−10	ms	18	6	7	46	596
	May 26	08 00	31 24	.....	.....	.....	.....	s	26	8	8	150	1565
									27	1	8		
	June 8	05 00	11 10	.....	.....	.....	.....	ms	9	5	6	34	465
	June 14	04 00	15 09	.....	.....	.....	.....	ms	14	7,8	6	51	420
	June 22	07 00	25 00	.....	.....	.....	.....	ms	22	7	7	74	711
									24	1	7		
	June 29	19 01	30 12	s.c.	+1	+3	+1	s	30	1,2	8	109	1236
	July 5	02 00	6 13	.....	.....	.....	.....	s	5	7	8	140	1275
	July 20	07 00	22 12	.....	.....	.....	.....	ms	20	6,7,8	6	67	845
									21	6	6		
		(*Note:* Heard Island continued on next page)											

PRINCIPAL MAGNETIC STORMS—Concluded

Observatory (Observer-in-Charge)	Greenwich date	Storm-time GMT of begin.	Storm-time GMT of ending[1]	Sudden commencement Type[2]	Amplitudes[3] D	H	Z	C-figure, degree of activity[4]	Maximal activity on K-scale 0 to 9 Gr. day	Gr. 3-hr. period	K-index	Ranges D	H	Z
(1)	(2)	(3)	(4)	(5)	(6)	(7)	(8)	(9)	(10)	(11)	(12)	(13)	(14)	(15)
	1952	*h m*	*d h*		′	γ	γ					′	γ	γ
ard Island—*Continued* (. N. Ingall)	Aug. 17	01 24	19 06	s.c.	0	+4	0	ms	17	7	6	52	319	325
									18	6	6			
	Aug. 29	14 00	30 09	.....	.....	.....	.....	ms	29	8	7	72	637	383
	Aug. 31	18 47	4 06	s.c.	+11	+5	−11	ms	1	6,8	7	85	953	346
	Sep. 7	17 00	10 15	.....	.....	.....	.....	ms	7	7,8	7	79	871	357
									8	7	7			
	Sep. 13	22 00	15 03	.....	.....	.....	.....	m	14	5	5	31	222	239
	Sep. 25	18 00	26 09	.....	.....	.....	.....	ms	25	8	7	94	851	500
									26	1	7			
	Sep. 27	03 00	27 18	.....	.....	.....	.....	m	27	6	5	24	319	203
	Sep. 28	.. ..	1 06	.....	.....	.....	.....	s	29	8	8	136	1549	581
									30	1	8			
		(*Note:* Incomplete record on Sep. 28)												
	Oct. 3	14 00	6 19	.....	.....	.....	.....	s	4	1	8	133	1249	527
	Oct. 21	10 10	22 09	s.c.*	+13	+46	+26	ms	21	5,7	7	105	813	359
	Oct. 25	17 00	27 06	.....	.....	.....	.....	ms	26	1,6	7	116	978	367
	Nov. 29	11 00	2 03	.....	.....	.....	.....	ms	30	6,7,8	7	124	1020	386
									31	5	7			
	Nov. 20	22 00	22 21	.....	.....	.....	.....	ms	21	4	6	53	378	256
	Nov. 26	09 00	29 21	.....	.....	.....	.....	ms	26	8	7	152	961	383
									27	4,5	7			
	Dec. 1	12 00	5 14	.....	.....	.....	.....	ms	2	1,7,8	7	103	927	425
	Dec. 13	00 00	13 15	.....	.....	.....	.....	ms	13	4,5	6	72	457	164
	Dec. 14	21 39	.. ..	s.c.*	+2	+7	+5	(Minor activity followed)						
	Dec. 24	01 15	26 03	s.c.*	−4	+21	−7	ms	24	5	7	52	657	270
	Dec. 27	16 00	3 03	.....	.....	.....	.....	s	27	8	8	93	1042	364
		(*Note:* No record from 03^h, Dec. 28, until 03^h, Dec. 30)												

LETTERS TO EDITOR

FURTHER REMARKS ON KELSO'S PAPER, "A PROCEDURE FOR THE DETERMINATION OF THE VERTICAL DISTRIBUTION OF THE ELECTRON DENSITY IN THE IONOSPHERE"[1]

In his paper, Kelso points out that the distribution of electron density in the ionosphere can be estimated from virtual height *versus* frequency data by a simple numerical procedure. It has been pointed out by Manning[2] that his method amounts to nothing more than the numerical evaluation of an integral which had been obtained by previous workers, merely by averaging with equal weights a number of equally-spaced ordinates. Although this is usually an inaccurate method of numerical integration, it has its advantages for this problem, and is in fact much more accurate than appears at first sight.

The method is not quite as accurate as Kelso claims. He claims to have found an integration formula using r ordinates which is exact when the integrand is a polynomial of degree $4r - 1$ (equation 5 of his paper). In fact, the integration formula which he has found is exact only when the integrand is an even polynomial of degree $4r - 2$. This error has arisen from his treatment on page 361. His integral I is given by $\int_0^{\pi/2} h'(\cos\theta)\, d\theta$. In order to apply his method, he supposes that the virtual height, h', is defined for negative values of f by $h'(-f) = h'(f)$, and he extends the range of integration as far as π. This process introduces a discontinuity in all the odd-order differential coefficients of h' when $\theta = \pi 2$, that is, right in the middle of the range. This is a definite disadvantage for numerical integration, and, of course, may lead to an inaccurate result. Incidentally, it is interesting to note that Kelso's equation (24), which is really the basis of his method, is stated by Whittaker and Robinson[3] to be due to Bronwin (1849); it appears to have been rediscovered in 1864 by Mehler (Kelso's reference [10]).

The Gauss-Christoffel process is not unique. Kelso supposes that $h'(\cos\theta)$ is a polynomial in $\cos\theta$, and therefore seeks for polynomials in $\cos\theta$ such that $\int_0^{\pi} p_n(\cos\theta)\, p_m(\cos\theta)\, d\theta = 0$ for all $m \neq n$, where $p_n(\cos\theta)$ is a polynomial of degree n in $\cos\theta$. One could equally well assume that $h'(\cos\theta)$ is a polynomial in θ, and seek for polynomials in θ such that $\int_0^{\pi} p_n(\theta)\, p_m(\theta)\, d\theta = 0$ for all $m \neq n$. This is in fact the more usual process (although there seems to be no universally applicable reason why it should be preferable). Kelso's extension of the range of integration has been shown above to lead to errors. The integral which must be evaluated is therefore $\int_0^{\pi/2} h'(\cos\theta)\, d\theta$. The polynomials which satisfy $\int_0^{\pi/2} p_n(\theta)\, p_m(\theta)\, d\theta = 0$ for all $m \neq n$ are simply related to the Legendre polynomials (as stated by Kelso on page 359). The required values of θ_i are given by the roots of the Legendre

[1] J. M. Kelso, J. Geophys. Res., 57, 357-367 (1952).

[2] L. A. Manning, *Letter to Editor*, J. Geophys. Res., 58, 117-118 (1953).

[3] E. T. Whittaker and G. Robinson, The calculus of observations, London, Blackie and Son, Ltd., pl. 59, 2nd ed. (1926).

polynomial of appropriate degree. The weights may then be obtained from Kelso's equation (6). As might be expected, the weights are not the same for all i; therefore, the integration rule does not amount merely to the average with equal weights of a number of ordinates. This integration rule is usually known as Gauss's formula. However, it is possible to determine values of θ_i such that the weights are the same for all i and also the integration formula is exact when h' (cos θ) is a polynomial in θ of degree less than or equal to r, where r is the number of ordinates. The resulting formula is known as Chebyshev's formula.

It is interesting to compare the three formulae, together with Simpson's well-known integration formula, and the formula due to Kraus (Kelso's reference [4]). These, for three ordinates, are as follows:

Kelso: $h(f_v) = \frac{1}{3}\{h'(f_v \cos 15°) + h'(f_v \cos 45°) + h'(f_v \cos 75°)\}$

where $h(f_v)$ is the true height of reflection of frequency f_v

Kraus: $h(f_v) = 0.440\, h'(0.939\, f_v) + 0.364\, h'(0.550\, f_v) + 0.196\, h'(0.124\, f_v)$

Gauss: $h(f_v) = \frac{1}{18}\{5h'(f_v \cos 10°.14) + 8h'(f_v \cos 45°) + 5h'(f_v \cos 79.86°)\}$

Chebyshev: $h(f_v) = \frac{1}{3}\{h'(f_v \cos 13°.18) + h'(f_v \cos 45°) + h'(f_v \cos 76°.82)\}$

Simpson: $h(f_v) = \frac{1}{6}\{h'(f_v) + 4h'(f_v \cos 45°) + h'(0)\}$

The first formula is exact when h' is an even polynomial in f of the tenth degree. The second formula is exact when h' is a polynomial in f of the fifth degree. The other formulae are exact for polynomials in $\cos^{-1}(f/f_v)$ of the fifth, third, and third degrees, respectively. Although Kraus's and Gauss's formulae give the greatest accuracy, they are too complicated for extensive practical use. Of the other three formulae, Kelso's and Chebyshev's are to be preferred to Simpson's. It is probable that Kelso's is better than Chebyshev's, provided that dh'/df tends to zero as f tends to zero. If this is not so, Chebyshev's is better than Kelso's. In cases of doubt, both formulae could be tried; the difference between the two results would then give an estimate of the error of either of them. In order to use Kelso's formula, all one requires is a table of cosines. For Chebyshev's formula, one needs in addition a table of the Chebyshev ordinates. These are given, up to $r = 9$, in "Numerical mathematical analysis" by J. B. Scarborough (John Hopkins Press, Baltimore, pl. 55, 2nd ed. (1950).

However, it seems to be unnecessary to use very accurate formulae in the analysis of (h', f) curves, since the curves themselves are subject to experimental error, and also the theory behind the analysis is not exact. The most disturbing feature of the theory is that the effect of the earth's magnetic field is neglected. For this reason, the analysis is valid only for the ordinary ray near the magnetic equator. For the ordinary ray reflected from a linear layer in England, it may be shown that the estimate of $h(f_v) - h_0$ from the above theory is too high by about 10.5 per cent when f_v is 4.6 Mc/sec, where h_0 is the height of the lower boundary of the layer. The error will be larger for smaller values of f_v, or for larger angles of dip of the earth's magnetic field. Since this error is much more than the errors in the integration formulae (which seldom exceed one per cent),

it would appear that it does not matter which integration formula is used, except when analysing observations from very near the magnetic equator. Further information on the effect of the earth's magnetic field on the group delay of the ordinary ray is given by Shinn and Whale.[4]

For medium and high latitudes, Rydbeck[5] has shown that it is possible to invert the integral equation approximately for the extraordinary ray. It seems likely that Kelso's and Chebyshev's integration formulae could be applied with advantage to this procedure.

D. H. Shinn

Research Laboratories, Marconi's Wireless Telegraph Co., Ltd.,
Great Baddow, Essex, England, May 13, 1953
(Received May 28, 1953)

ANNUAL VARIATION OF THE GEOMAGNETIC ELEMENTS

In the publication, "The Earth's Magnetism" (Methuen's Monographs on Physical Subjects, 1951), Prof. Chapman states that "the monthly mean values of the magnetic elements show very little systematic variation throughout the year, when the secular variation has been allowed for" (p. 37).

At the Magnetic Observatory, Hermanus, the monthly and annual mean values of the magnetic elements D (declination, reckoned positive to the east), H (horizontal intensity), and Z (vertical intensity, reckoned positive to the nadir), are plotted regularly on a large wall chart. An investigation of the annual variation revealed by this chart raises the question whether the periodicity can be wholly accounted for by the characteristic changes in level of the elements during magnetic disturbances. Figure 1 shows the mean monthly departures at Cape Town (1933-1940) and Hermanus (1941-1951) over the greater part of two sunspot-cycles. The secular variation has been eliminated by measuring the departures from a smoothed graph composed of straight joins between the annual means. The standard deviation of the mean monthly departures is of the order of 2 gammas in H and Z, and 0.2 minute in D.

The H and D curves show remarkable similarity. Both show the expected drop at the March, but not at the September equinox. A Fourier analysis of the annual variations yields only two prominent waves (Fig. 2), of which the second is considered to be partly or wholly due to the well-known increase in magnetic activity at the equinoxes. The side arrows indicate the direction of the characteristic changes in level during magnetic disturbances. (The annual variation of *magnetic activity* is illustrated on p. 107 of the above-mentioned publication.)

[4]D. H. Shinn and H. A. Whale, Group velocities and group heights from the magneto-ionic theory, J. Atmos. Terr. Phys., 2, 85-105 (1952).

[5]O. E. H. Rydbeck, A theoretical survey of the possibilities of determining the distribution of the free electrons in the upper atmosphere, Trans. Chalmers Univ. Tech., Gothenburg, No. 3 (1942); or, The propagation of electromagnetic waves in an ionised medium, and the calculation of the true heights of the ionised layers of the atmosphere, Phil. Mag., 30, 282-293 (1940).

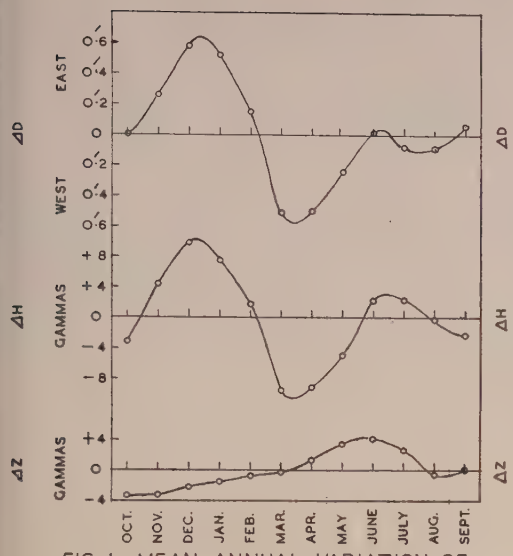

FIG. 1—MEAN ANNUAL VARIATION OF THE MAGNETIC ELEMENTS, 1933-1951

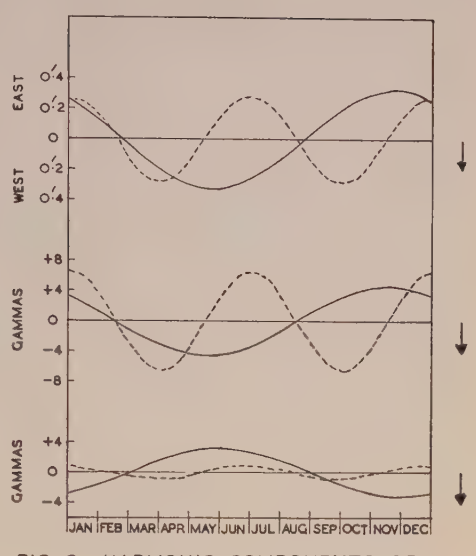

FIG. 2—HARMONIC COMPONENTS OF THE ANNUAL VARIATIONS

A different explanation must, however, be sought for the first harmonics in all three elements, which show a maximum (or minimum) about a month before perihelion and aphelion.

Further indications are (*a*) that, for the limited data at my disposal, the amplitude of the 12-monthly wave is greater for years of high than for years of low sunspot-activity, (*b*) that mean monthly values based on the five hours centered round local midnight likewise show a marked annual variation, and (*c*) that the 12-monthly wave persists in the analysis of data based on the five international quiet days of each month.

Since the observed annual variation of magnetic activity itself awaits explanation, it is felt that an investigation along these lines on a world-wide scale might throw some light on the problem.

I am indebted to the Director, Trigonometrical Survey Office, Department of Lands, for permission to publish the preliminary results of the investigation in this form.

MAGNETIC OBSERVATORY, A. M. VAN WIJK
Hermanus, South Africa, July 6, 1953
(Received July 14, 1953)

NOTES

(14) *New officers, American Geophysical Union*—The American Geophysical Union has elected the following officers, to serve until June 30, 1956: president, James B. Macelwane, St. Louis University; vice-president, Maurice Ewing, Columbia University, Palisades, N.Y.; general secretary, John P. Marble, National Research Council, Washington, D.C. Dr. Beno Gutenberg, Director of the Seismological Laboratory, California Institute of Technology, was the recipient of the William Bowie Medal of the American Geophysical Union.

(15) *Mount Wrangell Expedition, summer 1953*—An expedition directed toward the possible establishment of a scientific observing station on the summit of Mount Wrangell in Alaska was undertaken jointly this past summer (June to September) by New York University and the University of Alaska. The expedition was led by Dr. Serge A. Korff, professor of physics at New York University's College of Engineering, who served as scientific director and principal scientist, and Dr. Terris Moore, president of the University of Alaska, who as administrative director had charge of the logistics of establishing the station. The purposes of the summer's operation were (1) to determine the feasibility of a scientific station on Mount Wrangell, (2) to install as much in the way of shelters and equipment as possible in the event a suitable site for a permanent station should be discovered, and (3) to make cosmic-ray observations at the station during the summer. [On July 13, 1953, it was reported that a permanent high-altitude research observatory had been successfully established on the 14,006-foot summit of Mount Wrangell.]

(16) *New geophysical publication, India*—The Central Board of Geophysics, 27 Chowringhee Road, Calcutta 13, India, has initiated the publication of a "Geophysical Digest." It is to be issued quarterly to enable workers to acquaint themselves with the progress made from time to time in their own as well as in the other allied branches of geophysics by various organizations in India. The general presentation of the Digest is modeled on the lines of the Canadian Geophysical Bulletin issued by the National Research Council of Canada. The first number (January 1953, 55 pages) is in the form of cyclostyled copies, and covers information pertaining to the whole of the calendar year 1952. However, subsequent issues of the Digest will relate to the respective quarterly periods, and will be published in the months of January, April, July, and October of each year. The digest contains information pertaining to current geophysical work, both routine and research, carried on in different parts of the country by Government and private organizations. The topics are arranged conveniently under the different branches of geophysics, namely, meteorology, hydrology, oceanography, seismology, volcanology, terrestrial magnetism, geodesy, tectonophysics, etc. There is a separate section dealing with exploration geophysics.

(17) *New geophysical laboratory near Paris*—A new geophysical laboratory

has been established near Villepreux, some 30 kilometers southwest of Paris. The research program will include observations of atmospheric radioactivity, brightness of the night sky, atmospheric ozone, and cloud structure. Studies of rain and clouds with 3-cm radar are contemplated.

(18) *Central Radio Wave Observatory, Japan, under new ministry*—The Radio Regulatory Commission of Japan ceased to exist on August 1, 1952, and the Radio Regulatory Administrative Office was merged into the Ministry of Postal Service. Consequently, the Central Radio Wave Observatory has become an auxiliary department by the name of the Radio Research Laboratories within the said Ministry. The Radio Research Laboratories consists of three Administrative Divisions located in Tokyo and five radio wave observatories established at Wakkanai, Akita, Hiraiso, Inubo, and Yamagawa. The first division has the following three sections: (1) Ionospheric Propagation Section which shall carry on researches on ionosphere and wave propagation; (2) Tropospheric Propagation Section which shall carry on researches on troposphere and wave propagation; and (3) Data Coordination Section which shall conduct the collection and arrangement of observational results, supply of operational data relating to radio propagation, preparation of radio propagation forecasts and radio disturbance warning broadcasts of URSIGRAM, and physical basic studies of wave propagation in general.

(19) *Alaskan Science Conference*—The fourth Alaskan Science Conference, sponsored by the A.A.A.S. Alaska Division, will be held in Juneau, Alaska, September 28 to October 2, 1953.

(20) *Fall meeting of URSI-IRE*—The USA National Committee of the International Scientific Radio Union (URSI) is sponsoring a fall technical meeting jointly with the Canadian National Committee, URSI, and the IRE Professional Group on Antennas and Propagation. The meeting will be held at the National Research Council, and the Defence Research Board, Ottawa, Canada, on October 5-8, 1953. The participating Commissions are as follows: Commission 1—Radio measurement methods and standards, Commission 3—Ionospheric radio propagation, Commission 4—Terrestrial radio noise, Commission 5—Radio astronomy, and Commission 7—Electronics.

(21) *Conference on Radio Meteorology, University of Texas*—A conference on radio meteorology, at the University of Texas, Austin, is to be held on November 9-12, 1953. Commission 2 on Tropospheric Radio Propagation, of the USA National Committee of the International Scientific Radio Union (URSI) is a sponsor. Technical sessions are planned on cloud physics and precipitation mechanisms, radar rainfall determination, operation use of weather radar, tropospheric propagation and attenuation of radio signals, refractive index meteorology and climatology, thunderstorm and tornado atmospherics, fading characteristics of atmospheric and surface reflected radio signals, atmospheric turbulence and scattering, and radar analysis and meteorological structure of tropical and subtropical disturbances.

(22) *Seventh annual Midwestern Meeting of the Society of Exploration Geophysicists*—Plans are being made for a two-day meeting of oil exploration scientists at the Adolphus Hotel, in Dallas, Texas, on November 12 and 13, 1953. R. M. Nugent (Magnolia Petroleum Company, Midland, Texas) and L. H. Johnson (Honolulu Oil Corporation, Midland, Texas) are general chairman and co-chairman,

respectively, for the meeting, which is being sponsored jointly by the Dallas, Shreveport, Fort Worth, Tulsa, Oklahoma City, and Midland sections of the Society.

(23) *Geomagnetic activities of the United States Coast and Geodetic Survey*—Three volumes of a new series of publications, combining the HV and MG series, were issued; these were for Cheltenham, Sitka, and Tucson, and each volume contained results for the entire year 1950.

Mr. Clyde J. Beers was assigned to the College Magnetic Observatory, in June 1953, as Observer-in-Charge.

Miss Guro Gjellestad, a Fellow in cosmical and terrestrial magnetism of the University of Oslo, Norway, was a guest of the Survey, studying the magnetic work of the Division of Geophysics.

Dr. Lysandro V. Rodriguez, of the National Council on Geography of Brazil, continued his studies of the methods in magnetic work, as a guest of the Survey.

(24) *Corrigendum*—In the "Notice" on page 120 of the March 1953 issue of this Journal, the third line should be corrected to read "its fifty-eighth consecutive year of publication."

(25) *Personalia*—Dr. *S. Imamiti*, Director of the Kakioka Magnetic Observatory, in Japan, retired as of December 31, 1952, after 30 years of service in the field of geomagnetism and geoelectricity. Dr. *T. Yoshimatsu* has been appointed to succeed Dr. Imamiti.

Rosendo Octavio Sandoval, Chief of the Magnetic Department, Geophysical Institute of the National University of Mexico, died in Mexico City on April 2, 1953. He was well known in the field of terrestrial magnetism, to which he contributed much information pertaining to the values of the magnetic elements, maps, theory, and secular variation in Mexico.

NOTICE

The Journal has recently been fortunate in acquiring a complete set of the Journal of Terrestrial Magnetism and Journal of Geophysical Research through Volume 57, which it wishes to place where it will do the most good, presumably in a public or university library, since many of the numbers are now unobtainable. The set is bound in 39 brown buckram volumes, and will be sold at the price paid for it, $300, f.o.b. Washington, D.C. Inquiries should be addressed to the *Journal of Geophysical Research, 5241 Broad Branch Road, N.W., Washington 15, D.C., U.S.A.*

LIST OF RECENT PUBLICATIONS

By W. E. Scott

Department of Terrestrial Magnetism,
Carnegie Institution of Washington,
Washington 15, D. C.

(Received July 20, 1953)

A—*Terrestrial Magnetism*

Allen, P. J. A microwave magnetometer. Proc. Inst. Radio Eng., **41**, No. 1, 100-104 (1953).

Arley, N., B. Lunn, M. Nielsen, and C. Nörgaard. Magnetic measurements in deep-sea investigations. Construction of non-magnetic containers. Nature, **171**, 383-384 (Feb. 28, 1953). [Letter to Editor.]

Arley, N., P. Andreasen, J. Espersen, and J. Olsen. Magnetic investigations on the *Galathea* Expedition. Nature, **171**, 384-385 (Feb. 28, 1953). [Letter to Editor.]

Bartels, J., and J. Veldkamp. International data on magnetic disturbances, fourth quarter, 1952. J. Geophys. Res., **58**, No. 2, 261-265 (1953).

Bates, L. F., and G. Marshall. Heat effects in the magnetization of silicon iron. Rev. Modern Phys., **25**, No. 1, 17-33 (1953).

Bates, L. F., and D. H. Martin. Domains of reverse magnetization. Proc. Phys. Soc., A, **66**, No. 398, 162-166 (1953).

Bodle, R. R. Cheltenham three-hour-range indices *K* for January to March 1953. J. Geophys. Res. **58**, No. 2, 266 (1953).

Bozorth, R. M. Behavior of magnetic materials. Amer. J. Phys., **21**, No. 4, 260-266 (1953).

Bruckshaw, J. M. Magnetic properties of rocks. Nature, **171**, 500-502 (March 21, 1953). [Geophysical discussion at a joint meeting of the Royal Astronomical Society and the Geological Society, held in London, January 23, 1953, with Prof. E. C. Tilley (Department of Mineralogy and Petrology, Cambridge) in the chair.]

Bullard, E. C. Is the earth's dipole moment increasing? J. Geophys. Res., **58**, No. 2, 277-278 (1953). [Letter to Editor.]

Cardús, J. O. Influencia de la posición heliográfica de las fulguraciones cromosféricas en la producción de corchetes geomagnéticos. Urania, **37**, No. 231, 144-168 (1953).

Fukushima, N. Constitution of polar magnetic storms (II). Rep. Ionosphere Res. Japan, **6**, No. 4, 185-193 (1952).

Graham, J. W. Changes of ferromagnetic minerals and their bearing on magnetic properties of rocks. J. Geophys. Res., **58**, No. 2, 243-260 (1953).

Mauersberger, P. Betrachtungen über die zeitliche Änderung der Parameter des geomagnetischen Feldes auf Grund der vorliegenden Potentialentwicklungen. Berlin, Geophys. Inst. Potsdam, Abh. No. 5, 9-58 (1952).

Mayaud, P. N. Champ magnétique moyen et variation séculaire en Terre Adélie au 1er janvier 1952. Paris, C.-R. Acad. sci., **236**, No. 9, 954-956 (1953).

Mayaud, P. N. Position au 1er janvier 1952 du pôle magnétique Sud. Paris, C.-R. Acad. sci., **236**, No. 11, 1189-1191 (1953).

Néel, L. Some new results on antiferromagnetism and ferromagnetism. Rev. Modern Phys., **25**, No. 1, 58-63 (1953).

Néel, L. Thermoremanent magnetization of fine powders. Rev. Modern Phys., **25**, No. 1, 293-295 (1953).

Newton, H. W., and H. F. Finch. Geomagnetic storms and solar activity, 1952. Observatory, **73**, No. 872, 35-37 (1953).

Rikitake, T., I. Yokoyama, and Y. Hishiyama. The anomalous behavior of geomagnetic variations of short period in Japan and its relation to the subterranean structure. The 2nd report. Bull. Earthquake Res. Inst., Tokyo Univ., 31, pt. 1, 19-31 (1953).

Schumann, W. Erdmagnetische Anomalien in Europa und ihre Beziehungen zu den geologischen Verhältnissen. (Eine Studie über den Gesteinsmagnetismus.) Berlin, Geophys. Inst. Potsdam, Abh. No. 14, 147 pp. (1953). 30 cm.

Stoyko, N. Sur la variation de la rotation de la Terre et l'inversion de la polarité du champ magnétique terrestre. Paris, C.-R. Acad. sci., 236, No. 16, 1591-1593 (1953).

Sucksdorff, E. The Geophysical Observatory Sodankylä. Helsinki, Geophysica, 1, No. 5, 17-47 (1952).

Sucksdorff, E. The Magnetic Observatory Nurmijärvi. Helsinki, Geophysica, 1, No. 5, 48 (1952).

United States Coast and Geodetic Survey. Magnetograms and hourly values, Sitka, Alaska, 1950. Washington, D. C., U.S. Coast Geod. Surv., No. MHV-Si50, 161 pp. (1953). 25 cm.

United States Coast and Geodetic Survey. Magnetograms and hourly values, Tucson, Arizona, 1950. Washington, D.C., U.S. Coast Geod. Surv., No. MHV-Tu50, 140 pp. (1953). 25 cm.

Vestine, E. H. On variations of the geomagnetic field, fluid motions, and the rate of the earth's rotation. J. Geophys. Res., 58, No. 2, 127-145 (1953).

Wingst Observatorium. (1) Ergebnisse der erdmagnetischen Beobachtungen im Observatorium Wingst im Jahre 1948 (O. Meyer); (2) Bericht über die mit QHM-Magnetometern zwischen Rude Skov, Fürstenfeldbruch und Wingst ausgeführten Vergleichsmessungen April bis Oktober 1952 (V. Laursen). D. Hydrogr. Inst., Hamburg, Jahrb. No. 6, 88 pp. (1953). 25 cm.

Zentralanstalt für Meteorologie und Geodynamik. Jahrbücher, 1951. Wien, 88, Pub. No. 163, 144 pp. (1952). 32 cm. [Contains list of annual magnetic values of *D*, *H*, *I*, and *F* for Vienna, years 1851-1950.]

B—*Terrestrial Electricity*

Beiser, A. On the origin of auroral forms. J. Geophys. Res., 58, No. 2, 275-276 (1953). [Letter to Editor.]

Coile, R. C., and W. Culmsee. Note on thunderstorms at high altitudes in the tropics. J. Geophys. Res., 58, No. 2, 280-281 (1953). [Letter to Editor.]

Jensen, R. E., and B. W. Currie. Orientations of auroral displays in west-central Canada. J. Geophys. Res., 58, No. 2, 201-208 (1953).

Landseer-Jones, B. C. The streaming of charged particles through a magnetic field as a theory of the aurora. J. Atmos. Terr. Phys., 3, No. 1, 41-57 (1953).

Malan, D. J. Les dècharges dans l'air et la charge inférieure positive d'un nuage orageux. Ann. Geophys., 8, No. 4, 385-401 (1953).

McDonald, J. E. The earth's electricity. Sci. Amer., 188, No. 4,32-37 (1953).

Parkinson, W. D., and R. I. Weller. Atmospheric electric elements over the ocean. J. Geophys. Res., 58, No. 2, 270-272 (1953). [Letter to Editor.]

Vegard, L. Doppler displacement of auroral hydrogen lines and its bearing on the theory of aurora and magnetic disturbances. Geofys. Pub., Oslo, 18, No. 5, 3-15 (1952).

Vegard, L., and E. Tönsberg. Results from auroral spectrograms obtained at Tromsö during winter of 1950/51. Geofys. Pub., Oslo, 18, No. 8, 3-20 3 pls. (1952).

C—*Cosmic Rays*

Brunberg, E.-Å. Experimental determination of electron orbits in the field of a magnetic dipole. J. Geophys. Res., 58, No. 2, 272-275 (1953). [Letter to Editor.]

Galbraith, W., and J. V. Jelley. Light pulses from the night sky associated with cosmic rays. Nature, 171, 349-350 (Feb. 21, 1953). [Letter to Editor.]

George, E. P., J. W. MacAnuff, and J. W. Sturgess. Observations of extensive cosmic-ray showers below ground. Proc. Phys. Soc., A, 66, No. 400, 346-356 (1953).

Kameda, T., and M. Wada. Seasonal variation of large cosmic-ray bursts. Prog. Theoret. Phys., Kyoto, 7, No. 5-6, 586-588 (1952).

Matsumoto, T., and M. Sugawara. On the origin of primary cosmic radiation. Prog. Theoret. Phys., Kyoto, **9**, No. 1, 1-6 (1953).

Neher, H. V. An automatic ionization chamber. Rev. Sci. Instr., **24**, No. 2, 99-102 (1953).

Sarabhai, V., and R. P. Kane. World-wide effects of continuous emission of cosmic rays from the sun. Phys. Rev., **90**, No. 2, 204-206 (1953).

Sekido, Y., S. Yoshida, and Y. Kamiya. Comparison of cosmic-ray storms observed at various longitudes. Rep. Ionosphere Res. Japan, **6**, No. 4, 195-209 (1952).

D—*Upper Air Research*

Appleton, E. V., and W. R. Piggott. Ionospheric storms and the geomagnetic anomaly in the F_2 layer. J. Atmos. Terr. Phys., **3**, No. 2, 121-123 (1953). [Note.]

Argence, E., et M. Mayot. Méthode de détermination des hauteurs vraies des couches de l'ionosphère, compte-tenu de l'action du champ magnétique terrestre. I—Utilisation d'une expression approachée de l'indice de réfraction (cas du rayon ordinaire). J. Geophys. Res., **58**, No. 2, 147-165 (1953).

Atlas, D., M. Kerker, and W. Hitschfeld. Scattering and attenuation by non-spherical atmospheric particles. J. Atmos. Terr. Phys., **3**, No. 2, 108-119 (1953).

Auberger, L. Note sur l'origine du rayonnement du ciel nocturne. J. Geophys. Res., **58**, No. 2, 231-233 (1953).

Banerji, R. B. Some studies on random fading characteristics. Proc. Phys. Soc., B, **66**, No. 398, 105-114 (1953).

Berkel, P. L. M. van, and V. J. Hellendoorn. A camera for use with ionospheric recorders. Central Laboratory of Netherlands Postal and Telecommunications Services, 's-Gravenhague, Description No. 16 R.L., 8 pp., min. (Jan. 1952). 29 cm.

Chapman, S. The geometry of radio echoes from aurorae. J. Atmos. Terr. Phys., **3**, No. 1, 1-29 (1953).

Chapman, J. H. A study of winds in the ionosphere by radio methods. Can. J. Phys., **31**, 120-131 (Jan., 1953).

Closs, R. L., J. A. Clegg, and T. R. Kaiser. An experimental study of radio reflections from meteor trails. Phil. Mag., **44**, No. 350, 313-324 (1953).

Currie, B. W., P. A. Forsyth, and F. E. Vawter. Radio reflections from aurora. J. Geophys. Res., **58**, No. 2, 179-200 (1953).

Feinstein, J. Wave propagation in an anisotropic, inhomogeneous medium. J. Geophys. Res., **58**, No. 2, 223-230 (1953).

Findlay, J. W. Moving clouds of ionisation in region *E* of the ionosphere. J. Atmos. Terr. Phys., **3**. No. 2, 73-78 (1953).

Forsyth, P. A., B. W. Currie, and F. E. Vawter. Scattering of 56 Mc/s radio waves from the lower ionosphere. Nature, **171**, 352-353 (Feb. 21, 1953). [Letter to Editor.]

Gibbons, J. J., R. L. Schrag, and A. H. Waynick. Long-delay ionospheric echoes at 150 kc/s. Nature, **171**, 444-445 (March 7, 1953). [Letter to Editor.]

Herbstreit, J. W., K. A. Norton, P. L. Rice, and G. E. Schafer. Radio wave scattering in tropospheric propagation. Washington, D.C., Nation. Bur. Stan., Rep. No. 2459, 15 pp., 6 figs., mim. (April 15, 1953).

Hines, C. O. Reflection of waves from varying media. Q. Appl. Math., **11**, No. 1, 9-31 (1953).

Hok, G., N. W. Spencer, and W. G. Dow. Dynamic probe measurements in the ionosphere. J. Geophys. Res., **58**, No. 2, 235-242 (1953).

IRE Committee on Wave Propagation. Tropospheric propagation: A selected guide to the literature. Proc. Inst. Radio Eng., **41**, No. 5, 588-594 (1953).

Johnson, W. E. Semi-logarithmic rectangular coordinate recorder. Washington, D.C., Nation. Bur. Stan., Rep. No. 2288, 5 pp., 8 figs. (Feb. 6, 1953).

Jones, R. E., G. H. Millman, and R. J. Nertney. The heights of ionospheric winds as measured at long radio wavelengths. J. Atmos. Terr. Phys., **3**, No. 2, 79-91 (1953).

Kallmann, H. K. Physical properties of the atmosphere between $\sim$ 80 km and $\sim$ 250 km. J. Geophys. Res., **58**, No. 2, 209-217 (1953).

Kallmann, H. K. The continuous layer formation in the atmosphere under the influence of solar radiation. Phys. Rev., **90**, No. 1, 153-154 (1953). [Letter to Editor.]

Landmark, B. Determination of the sense of polarization of the magneto-ionic z-component. Tellus, **4**, No. 4, 319-323 (1952).

Lawrence, R. S. Continental maps of four ionospheric disturbances. J. Geophys. Res., **58**, No. 2, 219-222 (1953).

Lejay, R. P. La 10e Assemblée Générale de l'U.R.S.I. Onde Électrique, **33**, No. 312, 127-132 (1953). [The entire issue is devoted to the General Assembly at Sydney, Australia, August 11-21, 1952: also contains résumés of articles and reports of the various Commissions.]

Lewis, R. P. W. The reflection of radio waves from an ionized layer having both vertical and horizontal ionization gradients. Proc. Phys. Soc., B, **66**, No. 400, 308-316 (1953).

Lindblad, B.-A. A radar investigation of the delta aquarid meteor shower of 1950. Göteborg, Chalmers Tekn. Högsk. Handl., No. 130, 26 pp. (1953).

McKinley, D. W. R., and P. M. Millman. Long duration echoes from aurora, meteors, and ionospheric back-scatter. Can. J. Phys., **31**, 171-181 (Feb. 1953).

Morgan, M. G. A review of VHF ionospheric propagation. Proc. Inst. Radio Eng., **41**, No. 5, 582-587 (1953).

Munro, G. H. Travelling disturbances in the ionosphere: Diurnal variation of direction. Nature, **171**, 693-694 (April 18, 1953). [Letter to Editor.]

Nertney, R. J. The lower E and D region of the ionosphere as deduced from long radio wave measurements. J. Atmos. Terr. Phys., **3**, No. 2, 92-107 (1953).

Osborne, B. W. Some practical determinations of the electron content below the level of maximum ionization in the F_2 region of the ionosphere. J. Atmos. Terr. Phys., **3**, No. 1, 58-67 (1953).

Parasol, M. A method for the determination of the composition and temperatures of stratospheric clouds. J. Geophys. Res., **58**, No. 2, 279 (1953). [Letter to Editor.]

Pfister, W. Note on Lindquist's paper, "An investigation of the ionizing effect in the E-layer near sunrise." J. Geophys. Res., **58**, No. 2, 282 (1953). [Letter to Editor.]

Piddington, J. H. Thermal theories of the high-intensity components of solar radio-frequency radiation. Proc. Phys. Soc., B, **66**, No. 398, 97-104 (1953).

Piggott, W. R. The reflection and absorption of radio waves in the ionosphere. Proc. Inst. Elec. Eng., **100**, Pt. 3, No. 64, 61-72 (1953).

Rawer, K. Die Ionosphäre. Groningen, P. Noordhoff, Ltd., 189 pp. (1953). 24 cm.

Sen, H. K. An estimate of the density and motion of solar material from observed characteristics of solar radio outbursts. Aust. J. Phys., **6**, No. 1, 67-72 (1953).

Siedentopf, H. Fortschritte der Radioastronomie. Phys. Bl., **9**, Heft 1, 24-30 (1953).

Smith-Rose, R. L. International Scientific Radio Union: Meeting in Sydney. Nature, **171**, 628-631 (April 11, 1953). [General description of the tenth general assembly of the U.R.S.I. held in Sydney, August 11-21, 1952.]

Takakura, T. A method of analysis of the directivity of solar radio emission from sunspots. Nature, **171**, 445 (March 7, 1953). [Letter to Editor.]

Tousey, R. Rocket spectroscopy. J. Optical Soc. Amer., **43**, No. 4, 245-251 (1953).

Uyeda, H. Studies on ionospheric storms. Rep. Ionosphere Res. Japan, **6**, No. 4, 169-177 (1952).

Vassy, A., and E. Vassy. Lueur nocturne et activité aurorale. J. Geophys. Res., **58**, No. 2, 283-284 (1953). [Letter to Editor.]

Villard, O. G., Jr., and A. M. Peterson. Meteor scatter. QST, **37**, No. 4, 11-15, 124, 126 (1953).

Watanabe, K., F. Marmo, and E. C. Y. Inn. Formation of the D layer. Phys. Rev., **90**, No. 1, 155-156 (1953). [Letter to Editor.]

Weiss, A. A. Solar ionospheric tides in the F_2 region. J. Atmos. Terr. Phys., **3**, No. 1, 30-40 (1953).

Wells, H. W. Radio interferometer technique applied to measurement of meteor velocities. J. Geophys, Res., **58**, No. 2, 284-286 (1953). [Letter to Editor.]

E—*Earth's Crust and Interior*

Aldrich, L. T., J. B. Doak, and G. L. Davis. The use of ion exchange columns in mineral analysis for age determination. Amer. J. Sci., **251**, No. 5, 377-387 (1953).

BÅTH, M. The problem of microseismic barriers with special reference to Scandinavia. Stockholm, Geol. För. Förh., **74**, Heft 4, 427-449 (1952).

BIRCH, F. Uniformity of the earth's mantle. Bull. Geol. Soc. Amer., **64**, No. 5, 601-602 (1953). [Short note.]

JEFFREYS, H. The earth: Its origin, history, and physical constitution. Cambridge, University Press, 3rd ed., 392 pp. (1952). 27 cm.

RICKER, N. The form and laws of propagation of seismic wavelets. Geophysics, **18**, No. 1, 10-40 (1953).

SCRIPPS INSTITUTION OF OCEANOGRAPHY. Shipboard report, Capricorn Expedition, 26 September 1952-21 February 1953. Univ. of California, SIO Ref. 53-15, 60 pp., mim. (Feb. 25, 1953). 28 cm.

TOLSTOY, I., R. S. EDWARDS, AND M. EWING. Seismic refraction measurements in the Atlantic Ocean (Part 3). Bull. Seis. Soc. Amer., **43**, No. 1, 35-48 (1953).

WAIT, J. R., AND L. L. CAMPBELL. The fields of an oscillating magnetic dipole immersed in a semi-infinite conducting medium. J. Geophys. Res., **58**, No. 2, 167-178 (1953).

F—*Miscellaneous*

BRACEWELL, R. N. The sunspot number series. Nature, **171**, 649-650 (April 11, 1953).

CANADA. Canadian activities in geophysics. Can. Geophys. Bull., National Research Council, Ottawa, **5**, 59 pp., mim. (Dec. 1952). [Published annually; contains reports of sections of Atmospheric Ionization, Terrestrial Magnetism, Seismology and Physics of the Earth's Interior, etc.]

PENNDORF, R. On the phenomenon of the colored sun, especially the "blue" sun of September 1950. Air Force Cambridge Res. Center, Geophys. Res. Papers No. 20, 41 pp. (April 1953). 28 cm.

PIDDINGTON, J. H., AND R. D. DAVIES. Origin of the solar corona. Nature, **171**, 692-693 (April 18, 1953). [Letter to Editor.]

PORTER, J. G. Comets and meteor streams. New York, John Wiley and Sons, Inc., 123 pp. (1952). 24 cm. [Vol. 2, International Astrophysical Series.]

THIESSEN, G. Die magnetische Feldstärke in Sonnenflecken. Naturwiss., **40**, Heft 7, 218-219 (1953).

UREY, H. C. The planets: Their origin and development. New Haven, Yale University Press, 245 pp. (1952). 24 cm.

WALDMEIER, M. Provisional sunspot-numbers for January to March, 1953. J. Geophys. Res.. **58** No. 2, 266 (1953).

NOTE ON PUBLICATION COSTS

The future of scientific publication is difficult to visualize for two principal reasons.

The first and most important is the fact that the flood of publication is overwhelmingly out of proportion to the capacity of an individual mind for receiving information. Every specialized research area has its adjacent fields and its parent sciences, as well as its own principal journals. At our Department, we subscribe to and preserve 126 magazines, plus 56 additional journals which are kept for some years on a more expendable basis. No staff member can begin even to scan this flood of information during each month. Surprisingly, our observation is that the principal mechanism for information about important new researches is still by person to person contact, through visitors and meetings, and it is still an effective mechanism. The future of scientific publication clearly involves something more basic than the simple resolution by government subsidy of financial problems connected with publication. In every special subject, there are only a few places on the face of the earth which are currently centers of research activity and specialized knowledge. Contact with and between these centers in some way may prove the future bases for intelligent scientific publication and the archives problem, replacing the traditional system of broadcasting to every subscriber detailed basic reports on each research problem in all fields of a broad subject.

The second problem is financial, at present. Every scientific society has trouble with its publication costs. The fiscal problems of a small journal serving a specialized group can be briefly illustrated by the balance sheet of this JOURNAL.

Journal of Geophysical Research
Balance Sheet for 1953

Paid subscriptions	$2600	Printer's charges, 550 pages (currently $16 per page)	$8800
Page charges and reprints	2000	Postage	250
Total cash income	$4600	Office supplies	250
Subsidy from CIW	2000	Total cash outgo (no salaries)	$9300
Income	$6600	Cash deficit beyond subsidy	$2700

A small part of this deficit is covered by sale of back issues. The Department of Terrestrial Magnetism salary subsidy is roughly $7000, on basis of office time actually spent.

The deficit for this year is largely being taken care of by using up the operating reserves which had been accumulated during a series of years; a final cash deficit of several hundred dollars may require special consideration. The 900-odd subscribers of the JOURNAL might well perform the following simple arithmetic: The cash expenditures plus the salary costs for office time actually spent (with no charges for

service of editors or scientific referees) are $9300 plus $7000, or $16,300. Subscribers pay $2600, less than one-sixth of these actual costs. In other words, the four paper-bound issues per year represent an expenditure here of nearly $20 per subscriber. This is so far out of reach that the subscription price has been simply left at $3.50, especially because more than half are subscribers in foreign countries, and an increase of even $2 per year can represent a real hardship by reason of the foreign exchange situation.

It might be remarked that the compositor's charges for an edition of 1000 copies are more than 80 per cent of the printer's bill. Our JOURNAL would break even at $3.50 per year and 550 pages if we had about 8000 subscribers with no page charges; with $4 page charge the break-even number would be perhaps 5000 subscribers.

These figures are an old story, and most scientific publication represents a mixture of love and subsidy. Various mergers have been examined, and the JOURNAL is not in an emergency at present. Next year's deficits, since no operating reserves are available for emergency rations, might be met by increasing the subscription price somewhat and perhaps doubling the page charge. Another solution would be to ask all authors to present papers which have already been condensed to half or two-thirds of the author's estimate of an appropriate length, reducing the published pages to the old figure of about 400.

No emergency decision is being made, or indeed necessary, as this issue goes to press. We just thought it might be interesting to share the problem with our readers.

THE EDITOR

September 16, 1953

NOTICE

When available, single unbound volumes can be supplied at $3.50 each and single numbers at $1 each, postpaid.

Charges for reprints and covers

Reprints can be supplied, but prices have increased considerably and costs depend on the number of articles per issue for which reprints are requested. It is no longer possible to publish a schedule of reprint charges, but if reprints are requested approximate estimates will be given when galley proofs are sent to authors. Reprints without covers are least expensive; standard covers (with title and author) can be supplied at an additional charge. Special printing on covers can also be supplied at further additional charge.

Fifty reprints, without covers, will be given to institutions paying the publication charge of $4.00 per page.

Alterations

Major alterations made by authors in proof will be charged at cost. Authors are requested, therefore, to make final revisions on their typewritten manuscripts.

Orders for back issues and reprints should be sent to Editorial Office, 5241 Broad Branch Road, N.W., Washington 15, D.C., U.S.A.

Subscriptions are handled by The Editorial Office, 5241 Broad Branch Road, N.W., Washington 15, D.C., U.S.A.

CONTENTS—Concluded